Shape dynamics and clustering processes of particles transported by turbulent flows : a stochastic approach

Robin Guichardaz

Numéro National de Thèse : 2016LYSEN027

Thèse de Doctorat de l'Université de Lyon

opérée par

l'École Normale Supérieure de Lyon

École Doctorale 52
École Doctorale de Physique et d'Astrophysique de Lyon

Discipline : Physique

Soutenue publiquement le 13/10/2016, par :

Robin Guichardaz

Shape dynamics and clustering processes of particles transported by turbulent flows: a stochastic approach

Dynamique de formes et formations d'amas de particules transportées par un écoulement turbulent : une approche stochastique

---

Devant le jury composé de :

Médéric Argentina	Professeur	Université de Nice	Examinateur
Sergio Ciliberto	Directeur de recherche	CNRS	Examinateur
Bérengère Dubrulle	Directeur de recherche	CNRS	Rapporteure
François Pétrélis	Chargé de recherche	CNRS	Rapporteur
Alain Pumir	Directeur de recherche	CNRS	Directeur
Dario Vincenzi	Chargé de recherche	CNRS	Examinateur
Michael Wilkinson	Professeur	The Open University	Examinateur

Contents

Chapter 1

Introduction

1.1 Dynamical systems

When describing a given physical system, identifying the appropriate variables describing the dynamics of the system is a required first step. Consider the iconic example of a simple pendulum: one can follow the temporal evolution of the angle between the rod and the vertical. However, while this variable allows us to describe perfectly the position of the pendulum at time t, it is not sufficient to characterize completely its dynamics. Indeed, one still needs an information about the velocity of the mass. In classical mechanics and for a one dimensional system – that is, a system which physically evolves only in one direction –, one necessarily needs to know both the position and the velocity at a given time in order to predict the future evolution. This prescription is linked to the fact that the equations of motions are deterministic and involve a temporal derivative of order two. The relevant space where to display the evolution of a one dimensional physical system is then a two dimensional space: the phase space. For a system of N particles who can explore a three dimensional physical space with no constraints, the phase space has then $6N$ dimensions. In general, the dimension of the phase space corresponds to the number of degree of freedom of the physical system, which is the number of free and independent dynamical parameters.

A dynamical system is a function which describes the time dependence of a point in a given phase space. The physical evolution of the system is then represented by a trajectory in the phase space. A given trajectory may either wander off to infinity, or to a limited structure in the phase space. Those structures are called attractors and thus describe the long time behaviour of trajectories. An attractor is then a geometrical structure that can be a point, a curve or sometimes a more complicated set with a fractal structure – in this case one speaks of a strange attractor (see figure 1.1).

1.2 Stochastic description

For the pendulum experiment, after a certain time the oscillations will cease due to the friction (viscous friction caused by the air, or solid friction linked to the mechanical constraints in the attachment point). This dissipative term can be taken into account at the level of the evolution equation by addition of a phenomenological force which conserves the deterministic nature of the dynamics. However, it is of interest to ask about the fate of the energy thus dissipated: Global conservation of energy imposes that energy has to be transferred to other degrees of freedom, in the form of heat. This is typically described by microscopic degrees of freedom. These "microscopic" degrees of freedom – in opposition to the "macroscopic" motion of the pendulum – or "hidden" can also present an active influence on the dynamics. If the pendulum is of a size

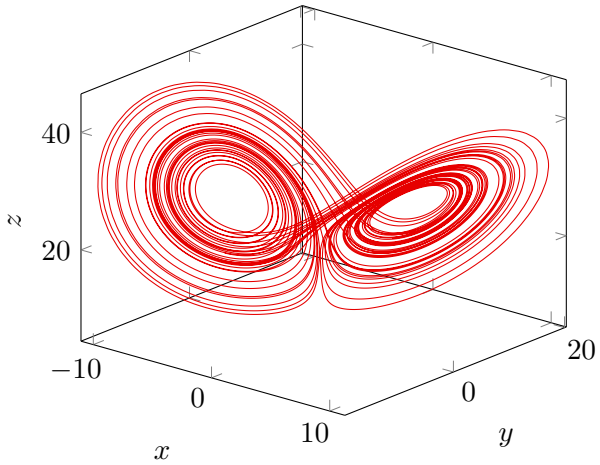

Figure 1.1 – Representation of the strange attractor of the deterministic Lorenz system $\dot{x} = \sigma(y - x)$, $\dot{y} = \rho x - y - xz$, $\dot{z} = xy - \beta z$ with $\sigma = 10$, $\rho = 28$ and $\beta = 8/3$.

and density comparable to the air molecules, a phenomenological viscous force is not enough to faithfully describe the dynamics. In fact, the continuous action of the molecules of the fluid on the pendulum will cause an erratic movement. In general, the random motion of particles suspended in a fluid is called a *Brownian motion* (or "pedesis"). In 1905 Einstein [Ein05] gave the first theoretical explanation of this phenomenon, and its predictions were later verified experimentally by Jean Perrin [Per13]. The dynamics can be understood as the result of repeated collisions between the particles and the molecules constituting the gas or the liquid.

In order to fully determine the dynamics, we should consider the action of all the fluid molecules interacting with the particle. As the number of involved molecules is of the order of the Avogadro number ($\mathcal{N}_\mathrm{A} \sim 6 \times 10^{23}$), it is impossible to follow each trajectory. Therefore, one adopts a stochastic description of the interactions between the particle and the bath, with the introduction of random forces in the equations describing the dynamics, thus obtaining a stochastic differential equation or Langevin equation [Lan08]. The evolution of the system is then reduced to the temporal description of a relatively small number of parameters, but such an evolution must induce stochastic actions. Consequentially, one can no longer consider individual realisations of the process, but rather an average over all the possible realisations of the stochastic terms involved in the dynamics.

1.3 Turbulent flows

The question of turbulence is largely considered as the last unresolved problem in classical physics, namely a problem that is older than the development of general relativity, quantum mechanics or particle physics. However, in a certain way, turbulence and generally fluid mechanics is already solved, as the motion equations, established by Navier and Stokes, are well known since the 18th century. Decades of careful experimental and numerical investigations have given ample evidence that turbulence is properly described by the Navier-Stokes equations. Nevertheless, Navier-Stokes equations are effectively integro differential equations, and apart from some very simple cases, their general solutions are difficult to understand, even at a qualitative level. Thus, turbulence can be seen as a typical high dimensional dynamical system. Experimental observations of real flows or direct simulations based on the Navier-Stokes equations reveal that the turbulent regime is characterized by strong fluctuations of the velocity field, and multiple spatial scales (see figure 1.2).

In fluid mechanics, two main points of view emerge: the Eulerian and the Lagrangian description. The Eulerian description deals with the velocity field $\vec{u}(\vec{x}, t)$ of the flow and is not constrained

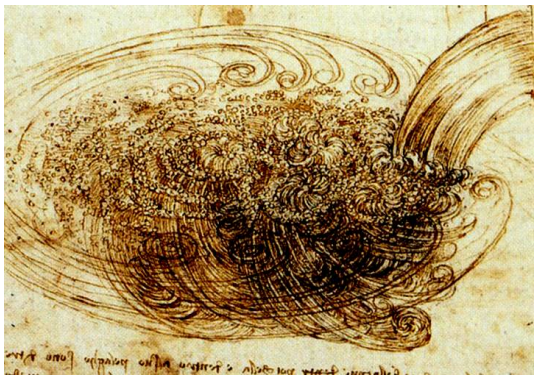

Figure 1.2 – Observations of turbulent flows by Leonardo da Vinci [Lum92].

to the particular tracking of an individual fluid particle. The field $\vec{u}(\vec{x}, t)$ is the one that appears in the Navier-Stokes equations. In the Lagrangian specification the observer follows the evolution of a real fluid particle as it moves through the flow. When we speak of trajectories, we implicitly adopt a Lagrangian description. As such particles are advected by the turbulent flow, their motion is described by a dynamical system. In this work, we do not start from the Navier-Stokes equation, but we rather introduce phenomenological models involving stochastic terms, in order to portray the fluctuating nature of turbulent flows.

1.4 Motivation of this thesis and guideline of the manuscript

The early motivation was to study a stochastic model describing the evolution of a triplet of Lagrangian fluid particles in a two-dimensional and incompressible turbulent flow. This model is introduced in detail in the next chapter, but the main feature is that the triangle formed by the triplet of points tends to flatten due to the action of the flow, so that an initial set of vertices randomly distributed tends to form quasi-linear structures, as observed in real flows. The analysis of the dynamics of flat triangles then led to evolution equations similar to an other class of model for particles in turbulent flows, but with density higher than that of the fluid. The two descriptions are then related to a class of simple noisy dynamical systems, in the sense that they involve fluctuating terms.

In a nutshell, this thesis consists in describing the relevant phase space for each particular dynamics, and studying the structures of attractors arising in those phase spaces (chapter 3 and 4), before generalizing the approach (chapter 5). To this end, we begin this text by a chapter introducing the state of the art concerning noisy dynamical systems and dynamics of particles in turbulent flows, and presenting in detail the outline of the manuscript.

Chapter 2

State of the art

Outline

We present here the main topics covered in this thesis, which deals with the dynamics of particles in turbulent flows. We focus on two different physical situations: first, we consider *tracers*, particles which perfectly follow the flow; second we study the motion of *inertial particles*, that is particles whom density differs from that of the fluid, so that their motion is not strictly following the fluid velocity field but is instead lagging behind it.

We are interested in that we call *clustering processes*, the deformation of initially isotropic structures into highly anisotropic structures. Such processes are of different nature for the two types of particles. On one hand, tracers initially homogeneously distributed in the flow tend to be flattened during the temporal evolution, resulting in an accumulation on a manifold of lower dimension. On the other hand, inertial particles usually concentrate on regions of high

concentration due to the dissipative character of the dynamics. Note that through this text we only deal with non-interacting particles.

First, we introduce the experimental and numerical observations reported in the literature about the dynamics of such particles, and we give the equations of motion for both types of dynamics. These equations are temporal differential equations and thus constitute a dynamical system, with an infinite number of degrees of freedom.

As the formation of structures is a general feature for dynamical systems, we then briefly present the main notions associated with the description of this phenomenon. In particular, we review notions such as Lyapunov exponents or strange attractors, structures presenting notably fractal characteristics.

Due to the very large number of degrees of freedom involved in hydrodynamical phenomenons, and since turbulent flows are intrinsically strongly fluctuating, we adopt a stochastic description of the dynamics, meaning that we use stochastic terms in the equations of motion representing the action of hidden degrees of freedom. As a consequence, we present the main mathematical tools used, and in particular, we introduce the Brownian motion as the iconic random process.

The dynamics of a trajectory near the attractor of a stochastically driven dynamical system can induce intermittency, a phenomenon which is largely described both in theory and in experiments. It generally leads to power-law distributions for the density of presence near the attractors, a signature of fractal structures.

One wishes to propose an effective description of the two physical situations, so we conclude by the introduction of the stochastic models used in the text to describe the dynamics of tracers and inertial particles, and present the outline of the text.

Notation

In the following, the vectors are written with an arrow, $\vec{v}$, while the matrix are written in **bold**:

$$\mathbf{A} = \begin{pmatrix} a & b \\ c & d \end{pmatrix}. \tag{2.1}$$

The i-component of the vector $\vec{v}$ is $[\vec{v}]_i = v_i$. The (i,j)-element of the matrix is $[\mathbf{A}]_{ij} = A_{ij}$, while ${}^T\mathbf{A}$ is the transpose of $\mathbf{A}$. The identity matrix is noted $\mathbf{Id}$.

We adopt the Einstein summation convention: when an index variable appears twice in a single term (and is not otherwise defined), it implies summation of that term over all the values of the index:

$$a_{ij}b_i = \sum_i a_{ij}b_i. \tag{2.2}$$

The time-derivative of a quantity $a(t)$ is written indifferently with the Leibniz or the Newton convention:

$$\dot{a}(t) = \frac{\mathrm{d}a(t)}{\mathrm{d}t}. \tag{2.3}$$

A constant scalar is noted cte, and a constant vector $\overrightarrow{\text{cte}}$.

2.1 Dynamics of particles in random flows

We adopt in this text a Lagrangian point of view, as we consider particles advected by turbulent flows. Contrary to the Eulerian one, the experimental Lagrangian tracking is more complex to realize but has been expanding for the last fifteen years [Mor+01; TB09; PPR09; GRH07].

We are specifically interested in two cases: *passive tracers* and *inertial particles*. The Eulerian underlying flow will be denoted by $\vec{u}(\vec{x}(t), t)$ in the following.

We begin by the description of tracers in incompressible flows, and then the motion of inertial particles.

2.1.1 Tracers and advected clusters in incompressible flows

Passive tracers are ideal fluid particles, as they are supposed to have no influence on the flow and to stay on pathlines. The passive scalar problem (dispersion of a pollutant with density close to that of the fluid, convection of temperature, etc.) is strongly related to the understanding of the motion of the flow itself [SS00; Sre91; AV78], and consequentially to the dynamics of tracers. As such tracers are simply advected by the flow, the equation of motion is

$$\dot{\vec{x}}(t) = \vec{u}(\vec{x}, t). \tag{2.4}$$

To begin, consider the advection of a single Lagrangian particle. In his pioneer work Taylor [Tay22] predicts that a large times an advected tracer will undergo a diffusion motion, but that the dynamics at small times is non-trivial, and in particular the acceleration evolution [MCB04].

In isotropic homogeneous turbulence, to study the growth of an initial structure of Lagrangian particles, now consider two particles in the flow. On one hand, on time scales much larger than the turnover time of the largest eddy their separation $\vec{R}(t) = \vec{x}_1(t) - \vec{x}_2(t)$ experiences a diffusion process. On the other hand if they are separated by a scale smaller than that of the largest eddy, $\vec{R}(t)$ is predicted to grow according to the Richardson law [TL72; MY71; Ric26]:

$$\left\langle \vec{R}^2(t) \right\rangle \propto \epsilon\, t^3 \tag{2.5}$$

where ϵ is the rate of energy dissipation. Note however that this prediction is quite difficult to observe in real turbulent flows, and the initial separation of the two particles can sometimes plays a crucial role in the scaling laws of separation [XOB08].

Nevertheless, considering only the separation of two particles is not enough to fully characterize the evolution of structures in the flow. We rather need to study the geometrical evolution of a larger set of points [Oue12]. At least, the minimal Lagrangian structure can be defined as the number of particles needed to span the space: four a in three-dimensional space (a tetrad), and three a in two-dimensional space (a triangle). For a size structure larger than the integral scale, the particles split uniformly in the flow. However, for scales smaller than the integral scale, an advected scalar field tends to form fronts of high gradients [Mes82; HS94; CK98]. Such structures can be understood as follows: due to the volume conservation, if a blob of fluid is stretched in a given direction, it will necessary be flattened in the perpendicular directions, thus leading to a high probability for multipoint clusters to become nearly coplanar. The formation of sharp gradients increases the mixing properties of the turbulent flow, as it produces regions where diffusion can occur rapidly.

In this text we mainly focus on the case of three particles in a bidimensional flow. The space were the clustering process occurs is then the *shape space* of the triangle [Ken89], homeomorphic to the 2-sphere, in which equilateral triangles are at the poles and flat triangles correspond to points on the equator. During the dynamics a triangle will then be flattened and the representative point of its shape will converge towards the equator.

2.1.2 Inertial particles

The tracers are an ideal limit case where the particles have exactly the same properties as whose of the fluid. In many natural situations, however, the density of the fluid differs from that of

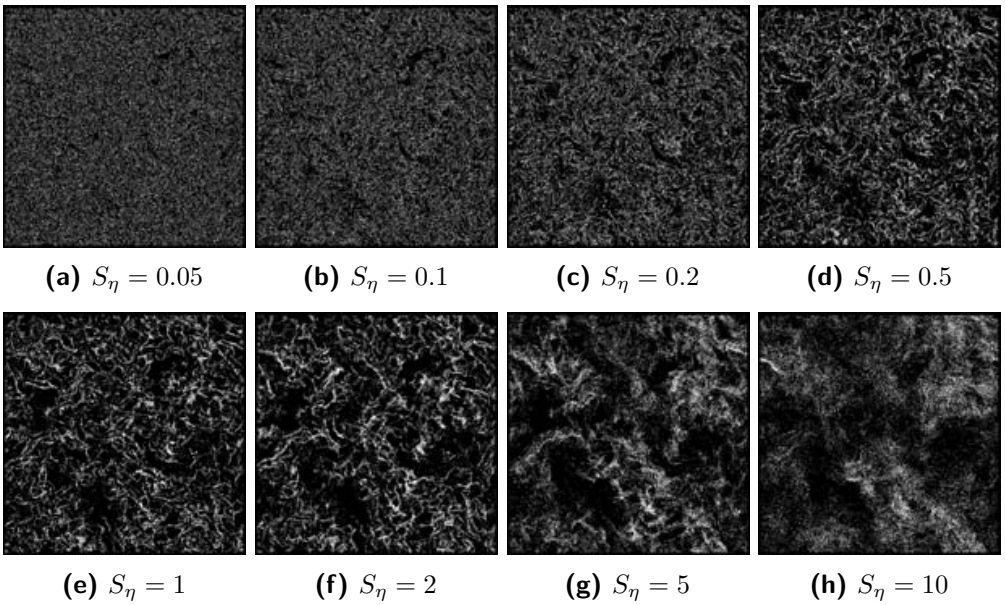

(a) $S_\eta = 0.05$ **(b)** $S_\eta = 0.1$ **(c)** $S_\eta = 0.2$ **(d)** $S_\eta = 0.5$

(e) $S_\eta = 1$ **(f)** $S_\eta = 2$ **(g)** $S_\eta = 5$ **(h)** $S_\eta = 10$

Figure 2.1 – Numerically computed spatial distribution of particles inside a thin layer of width $5\eta_\mathrm{K}$ for eight different Stokes numbers. The side length of plots is approximately $1100\eta_\mathrm{K}$. The plots are taken after the particle distributions become statistically stationary, for $t \approx 2.1T$, T being the integral time. On the first panel the particles are homogeneously distributed, but as inertia comes into play, strong inhomogeneities appear. These snapshots are issued from [YG07].

the particle, whose size has also to be taken into account. As a consequence, these particles, called inertial particles, do not exactly follow the carrying fluid. In the following we focus on *heavy* particles. The understanding of this particular dynamics has many applications: growth of raindrops in subtropical clouds [FFS02], formation of planetary objects in the beginning of the solar system [Bra+99], dispersion of some atmospheric pollutants [Csa73], or transport and coexistence of plankton in the oceans [Abr98; Kár+00].

The dynamics of inertial particles in turbulent flows exhibits a phenomenon known as *preferential concentration*: the particle concentration field is generally strongly inhomogeneous, meaning that particles cluster in some particular regions of the physical space. This effect was reported both from experimental observations or direct simulations using various methods to obtain the turbulent flow [CGT85; CC88; Tan+92; Wen+92; Kob+92; MBC10]. For a global review about preferential concentration, see [MBC12].

Figure 2.1 shows different snapshots from numerical simulations presented in [YG07]. The particles are in a homogeneous and isotropic turbulence and have increasing inertia, characterized by the Stokes number:

$$S_\eta = \frac{\tau_\mathrm{S}}{\tau_\eta} \tag{2.6}$$

where the Stokes time τ_S is defined infra (2.9) as the time response of the inertial particles, and τ_η is the Kolmogorov time scale. Such a clustering is qualitatively captured by the behaviour of the pair correlation function $g(\ell)$ of particle distribution, defined as the total number of pairs of particles whose distance is less that ℓ, and which shows power-law dependence with ℓ. This is linked to the fractal structure of the agglomerated set of particles, as we will show in section 2.2.2.

Due to the inertia and the finite size of the particle, the equation of motion is significantly more complex than (2.4). If the particles have radius a smaller than the Kolmogorov scale of the flow, and relative velocities with respect to fluid sufficiently small, one can approximate the flow

around the particles by a Stokes flow, and one typically has [Gat83; MR83]

$$\begin{aligned} m_{\mathrm{p}}\ddot{\vec{x}}(t) = m_{\mathrm{f}}\frac{\mathrm{D}\vec{u}(\vec{x},t)}{\mathrm{D}t} - 6\pi\eta a\left[\dot{\vec{x}} - \vec{u}(\vec{x},t)\right] - \frac{m_{\mathrm{f}}}{2}\left[\ddot{\vec{x}}(t) - \frac{\mathrm{d}}{\mathrm{d}t}\vec{u}(\vec{x},t)\right] \\ - \frac{6\pi\eta a^2}{\pi\nu}\int_0^t \frac{\mathrm{d}s}{\sqrt{t-s}}\frac{\mathrm{d}}{\mathrm{d}s}\left[\dot{\vec{x}} - \vec{u}(\vec{x},s)\right] \end{aligned} \tag{2.7}$$

where $\frac{\mathrm{D}\vec{u}}{\mathrm{D}t}$ is the derivative of the velocity of the fluid along a path of a fluid element, m_{p} is the mass of the inertial particle, m_{f} the mass of the fluid displaced by the particle and η, ν are respectively the dynamic and kinematic viscosities of the fluid. The terms acting on the right hand side of (2.7) are in order of appearance the force exerted by the unperturbed flow, the Stokes viscous drag, the inertia force of added mass and finally the Basset-Boussinesq history force due to unsteady relative acceleration.

Note that another process can contribute to the formation of spatially inhomogeneities: structures known as caustics may emerge in the physical space, resulting from projection of folded manifolds onto a space of lower dimension [WM05; PW15]. As the inertial particles do not follow the flow, two particles close in the physical space can have different velocities, leading to the apparition of such structures, named in analogy with the caustics in optics. This phenomenon is distinct from the preferential concentration one, because particles with large relative velocities do not tend to form clusters but rather logically separate.

To determine the dynamics of an inertial particle of finite extent, one could try to solve exactly the equation of motions (2.7), but in the general case such a task is nearly impossible, especially because of the history force. However, for very small particles of density much higher than that of the fluid, the Stokes drag is the dominant force, so that it is legitimate to only conserve the third term on the RHS of (2.7), leading to the simplified motion:

$$\ddot{\vec{x}} = -\frac{1}{\tau_{\mathrm{S}}}(\dot{\vec{x}} - \vec{u}(\vec{x},t)) \tag{2.8}$$

where $\vec{u}(\vec{x},t)$ is the velocity field and

$$\tau_{\mathrm{S}} = \frac{2}{9}\frac{a^2}{\nu}\frac{\rho_{\mathrm{particle}}}{\rho_{\mathrm{fluid}}} \tag{2.9}$$

is the particle relaxation time or Stokes time (ρ_{A} is the mass density of A). The dynamics can be written as a $2d$-dimensional dynamical system (where d is the dimension of the space):

$$\begin{cases} \dot{\vec{x}} = \vec{v}\,, \\ \dot{\vec{v}} = \dfrac{1}{\tau_{\mathrm{S}}}[\vec{u}(\vec{x},t) - \vec{v}]\,. \end{cases} \tag{2.10}$$

The phase space is the space $(\vec{x},\vec{v})$, and the dynamics is dissipative. This can be shown by computing the divergence of the dynamical system:

$$\partial_{\vec{x}}[\dot{\vec{x}}] + \partial_{\vec{v}}[\dot{\vec{v}}] = -\frac{1}{\tau_{\mathrm{S}}} < 0. \tag{2.11}$$

This contraction leads to the existence of complex attractors in the phase space.

One usually sees the preferential concentration of inertial particles as a process induced by the centrifugal force, the particles being expelled from vortices. The argument was first presented by Maxey [Max87] and can be summarized as follows. One look for the expression of the effective advecting field $\vec{v}$ in (2.10), which transports the particles. The integration of the second line of (2.10) gives

$$\vec{v}(t) = \frac{1}{\tau_{\mathrm{S}}}\int_{-\infty}^{t} \mathrm{d}t'\,\vec{u}(\vec{x}(t'),t')\exp\left(-\frac{t-t'}{\tau_{\mathrm{S}}}\right) \tag{2.12}$$

so that at small Stokes time τ_S it reduces to[1]

$$\vec{v}(t) = \vec{u}(\vec{x}(t), t) - \tau_S \frac{D}{Dt}[\vec{u}(\vec{x}(t), t)] + \mathcal{O}(\tau_S^2). \tag{2.13}$$

Thus, the advecting velocity field $\vec{v}$ is in fact *compressible*, even if the underlying flow is not. If we compute its divergence one has

$$\vec{\nabla} \cdot \vec{v} = 0 - \tau_S \frac{\partial u_i}{\partial x_j} \frac{\partial u_j}{\partial x_i} = -\tau_S \, \mathrm{tr}\mathbf{A}^2 \tag{2.14}$$

where $\mathbf{A}$ is the *velocity gradient tensor*, defined as

$$A_{ij} = \partial_j u_i. \tag{2.15}$$

By writing $\mathbf{A} = \mathbf{M} + \mathbf{\Omega}$ where $\mathbf{M}$ is the *strain rate symmetric tensor*, and $\mathbf{\Omega}$ is the *vorticity antisymmetric tensor*, one obtains

$$\vec{\nabla} \cdot \vec{v} = -\tau_S \left[\mathrm{tr}\mathbf{S}^2 - \frac{1}{2} \vec{\omega} \cdot \vec{\omega} \right] \tag{2.16}$$

where $\vec{\omega}$ is the axial vorticity vector, which corresponds to the antisymmetric tensor: $\vec{\omega} = \vec{\nabla} \times \vec{u}$. Thus, the effective advecting flow is contracting in regions of high strain and expanding in regions of high vorticity.

The phenomenon of preferential concentration is intrinsically linked to the Stokes drag force, which is effectively prominent for heavy particles. In fact, the Stokes time alone is insufficient to characterize this behaviour, as experiments showed that the dynamics of buoyant particles (that is, particles of density comparable to that of the fluid) do not lead to preferential concentrations, independently of the value of their Stokes time [Fia+12; Fia+13]. In this particular case, the drag force is not the dominant term in the equations of motion.

2.2 Dynamical systems

Both equations (2.4) and (2.10) describe a dynamical system. However, we have not yet described one term, the Eulerian velocity field, denoted here as $\vec{u}(\vec{x}, t)$. In general, but especially if the flow is turbulent, the dynamics of the Eulerian flow, and consequentially the dynamical systems presented supra, are *extremely complicated*, with a large number of degrees of freedom and no time periodicity. Nevertheless some simple characteristics of the motion of tracers or inertial particles can be understood in a general framework; for example, formation of patterns in the physical space are a common feature for high-dimensional dynamical systems. We present here some tools to describe the dynamics of both types of particles.

2.2.1 Lyapunov exponents

The behaviour of close trajectories, and thus the chaotic behaviour of a dynamical system, is determined by the Lyapunov exponents of the dynamics.

Consider a generic dynamical system described by the differential equation

$$\dot{\vec{X}}(t) = \vec{F}(\vec{X}(t), t). \tag{2.17}$$

As first approximation, the Lyapunov exponent characterizes the rate of separation of infinitesimally close trajectories in the phase space. Typically, take two close trajectories $\vec{X}_1(t), \vec{X}_2(t)$

[1] The idea is to perform an integration over parts of the integral, and use the identity $\exp(-t/\tau)/\tau \to \delta(t)$ when $\tau \to 0$.

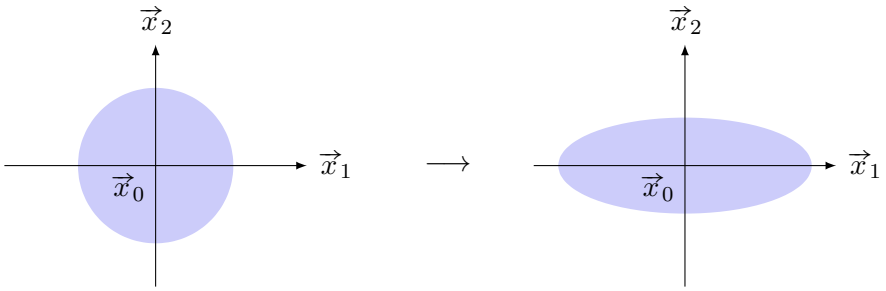

Figure 2.2 – Deformation of a fluid particle in a bidimensional space at $\vec{x}_0$. The direction $\vec{x}_1$ (resp. $\vec{x}_2$) is dilating (resp. contracting) with rate $\lambda_1 > 0$ (resp. $\lambda_2 < 0$). As $\lambda_1 + \lambda_2 = 0$, the volume is conserved.

in the phase space, and note $\delta\vec{X}(t)$ the separation between them: $\delta\vec{X}(t) = \vec{X}_2(t) - \vec{X}_1(t)$. The (largest) Lyapunov exponent reads

$$\lambda = \lim_{t\to\infty} \lim_{|\delta\vec{X}(0)|\to 0} \frac{1}{t} \ln \frac{|\delta\vec{X}(t)|}{|\delta\vec{X}(0)|}, \tag{2.18}$$

meaning that approximatively the separation of trajectories acts like

$$\delta\vec{X}(t) = \delta\vec{X}(0) \exp(\lambda t). \tag{2.19}$$

A positive Lyapunov exponent implies a separation of trajectories, and a negative one indicates a clustering of paths.

There usually exists a spectrum of Lyapunov exponents rather than a single one, whose number of elements is equal to the dimension of the phase space. More rigorously, if the trajectories are sufficiently close, one can linearise the system (2.17) and obtain

$$\frac{\mathrm{d}}{\mathrm{d}t}\delta\vec{X} = \mathbf{M}(t)\delta\vec{X}(t). \tag{2.20}$$

Define the Jacobian matrix $\mathbf{J}(t)$ as the Green function of this differential equation, one has

$$\mathbf{J}(t) = \mathbb{T}\left[\exp\left(\int_0^t \mathrm{d}t'\mathbf{M}(t')\right)\right] \tag{2.21}$$

where $\mathbb{T}$ denotes the time-ordered product. Under certain assumptions [Ose68], the limit matrix

$$\lim_{t\to\infty} \left(\mathbf{J}(t)^{\,T}\mathbf{J}(t)\right)^{1/(2t)} \tag{2.22}$$

exists and its eigenspectrum is the Lyapunov exponents set.

The sum of the Lyapunov exponents is the rate of growth of an infinitesimal volume in the phase space. In figure 2.2, we illustrate a conservative 2-dimensional dynamics with $\lambda_1 = -\lambda_2 > 0$. One direction is dilating while the other is contracting. If all the Lyapunov exponents are negative, we speak of a strongly aggregative dynamical system, where all the trajectories tend to a single one.

2.2.2 Strange attractors and fractal structure

For deterministic dynamical systems of dimension higher than three, attractors with fractal structures can occur. A fractal set is an irregular structure exhibiting a repeating pattern that displays at every scale. This *self-similar* property is often caused by the application of deterministic or stochastic homothetic rules. Due to their irregularity, fractals are usually nowhere differentiable.

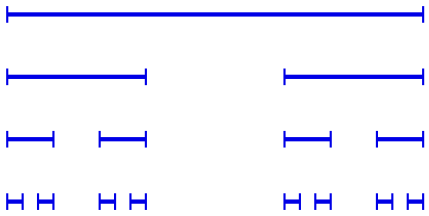

Figure 2.3 – The Cantor set is obtained by deleting the open middle third from each of a set of line segments repeatedly. The resulting set exhibits a fractal structure of dimension $D_{\text{box}} = \ln_3(2) < 1$.

The term fractal was first used by Benoît Mandelbrot in 1975 [Man90]. If a large number of ideal fractal sets are described in the mathematical literature, yet such structures can also emerge from natural processes [Man83; Tan+09; LZY03].

There exists several definitions for the dimension of a fractal set, which do not always give equivalent results. Mathematically, the most rigorous one is the Hausdorff D_{H}, but it is also technically one of the hardest to work with. Another more convenient definition is the Minkowski-Bouligand our "box counting" dimension. Let $\mathcal{N}(\varepsilon)$ be the minimal number of hypercubes of side length ε necessary to totally cover the set. If we consider a line of length L in a bidimensional space, one needs $\mathcal{N}(\varepsilon) = L/\varepsilon$ squares to cover it, so $\mathcal{N} \sim \varepsilon^{-1}$. For a surface one obtains $\mathcal{N} \sim \varepsilon^{-2}$. The box dimension is then defined as the exponent in the power-law dependence of $\mathcal{N}$ in ε, for small values of ε. One has

$$D_{\text{box}} = \lim_{\varepsilon \to 0} \frac{\ln \mathcal{N}(\varepsilon)}{\ln 1/\varepsilon}. \tag{2.23}$$

Fractal dimensions are non-integer. Consider the Cantor set defined as follows: one starts from the segment $[0, 1]$ which we divide in three equal segments. One deletes the middle segment and performs the same process on the two remaining segments, and so on (see figure 2.3). The Cantor set is then the limited result of this process. To compute its box counting dimension, one remarks that at the step n, the set is covered by 2^n segments of size 3^{-n}, so that

$$\begin{aligned} D_{\text{box}} &= \lim_{n \to \infty} \frac{\ln(2^n)}{\ln(3^n)} \\ &= \frac{\ln 2}{\ln 3}. \end{aligned} \tag{2.24}$$

The dimension of this fractal set is then $\ln_3(2) \approx 0.63 < 1$. Consequentially, the Cantor set is "a little more" than a point or a finite union of points – which would have a zero dimension –, but also "a little less" than a simple line of dimension one.

For an attractor of a dynamical system, the natural dimension to use is the correlation dimension D_2 [GP83; GP84]. Consider a set $\{\vec{x}_i\}$ of points on the attractor, which can be obtained for example from a time series of a single trajectory: $\vec{x}_i = \vec{x}(t_i = i\tau)$ with τ a fixed time increment, taken large enough to neglect the temporal correlations between the x_i. A strange attractor presents at least one positive Lyapunov exponent, so that each point will separate from the others. The points are then dynamically decorrelated but spatially correlated, as they live on the attractor (or very close to it). To measure this correlation, we introduce the correlation integral $C(\Delta x)$, defined as

$$C(\Delta x) = \lim_{N \to \infty} \frac{g(\Delta x)}{N} \tag{2.25}$$

where $g(\Delta x)$ is the total number of pairs of points (i, j) whose distance $|\vec{x}_i - \vec{x}_j|$ is less that Δx. The correlation dimension relies on the assumption that $C(\Delta x)$ follows a power law for small values of Δx:

$$C(\Delta x) \sim \Delta x^{D_2} \tag{2.26}$$

or more rigorously

$$D_2 = \lim_{\Delta x \to 0} \frac{\ln C(\Delta x)}{\ln \Delta x}. \tag{2.27}$$

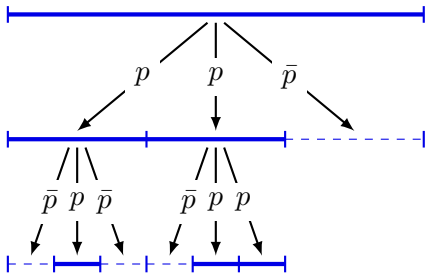

Figure 2.4 – Example of a realisation of a random Cantor set. Each cell gives birth to three daughter cells, each having a probability p to "live" and $\bar{p} = 1 - p$ to "die". In the next step the process is repeated for the remaining living cells.

Contrary to the box-counting dimension, the correlation dimension is linked to the spatial distribution of the attractor [ER85]. If the attractor is spatially inhomogeneous, one has $D_2 \leq D_{\text{box}}$. Note that in general [Fal04]

$$D_2 \leq D_{\text{H}} \leq D_{\text{box}}. \tag{2.28}$$

2.2.3 Strongly contracting processes and negative fractal dimension

Fractal sets usually have positive dimension, meaning that the number of hypercubes necessary to cover the set grows as the size of the cubes decreases, and for the correlation dimension that the mass of trajectories in a ball of size Δx decreases with Δx. Nevertheless it is sometimes of interest to consider processes which contract the dynamics up to a single point structure: inertial particles collapsing on a single path, or triangles becoming infinitely flat. The dimension of the attractor is then often set to zero. However, we briefly show here how to extend the notion of fractal dimension to *negative cases*.

To understand the notion of negative fractal dimension, let us return to the Cantor set. Yet, we suppose that the process is not deterministic but *stochastic*: a "mother" segment is divided in three equal "sister" segments, each having a probability p to "live" and $\bar{p} = 1 - p$ to "die". We then repeat the same process to the surviving segments, and so on (see figure 2.4). The mean number of living segments created from a single one is then

$$\begin{aligned} \langle N \rangle &= 0 \cdot \bar{p}^3 + 1 \cdot 3 \cdot \bar{p}^2 p + 2 \cdot 3 \cdot \bar{p} p^2 + 3 \cdot p^3 \\ &= 3p, \end{aligned} \tag{2.29}$$

so that at step n of the process, the average of the total number of segments of size 3^{-n} is $\langle \mathcal{N} \rangle = \langle N \rangle^n = (3p)^n$. If the number of daughter cells decreases, i.e. if $3p < 1$, the set tends in average to a empty set. Generalise (2.23) by writing

$$\begin{aligned} D_{\text{box}} &= \lim_{n \to \infty} \frac{\langle \mathcal{N} \rangle}{\ln(3^n)} \\ &= \ln_3(3p), \end{aligned} \tag{2.30}$$

one obtains a *negative* value for the fractal dimension in the case of a vanishing set ($3p < 1$). Note that $p = 2/3$ gives the same dimension as the deterministic Cantor set, meaning that the two ensembles have the same intrinsic structure, even if their generating processes differ. In fact, the Cantor set is a typical realisation of the stochastic Cantor set with $p = 2/3$. As the number of covering cells must be non-integer to obtain negative fractal dimensions, the randomness of the process generating the fractal is essential [Man90].

The extension to dynamical attractors is straightforward. If the correlation dimension D_2 is negative, then from (2.26) it means that the number of trajectories inside a ball of radius Δx

centered around a single one *increases* then Δx decreases. The link between the density of probability for separation of trajectories and $C(\Delta x)$ being

$$C(\Delta x) = \int_0^{\Delta x} \mathrm{d}(\Delta x') P(\Delta x') \quad \text{which gives} \quad P(\Delta x) = \frac{\mathrm{d}C(\Delta x)}{\mathrm{d}(\Delta x)}, \tag{2.31}$$

one obtains

$$P(\Delta x) \sim \Delta x^{D_2 - 1}. \tag{2.32}$$

The condition $D_2 < 0$ implies a non-normalisable distribution. One then needs a *regularisation process*, in order to avoid trajectories to collapse on the attractor. We will come back to this notion thereafter, but before that we present the mathematical canvas for stochastic dynamics.

2.3 Stochastic processes

2.3.1 Random walk and Brownian particle

The emblematic example of a stochastic process is the random walk: a man[(2)] moves along a line and can make steps to the left or to the right with same probability 1/2. We note τ the time between each step, and a the size of a step. This motion is a representation of a *diffusion process*. As the dynamics is random, we look for the probability $P(ia, n\tau)$ for the walker to be at position ia at time $n\tau$, with $i \in \mathbf{Z}$ and $n \in \mathbf{N}$. A simple calculus leads to

$$P(ia, n\tau) = \frac{1}{2^n} \binom{n}{\frac{n+i}{2}}. \tag{2.33}$$

By symmetry, the mean of the position $\langle x(t) \rangle$ is equal to zero: the walk is unbiased. One can also compute the variance of the position, and obtain

$$\langle x^2(t) \rangle = \frac{a^2}{\tau} t \tag{2.34}$$

with $t = n\tau$. The coefficient $D = a^2/(2\tau)$, equal to half the mean square distance travelled per unit time, is then a diffusion coefficient. In the limit of continuous time ($\tau \to 0$) and infinitesimal small step size ($a \to 0$) with D fixed, one obtains formally a *Wiener process* [Gar+85]. Introduce the probability density function $P(x, t)$; the probability for the particle to be between x and $x + \mathrm{d}x$ at time t is by definition $P(x, t)\,\mathrm{d}x$. The probability density function is an evaluation of the chance to find the particle in a given position and for a given time, and thus it is the continuous analogous of $P(ia, n\tau)$. After taking the continuous process limit, one obtains

$$P(x, t) = \frac{1}{\sqrt{4Dt}} \exp\left(\frac{x^2}{2D}\right). \tag{2.35}$$

If we see $P(x, t)$ as a concentration $n(x, t)$ of particles undergoing a one dimensional diffusion in a given medium with diffusion coefficient D, then we know that $n(x, t)$ follows the diffusion equation

$$\frac{\partial n}{\partial t} = D \frac{\partial^2 n}{\partial x^2}, \tag{2.36}$$

and it is straightforward to see that $P(x, t)$ as defined in (2.35) is solution of (2.36). Here appears a link between stochastic processes and partial differential equations, which will be formally presented thereafter with the introduction of the Fokker-Planck equation.

(2) Usually named Robert.

In the continuous limit, the process $x(t)$ formally follows the evolution equation

$$\dot{x} = \sqrt{2D}\,\xi(t), \tag{2.37}$$

where $\xi(t)$ is a *Gaussian white noise process*. Such a process is of fundamental interest in stochastic dynamics, as it is the most used representation of a noise process. The statistics of a white noise process are *Gaussian* and *uncorrelated in time*, that is

$$\langle \xi(t) \rangle = 0 \ , \ C(t_1, t_2) \overset{\text{def.}}{=} \langle \xi(t_1)\xi(t_2) \rangle = \delta(t_1 - t_2) \tag{2.38}$$

and all the other joint cumulants are zero:

$$\begin{aligned} 0 &= \langle \xi(t_1)\xi(t_2)\xi(t_3) \rangle \,, \\ 0 &= \langle \xi(t_1)\xi(t_2)\xi(t_3)\xi(t_4) \rangle - C(t_1,t_2)C(t_3,t_4) - C(t_1,t_3)C(t_2,t_4) - C(t_1,t_4)C(t_2,t_3) \text{ etc.} \end{aligned} \tag{2.39}$$

Here the mean $\langle A \rangle$ of an observable A is taken indifferently as a, average over an ensemble of realisations of the noise, or as computed over a single trajectory after a sufficiently long time. When the two results are the same the system is called ergodic, and we will suppose that it is always the case.

The Gaussian white noise is formally the time derivative of a Brownian motion (see equation (2.37)). Its variance is infinite, which is a consequence of continuous time and infinitely small jumps limit previously taken: the time derivative of the discrete process is

$$\frac{\Delta x}{\Delta t} = \pm \frac{a}{\tau} \tag{2.40}$$

which goes to infinity when a and τ goes to zero with a^2/τ fixed. Although being widely used especially in the physics community, the Gaussian white noise process is thus not rigorously defined mathematically speaking, and one can prefer use its time integral $\mathrm{d}W(t)$, so that

$$\mathrm{d}x(t) = \sqrt{2D}\,\mathrm{d}W(t). \tag{2.41}$$

Its statistics are naturally close to the ones defined in (2.39), with $\langle \mathrm{d}W \rangle = 0$ and $\langle \mathrm{d}W^2 \rangle = \mathrm{d}t$.

As we will see, if we use a white noise process in the description of the dynamics, then the literature provides us convenient mathematical tools for pushing the analysis quite far.

2.3.2 The Langevin equation

The memoryless property of a Gaussian white noise process makes it a good candidate for describing a noise process with a correlation time very short compared to the other characteristic times involved in the dynamics. Consider a generic dynamical system with the addition of a Gaussian white noise:

$$\dot{x} = a(x) + \sqrt{2D}\,\xi(t), \tag{2.42}$$

in order to take into account hidden fast variables, where $a(x)$ is a sufficiently smooth function. The equation of motion contains a stochastic term, meaning that its solution is not a given function, but rather an ensemble of solutions, each related to a single realisation of the stochastic process. A differential equation involving as a random term a Gaussian white noise process is called a *Langevin equation*.

If the diffusion coefficient depends of the position x, the equation (2.48) is not rigorously defined, as the choice of the time at which the term $\sqrt{2D(x)}\,\xi$ is evaluated is not specified. Two main prescriptions are used in the literature: the Itō and the Stratonovitch convention. As we will always deal with a linear noise, when the diffusion coefficients are constant, we will not follow one prescription or the other.

2.3.3 The Fokker-Planck equation

One needs to obtain a convenient description of the statistical properties of the process described by (2.42). One can show [Van92; Gar+85] that the distribution $P(x,t)$ follows a partial differential equation called a *Fokker-Planck equation*:

$$\frac{\partial P}{\partial t} = -\frac{\partial}{\partial x}[a(x)P(x,t)] + D\frac{\partial^2}{\partial x^2}[P(x,t)]. \tag{2.43}$$

The term $a(x)$ is the drift velocity, which is related to the infinitesimal increase δx during an infinitesimal increase in time δt:

$$\langle \delta x \rangle = a(x)\,\delta t, \tag{2.44}$$

and D is the diffusion coefficient. The diffusion equation (2.36) is then a particular Fokker-Planck equation, although a very simple one, with no drift velocity and a constant diffusion coefficient.

The generalization to larger dimensions is straightforward. Consider the n-dimensional Langevin equation

$$\frac{\mathrm{d}\vec{x}}{\mathrm{d}t} = \vec{a}(\vec{x}) + \mathbf{b}\cdot\vec{\xi}(t) \tag{2.45}$$

where $\mathbf{b}$ is a $n \times n$ matrix independent of $\vec{x}$, and $\vec{\xi}(t)$ an n-dimensional Gaussian white noise process with statistics

$$\langle \xi_i(t_1)\xi_j(t_2)\rangle = \delta_{ij}\delta(t_1 - t_2). \tag{2.46}$$

Then the joint density of probability $P(\vec{x},t)$ follows the multivariate Fokker-Planck equation:

$$\frac{\partial P}{\partial t} = -\frac{\partial}{\partial x_i}[a_i P] + \frac{\sigma_{ij}}{2}\frac{\partial^2 P}{\partial x_i \partial x_j} \tag{2.47}$$

where $\boldsymbol{\sigma} = \mathbf{b}^T\mathbf{b}$ is the diffusion matrix.

2.3.4 Application: sedimentation of Brownian particles

Let a heavy particle of mass m in a thermal bath, whom the position is labelled by its altitude z. One wants to properly describe its dynamics, but without computing the trajectories of all the fluid molecules in the bath. To proceed, we suppose that the particle is subject to the gravitational field, and we decompose the action of the fluid into two forces:

▷ a drag force opposed to the velocity particle $F_{\text{drag}} = -\gamma\dot{z}$;
▷ a random force F_{rand} with zero mean.

After writing the Newton's second law applying on the particle, one obtains, the z axis being directed upwards:

$$m\ddot{z} = -mg - \gamma\dot{z} + F_{\text{rand}}. \tag{2.48}$$

The inertia of the particle relaxes with a characteristic time $\tau = m/\gamma$. For typical Brownian particles $\tau \sim 10^{-8}$ s. For times intervals Δt larger than τ, we can neglect the inertia term in (2.48) and get

$$\dot{z} = v_0 + \sqrt{2D}\,\xi(t) \tag{2.49}$$

with $v_0 = -mg/\gamma$ the drift velocity, and $\sqrt{2D}\xi(t) = F_{\text{rand}}/\gamma$ the noise term. As the last one represents the actions of fast degrees of freedom, one can suppose that it can be modelled by a Gaussian white noise with diffusion coefficient D. Thus, the Fokker-Planck equation for the density of probability $P(z,t)$ reads

$$\frac{\partial P}{\partial t} = -v_0\frac{\partial P}{\partial z} + D\frac{\partial^2 P}{\partial z^2}. \tag{2.50}$$

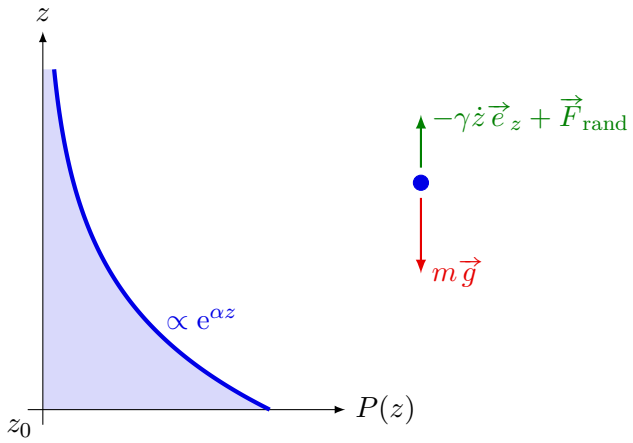

Figure 2.5 – Density of probability of a heavy particle in a thermal bath.

The stationary distribution reads

$$P_{\text{stat.}}(x) = \mathcal{A} \exp\left(\frac{v_0}{D} z\right) \tag{2.51}$$

where $\mathcal{A}$ is a normalization constant. Note that in order to be normalized, the distribution cannot be defined on $\mathbf{R}$, and one must assume the existence of a reflective wall at some $z = z_0$ (see figure 2.5). This system is the simplest example of a *sedimentation problem*, where a particle is advected by a drifted noise. If the statistics of the noise does not depend on the position (which is the case here), then one expect that the stationary density of probability has the translational invariant form

$$P_{\text{stat}}(x) = \mathcal{A} \exp(\alpha x). \tag{2.52}$$

For the Brownian particle in a bath we obtain $\alpha = v_0/D$. If we consider that the bath is a thermal bath at temperature T, then the density of probability $\rho(y)$ follows

$$\rho(y) \sim \exp\left(-\frac{mgy}{k_{\text{B}}T}\right). \tag{2.53}$$

We have consequentially the Einstein relation [Ein05]:

$$D = \mu k_{\text{B}} T \tag{2.54}$$

where $\mu = -v_0/mg$ is the mobility of the particle. In the case of a sphere of radius R for small Reynolds number, Stokes law gives

$$\mu^{-1} = \gamma = 6\pi\eta R, \tag{2.55}$$

with η the dynamic viscosity of the fluid.

2.3.5 Generalizations of the Fokker-Planck equation

The Fokker-Planck equation deals with a first derivative in time t, and does not involve earlier times $t' < t$. It is linked to the fact that the Langevin equation describing the dynamics is *Markovian*, that is, the process is memoryless: the dynamics at time $t_2 > t_1$ only depends on the state of the system at times t_1, and not on previous times $t_0 < t_1$. In the reminder of the thermal bath case, the Markov property relies on the temporal decorrelation of the action of the fluid molecules.

When dealing with a Markov process, the general equation describing the temporal evolution of the probability density function is the *Master equation*. The Master equation is formally equivalent to the Chapman-Kolmogorov equation. It reads in one dimension

$$\frac{\partial P(x,t)}{\partial t} = \int \left[W(x|x')P(x',t) - W(x'|x)P(x,t)\right] \mathrm{d}x' \tag{2.56}$$

where $W(x_2|x_1)$ is the transition probability per unit time from x_1 to x_2, and might depend on the time. The Master equation can be understood as a gain-loss equation for the probability to be at position x.

In this form, the Master equation is not easy to deal with (for example the first moments of the distribution are not accessible through this formulation), and tremendous efforts were made to obtain developments in partial differential equations rather than in integro-differential equations. The best known is the Kramers-Moyal development [Moy49]: by writing

$$W(x_2|x_1) = W(x_1; x_2 - x_1) \tag{2.57}$$

where $r = x_2 - x_1$ is the size of the jump, and after performing a Taylor expansion of $W(x_1; r)$ in r, one formally obtains

$$\frac{\partial P(x,t)}{\partial t} = \sum_{n=1}^{\infty} \frac{(-1)^n}{n!} \frac{\partial^n}{\partial x^n}[a_n(x)P(x,t)] \tag{2.58}$$

where the $a_n(x)$ are the jump moments defined as

$$a_n(x) = \int_{-\infty}^{\infty} r^n W(x; r)\, \mathrm{d}r. \tag{2.59}$$

If the dynamics follows a Langevin equation one can show that the development stops after the two first terms, and one recovers the Fokker-Planck equation. However, the Kramers-Moyal development is not an expansion in powers of some small parameters. Van Kampen [Kam61] suggested a general development known as the system size expansion. If we note Ω the "size" of the system (its volume, or the number of atoms), the natural small parameter to consider is Ω^{-1}. Two characteristic scales emerge: the first one is determined by the size of the jumps and is an extensive scale, in the sense that it does depend of the global size of the system (for a system with N atoms, the fluctuations are roughly speaking of order $N^{1/2}$); the other one is the one on which the macroscopic properties of the system vary, and is therefore intensive. Formally, we write

$$W(x_2|x_1) = \Phi\left(\frac{x_1}{\Omega}; r\right) \tag{2.60}$$

and perform the expansion in powers of Ω^{-1}. In leading order, we recovers the Fokker-Planck equation.

If the evolution of the system is not Markovian, one cannot write a Master equation, and we must adopt a finer description. Considering for example a particle driven by an Ornstein-Uhlenbeck process, that is a process $v(t)$ following the Langevin equation

$$\dot{v} = -kv + \sqrt{2\mathcal{D}}\xi(t). \tag{2.61}$$

One speaks of a Rayleigh particle [Dri81]. The equation of motion being $\dot{x} = v$, in this case the joint density of probability $P(x, v, t)$ follows a Fokker-Planck equation:

$$\frac{\partial P}{\partial t} = -v\frac{\partial P}{\partial x} + k\frac{\partial}{\partial v}[vP] + \mathcal{D}\frac{\partial^2 P}{\partial v^2} \tag{2.62}$$

but we cannot write something similar to (2.43) involving only the marginal distribution $P(x, t)$. Concerning the motion equation in the general form

$$\dot{x} = f(x) + g(x)y(t) \tag{2.63}$$

where $y(t)$ is a complex noise and f, g smooth functions, a large work has been made to obtain different approximative expansions in the form of (2.43), using several techniques such as cumulant expansions [SSS86; Van74; Fox78] or path integral formulations [Wio+89].

2.4 Behaviour at the onset of stability: intermittency

Let us briefly return to the transition between a strange attractor and a point-like structure, that is a stable point. For a strange attractor at least one of the Lyapunov exponent is positive, while a stable point is characterized by a set of negative Lyapunov exponents. Nevertheless, when the dynamical system is driven by a stochastic process, as presented in the previous section, the Lyapunov exponents are then fluctuating quantities. Consider a one dimensional dynamical system with a fixed point and its unique Lyapunov exponent $\lambda(t)$. If the mean of $\lambda(t)$ is negative then the fixed point is stable in average, but positive fluctuations can lead to bursts of trajectories.

We present here a class of dynamical systems driven by a stochastic process, the driving process being either the result of a exterior sufficiently chaotic dynamical system or an ideal random process characterized by its density of probability. We focus on the evolution of the driven system near an attractor of the dynamics.

Generically, intermittency is a term given to the behaviour of a system which can stay in one state for a long duration (a laminar state), and have unpredictably jumps which drive it far away from this laminar state during short periods of times, before returning to a possibly different laminar state. The notion of intermittency was historically derived for discrete time dynamics, while the dynamical systems studied in this text all present continuous time. Though, it will not change the main results.

Note that while the intermittency behaviour of velocity fields in turbulent flows remains a fruitful topic of research – as it partly responsible in the breaking of scaling laws in the turbulent cascade –, it will play no part in this text. Indeed, we only consider intermittent behaviour of dynamical systems driven by turbulent flows, and not the possibly very complex structure of the flow itself.

2.4.1 Pomeau-Manneville intermittency

One of the first examples of an intermittent scheme was proposed by I. Pomeau and P. Manneville in [PM80]. Consider a deterministic system with one or many *quasi fixed* point, that is point around which the system is able to stay a long duration (see figure 2.6). The goal was to characterize the transition to turbulence as a cascade process, and more generally to give a framework of the transition towards chaotic regimes.

However, other physical systems are not described by a deterministic dynamical system, but rather present a dynamics driven by stochastic processes. Another type of intermittency was then introduced.

2.4.2 "On-off" intermittency

The "on-off" intermittency occurs typically for a system close to a weakly unstable fixed point and driven by a random process or a chaotic deterministic process. The main idea is that the rate of variation on the fixed point is function of the driving system. It was first introduced in [PST93; PHH94; HPH94], with the following generic example:

$$x_{n+1} = a\xi_n x_n(1 - x_n) \tag{2.64}$$

so that $r_n = a\xi_n$ is also a chaotic function of the time. The ξ_n are independent and uniformly distributed on the interval $[0, 1]$. We assume that the process which causes the intermittency is local, meaning that it is governed by the linear dynamics near the fixed point $x = 0$. The non-linear part only occurs as a re-injection mechanism back toward small values of x_n. It is then essential to sustain the dynamics, but does not seed nor produce the intermittent dynamics.

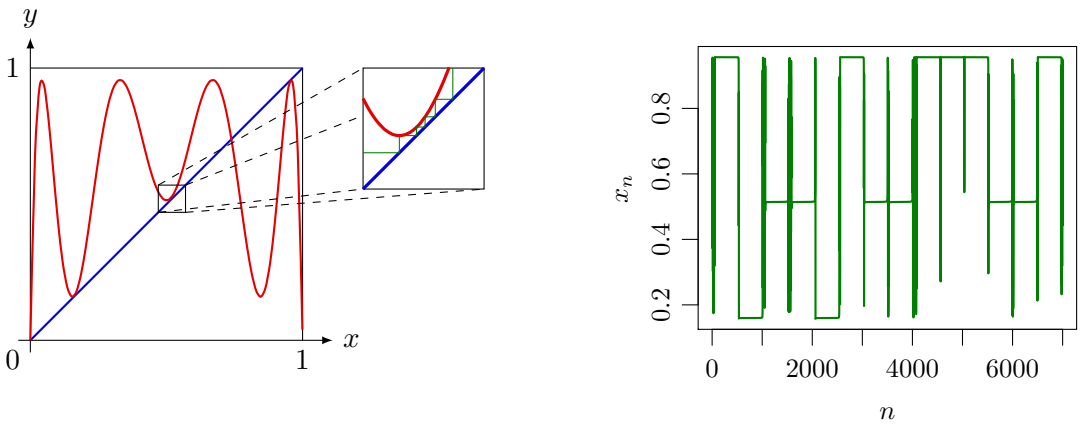

(a) Plot of $g(x)$ with respect to x. One can observe three quasi fixed points, and the zoom enhances the dynamics near to the second one.

(b) Plot of x_n with respect to the discrete time n, with $x_0 = 0.1$. The system undergoes transients between three laminar states.

Figure 2.6 – One typical example of a deterministic Pomeau-Manneville intermittency. The discrete-time dynamics reads $x_{n+1} = g(x_n)$ where g is the third iterated of the logistic application $f(x) = rx(1-x)$ with $r = 1 + \sqrt{8}$.

In the vicinity of this fixed point, one obtains $x_{n+1} = a\xi_n x_n$, leading to $x_n = a^n \left(\prod_{i=0}^{n} \xi_i\right) x_0$, so that the dynamics is linked to the asymptotic behaviour of the random product

$$P_n = a^n \prod_{i=0}^{n} \xi_i. \tag{2.65}$$

For large n one has $\ln P_n \sim n \langle \ln \xi \rangle$. As $\langle \ln x \rangle = \int_0^1 \mathrm{d}\xi \ln \xi = -1$, one obtains

$$P_n \sim \left(\frac{a}{\mathrm{e}}\right)^n. \tag{2.66}$$

The *onset* of the intermittency is then for $a_\mathrm{c} = \mathrm{e}$. For $a > a_\mathrm{c}$, the trajectories are on average exponentially unstable, but the dynamics still remains near the laminar state $x = 0$ for long duration. The figure 2.7a shows a typical trajectory for $a = 2.74 > \mathrm{e}$: the dynamics exhibits large bursts between laminar states in the vicinity of $x = 0$. The numerical simulations use a different map $x_{n+1} = f(x_n)$ than the one defined in (2.64) but with the same linear properties:

$$x_{n+1} = \begin{cases} a\xi_n x_n & \text{if } |x_n| \leq 0.25, \\ a\xi_n \dfrac{1 - x_n}{3} & \text{if } x_n > 0.25, \\ a\xi_n \dfrac{1 + x_n}{3} & \text{if } x_n < -0.25. \end{cases} \tag{2.67}$$

Such a mechanism is generic for a lot of physical systems, where a dynamical system near a bifurcation is driven by another chaotic system. A mechanism of on-off intermittency has been observed experimentally in various systems including electronic devices [Ham+94], gas discharge plasmas [Fen+98], electrohydrodynamic convection in nematics [JSB99] or spin-wave instabilities [RČB95]. Intermittency was also studied in the case of two coupled dynamical systems [YF86; FY86; Fuj+86].

Another characterization of the on-off intermittency is the distribution of the time spent in the laminar state. To proceed, it is easier to see the intermittency mechanism as a *random walk*.

2.4.3 Random walks formulation

For a typical dynamical system in the form

$$x_{n+1} = r_n x_n + \text{non-linear terms} \tag{2.68}$$

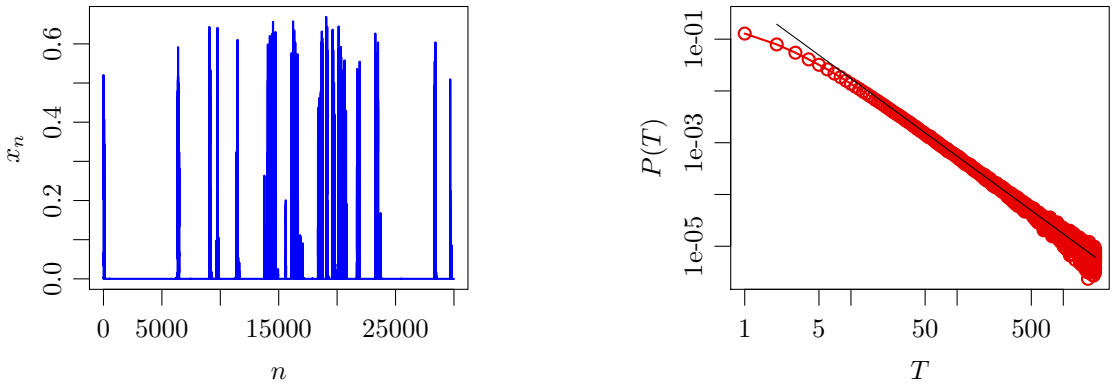

(a) Plot of x_n with respect to the discrete time n, with $x_0 = 0.1$. The laminar state is at $x = 0$, and the dynamics exhibits large bursts.

(b) Density of probability for the waiting times $P(T)$ with respect to T, in logarithmic scale. The black solid line shows a power law in $T^{-3/2}$.

Figure 2.7 – Example of stochastic driven intermittency. The discrete-time dynamics reads $x_{n+1} = f(x_n)$ with f defined in (2.67).

in the vicinity of the fixed point $x = 0$, the dynamics can be alternatively written as

$$y_{n+1} = y_n + z_n \tag{2.69}$$

where $y_n = \ln x_n$ and $z_n = \ln r_n$. The onset of the intermittency corresponds to the condition $\langle z_n \rangle = 0$, which gives for the system in (2.64) the same critical value $a_c = \mathrm{e}$. The intermittency then can be seen as a *non-biased* random walk. Such a description allows us to compute the asymptotic law for the waiting times for $a > a_c$, that is the density of probability $P(T)$ to stay during T below a given threshold. One obtains generically (see figure 2.7b)

$$P(T) \sim T^{-3/2}. \tag{2.70}$$

Note that while this law is general for on-off intermittency, it does not completely characterize it, as the Pomeau-Manneville intermittency also exhibits a $-3/2$ power law. One of the main difference, besides the fact that on-off intermittency is fundamentally a dynamic process while Pomeau-Manneville one is static, relies on the typical trajectories: in the Pomeau-Manneville scheme the intermittent signals exhibit bursts about either sides of the fixed point, which is not the case in on-off intermittency.

Below the onset of intermittency (for $a < a_c$), all the trajectories will go to $x = 0$ on average. In order to produce intermittency behaviour, one then needs a *re-injection process* that prevents the trajectories to collapse. Such a role can be played by an additive noise in the equations of motion. The effect of additive noise to produce intermittency behaviour even if the system collapses on average on the attractor was first studied in [PHH94].

2.5 Phenomenological stochastic models of particles dispersion

Both types of particles (tracers and inertial particles) can under certain conditions form complex dynamical structures in the phase space. We do not simulate the flow by a numerical resolution of Navier-Stokes equations. Instead, we use phenomenological models with a limited number of parameters to recreate the main properties of the dynamics, using stochastic terms and the tools introduced previously.

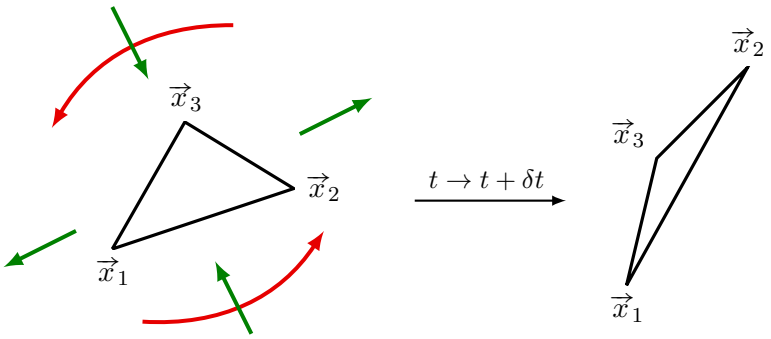

Figure 2.8 – Representation of the action of the matrix $\mathbf{A}$ defined for the model (2.71), in the case of three particles in a bidimensional flow. Two effects occur simultaneously: the triangle is globally rotated (red arrows) by the anti-symmetric part of $\mathbf{A}$, and in a given orthogonal basis one direction is stretched while the other perpendicular direction is contracted (green arrows) due to the symmetric part of $\mathbf{A}$. This last action tends to flatten the triangle.

2.5.1 Advected triangles

Direct numerical simulations of incompressible flows [PSC00] showed the possible existence of a self-similar regime for scales between the integral and the Kolmogorov ones. In consequence, we will mostly use a phenomenological model based on a *scale decomposition* method, first introduced in [SS95]. The turbulent velocity field is arbitrary divided in three contributions: velocities with small scales numbers, large waves numbers, and waves numbers comparable with the size of the cluster of points. The effect of large waves number velocities is just a global advection and does not affect the multipoint structure, whereas the contribution of small scales can be supposed independent for each point of the cluster. The remaining effect of the like-scale part of the velocity is coherent over the scale of the cluster and tends to flatten the set of points, consistently with the volume preservation. The typical model for the dynamics of N tracers is then

$$\frac{\mathrm{d}\vec{x}_i(t)}{\mathrm{d}t} = \mathbf{A}\,\vec{x}_i + R\,\vec{\xi}_i \tag{2.71}$$

where R is the radius of gyration of the cluster,

$$R^2 = \frac{1}{2N}\sum_{i,j}(\vec{x}_i - \vec{x}_j)^2\,, \tag{2.72}$$

which is a definition of its size, $\vec{\xi}_i$ are random, independent increments corresponding to the action of small-scale eddies acting independently on each point of the cluster, and $\mathbf{A}$ is the velocity gradient tensor (2.15), which is the resultant of the action of eddies of scale comparable to that of the cluster. As the flow is incompressible, this matrix is traceless. In homogeneous and isotropic turbulence, the global rotation of a set of points, just as its position in the space, is immaterial, so that one usually only consider the symmetric part of $\mathbf{A}$, noted $\mathbf{M}$. Thus, we suppose that $\mathbf{M}$ is a random, traceless and symmetric matrix.

During the dynamics each pair of points separates according to Richardson's law (2.5), so that the size of the cluster grows as the global structure ascends the spatial scales of the flow.

The phenomenological model for the random strain matrix $\mathbf{M}$ and the random increments $\vec{\xi}_i$ is described in [CP01; PW13]. The first possibility is to take Gaussian white noise increments, which reads explicitly

$$\mathbf{M} = \begin{pmatrix} a(t) & b(t) \\ b(t) & -a(t) \end{pmatrix} \quad \text{and} \quad \vec{\xi}_i = \begin{pmatrix} \eta_i^{(1)}(t) \\ \eta_i^{(2)}(t) \end{pmatrix} \tag{2.73}$$

where $a(t)$, $b(t)$ and $\eta_i^{(j)}$ are Gaussian white noises with statistics

$$\langle a(t)\rangle = \langle b(t)\rangle = \langle \eta_i^{(j)}\rangle = 0, \tag{2.74}$$

$$\langle a(t)a(t')\rangle = \langle b(t)b(t')\rangle = 2D_{\mathrm{s}}\delta(t-t'), \tag{2.75}$$

$$\langle \eta_k^{(i)}(t)\eta_\ell^{(j)}(t)\rangle = 2D_{\mathrm{b}}\delta_{ij}\delta_{k\ell}\delta(t-t'), \tag{2.76}$$

$$\langle a(t)b(t')\rangle = \langle a(t)\eta_i^{(j)}(t')\rangle = \langle b(t)\eta_i^{(j)}(t')\rangle = 0. \tag{2.77}$$

This model implicitly assumes that the eddies are uncorrelated in time. To take into account temporal correlations, we will introduce a modification of this model.

In the absence of the small scale eddies the triangles tend to be flattened (see figure 2.8), and the attractor is then the equator of the 2-sphere. Introduce $z = \cos\theta$ where θ is the latitude on the sphere, this parameter measures the flattening of the set, z being equal to zero for a flat triangle. The main goal is to obtain an evolution equation for $y = \ln z$ in the form

$$\dot{y} = F(t) \tag{2.78}$$

where the random process $F(t)$ depends only of the strain matrix $\mathbf{M}$ and has a negative mean, so that in the absence of the diffusion $\vec{\xi}_i$ all the trajectories will collapse on the equator on average.

2.5.2 Inertial particles

For simplicity reasons, we restrain ourselves to the one-dimensional case $d = 1$, so that only one Lyapunov exponent needs to be computed:

$$\begin{cases} \dot{x} = v\,, \\ \dot{v} = -\dfrac{1}{\tau_{\mathrm{S}}}[v - u(x,t)]. \end{cases} \tag{2.79}$$

As we are interested in the dynamics of the particles rather than in the evolution of the underlying fluid, we usually model the latter by a stochastic process whose statistics have a translational invariance both in time and space:

$$\langle u(x,t)\rangle = 0 \quad \text{and} \quad \langle u(x,t)u(x',t')\rangle = c(x-x',t-t')\,, \tag{2.80}$$

and we choose specifically the following form for $c(x-x',t-t')$, correlated in space but uncorrelated in time:

$$c(x-x',t-t') = A^2 \exp\left(-\frac{(x-x')^2}{\ell_{\mathrm{c}}^2}\right)\delta(t-t') \tag{2.81}$$

where ℓ_{c} is the correlation length of the fluid and A a constant. The dynamics of the inertial particles then becomes also a stochastic process. One can observe a *path coalescence* transition [WM03]: either the trajectories all collapse into a single one, resulting in the formation of a point-like dynamical structure, or either close trajectories exponentially separate on average and the resulting pattern seems to fill the whole space. The equation of motion for the separation δx of two close trajectories is

$$\delta\dot{x} = Z(t)\delta x \quad \text{where} \quad Z(t) = \frac{\partial v}{\partial x}(x,t). \tag{2.82}$$

The term $Z(t)$ is a local Lyapunov exponent. When its mean becomes negative, all the particles then cluster upon a single trajectory, and the attractor in physical space is a point-like structure. By writing $y = \ln \delta x$, which is a classical mapping used in dynamical systems , one obtains

$$\dot{y} = Z(t) \tag{2.83}$$

which is the motion equation of a random walk. Nevertheless, introducing an additive noise in the dynamical equations, representing the diffusion of the particles,

$$\dot{x} = v(x,t) + \sqrt{2\mathcal{D}}\,\xi(t), \tag{2.84}$$

as a consequence of a diffusion process due to local inhomogeneity of the flow at the scale of the particle, it gives the opportunity for the system to experiment large deviations from the collapsing trajectory [Wil+15], and thus to generate intermittency bursts.

2.6 Summary and outline of the manuscript

2.6.1 Differences and similarities between the two physical situations

We are interested in two very different physical situations: evolution of tracers structures (in two dimensions), and dynamics of inertial particles (in one dimension), both in turbulent flows. For the first one, action of like-scale eddies tends to flatten a triangle and results to a contraction of trajectories towards the equator of the shape sphere, only counterbalanced by a homogeneous diffusion in the physical space induced by small scales eddies. As for the inertial particles, the Stokes drag lead to a path coalescence of trajectories, which is that time counteracted by the diffusion of particles.

For both situations though, the description of the dynamics for two close trajectories in the inertial particles case – equation (2.83) –, or near the equator in the tracers case – equation (2.78), which characterizes the properties of the attractor, can be described by the same class of equations. A random walk formulation arises, derived originally for the intermittency process (2.69). Intermittency bursts can occur, even if the dynamics is totally contracting in the phase space, providing the presence of an additional noise for the equations of motion in the physical space. Large deviations generally lead to power-law distributions for the separation of trajectories, which is a signature of the fractal structures of the attractors.

The general equation

$$\dot{y} = \zeta(t), \tag{2.85}$$

where $\zeta(t)$ is a fluctuating quantity independent of y and with a *non-zero* mean, describes a *sedimentation process*. The power-law form for $P(\Delta x)$, the probability density function of the separation of trajectories, can be understood as follows. As the dynamics for $y = \ln \Delta x$ is described by a sedimentation equation, by analogy with the sedimentation process for Brownian particles studied in section 2.3.4 one can expect a exponential distribution for the distribution of y: $p(y) \sim \mathrm{e}^{\alpha y}$. As

$$p(y)\mathrm{d}y = P(\Delta x)\mathrm{d}(\Delta x) \tag{2.86}$$

one obtains

$$P(\Delta x) \sim \Delta x^{\alpha - 1}. \tag{2.87}$$

This mechanism breeds the fluctuation around the attractor, which can then be amplified by the unperturbed stochastic process, leading to power-law distributions. The coefficient α introduced in (2.87) is then equal to the correlation dimension D_2.

2.6.2 Organization of the text

The chapter 3 is devoted to the motion of three particles in a bidimensional turbulent flow. We present the shape space of a triangle as a 2-sphere, the Kendall sphere. The resolution of a totally uncorrelated eddies model [PW13] is briefly presented while we are mostly interested in the influence of the correlation time of the like-scale eddies on the dynamics. A Langevin equation for the evolution on sphere is obtained.

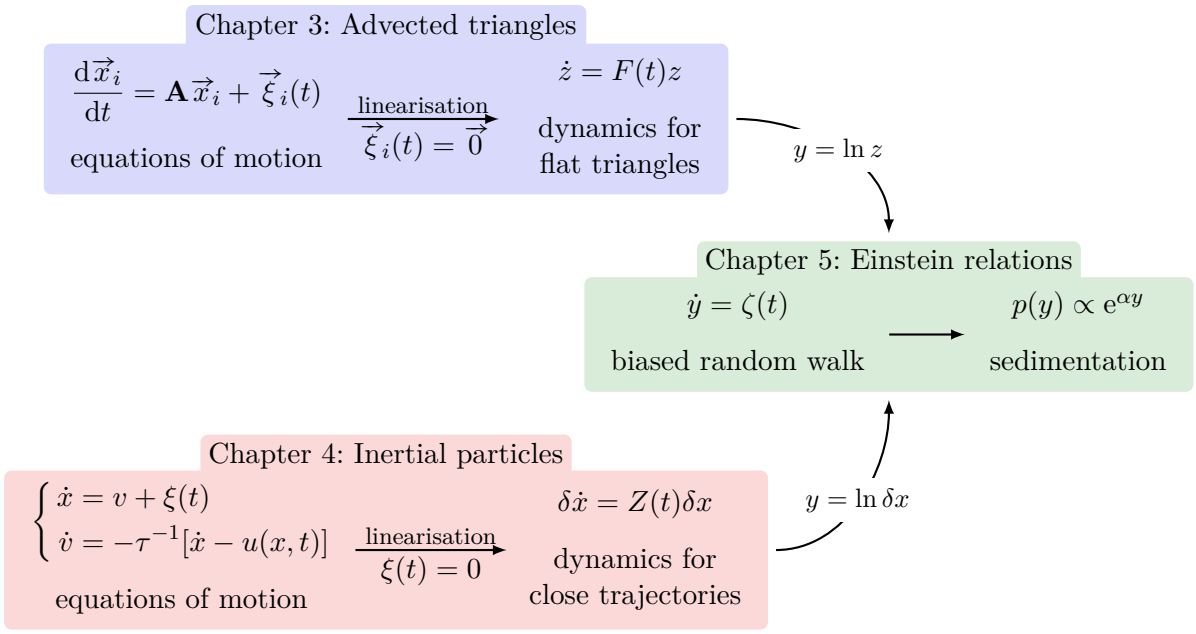

Figure 2.9 – Schematic view of the organization of the text.

In chapter 4 we study the phenomenological model (2.79) used to describe the motion of inertial particles in a turbulent flow. The complete resolution of the linearises motion for close trajectories is presented, and we show numerical evidence of a negative correlation dimension D_2. We compute numerically the evolution of D_2 as a function of the model parameters, and compare it with perturbative approaches.

Finally in chapter 5 we treat the general problem of the sedimentation process from a random walk. In particular, we obtain an implicit expression for the sedimentation coefficient α, using a large deviation approach. We establish a relation with the dynamics near the attractor obtained in the two previous chapters, and we finally present some perturbation tools in the case of a sedimentation process driven by weakly non-linear Langevin equations.

Chapter 3

Advected triangles in a bidimensional turbulent flow

Outline

We consider the evolution of three fluid particles advected by a bidimensional turbulent flow. We denote the positions of the particles during the temporal evolution by $\vec{x}_i(t)$ with $i \in \{1;2;3\}$. The equations of the dynamics are simply

$$\frac{\mathrm{d}\vec{x}_i}{\mathrm{d}t} = \vec{u}(\vec{x}_i(t), t) \tag{3.1}$$

where $\vec{u}(\vec{x}_i(t), t)$ is the Eulerian velocity field of the fluid.

We are interested in the dynamics of a triangle because it is the minimal cluster of points needed to span the space in two dimensions, and so it represents the simplest set to study in order to see geometrical effects, such as a change of topology or the clustering of points into a line. In homogeneous and isotropic turbulence, the absolute location of a structure is immaterial to the properties of the flow, just as its global orientation. Moreover, while the particles tend to separate during the dynamics, we assume the existence of a self-similar regime in which the dynamics does not depend on the global size of the triangles. It is then natural to introduce a phenomenological size-independent model for the dynamics of advected triangles in a turbulent flow.

In this chapter we first present the natural space to describe the shape of a triangle, which happens to be a sphere. Then, we determine the dynamics on this sphere for the phenomenological

model with white noise increments. Finally, we analyse the influence of time-correlated eddies on the changes in topological configuration of a triangle, and on the stationary distribution of the representative points in the shape space.

3.1 Shape of a triangle: the Kendall sphere

The general description of the *shape* of n points lying in a d-dimensional space is due to the mathematician D. G. Kendall [Ken89]. Initially, the goal was to determine if a set of 52 standing stones near Land's End, Cornwall, presented alignments which were "too nearly" collinear, thus indicating a deliberate planning. Kendall then wanted to obtain a quantitative process to measure the randomness of shapes distributions, and consequentially built his statistical theory of shape.

We will not present extensively the mathematical developments in this very large topic, and will rather concentrate on the simple case of three points in two dimensions. One already can have the intuition of the number of parameters needed to describe the shape of a triangle: because the shape of a triangle depends only on its angles, we need two parameters, namely two of the angles, as the sum of the three angles is equal to π rad. Nevertheless such a parametrisation is not very useful, and this is why Kendall introduced another one, which can be easily generalized to a larger set of points and higher dimensions. In this section we will first derive the natural parametrisation of the shape of a triangle, and show that the shape space is in this case the surface of a sphere. We want to describe the shape dynamics of a triangle advected by a random flow, so that the representative point will undergo a random motion on the sphere. As a typical example we will then recall in an elementary way the Brownian motion on a sphere of given radius R.

3.1.1 Shape space

To begin, we consider three point-like particles labelled by three vectors $\vec{x}_1$, $\vec{x}_2$ and $\vec{x}_3$. We always suppose that the three particles do not completely coincide. All the informations are contained in a 2×3 matrix

$$\mathbf{X} = \begin{pmatrix} \vec{x}_1 & \vec{x}_2 & \vec{x}_3 \end{pmatrix}. \tag{3.2}$$

which corresponds to six parameters. As the position of the centre of mass of the triplet, its size, and its global orientation in space do not affect its shape, we are left with two parameters, obtained after successive transformations of the matrix $\mathbf{X}$.

First, we perform the orthogonal transformation[(1)]

$$\begin{cases} \vec{u}_0 = \dfrac{1}{\sqrt{3}}(\vec{x}_1 + \vec{x}_2 + \vec{x}_3), \\ \vec{u}_1 = \dfrac{1}{\sqrt{2}}(-\vec{x}_1 + \vec{x}_2), \\ \vec{u}_2 = \dfrac{1}{\sqrt{6}}(-\vec{x}_1 - \vec{x}_2 + 2\vec{x}_3). \end{cases} \tag{3.3}$$

The vector $\vec{u}_0$, up to a constant, parametrizes the centre of the set of points, and thus is of no interest to the shape. We are then left with a 2×2 matrix:

$$\mathbf{u} = \begin{pmatrix} \vec{u}_1 & \vec{u}_2 \end{pmatrix} = \begin{pmatrix} u_{1,1} & u_{2,1} \\ u_{1,2} & u_{2,2} \end{pmatrix}. \tag{3.4}$$

[(1)] The transformation is orthogonal because we multiply on the right the matrix $\mathbf{X}$ by an orthogonal matrix.

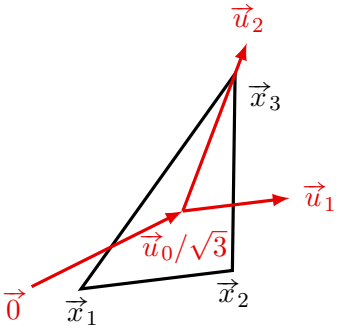

(a) Definition of $\vec{u}_0$, $\vec{u}_1$ and $\vec{u}_2$ after the orthogonal transformation (3.3). The vectors $\vec{u}_1$ and $\vec{u}_2$ lie in the pre-shape space.

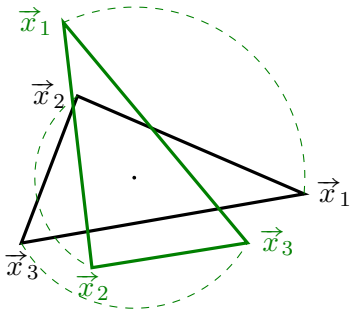

(b) Effect of the angle χ, going from $3\pi/2$ to $13\pi/6$, resulting in a global rotation around the centre of mass.

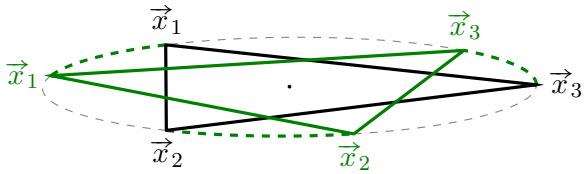

(c) Effect of the angle ϕ, going from 0 to $\pi/2$ at fixed $z \approx 0.38$. In gray, the ellipse in which the triangle is inscribed.

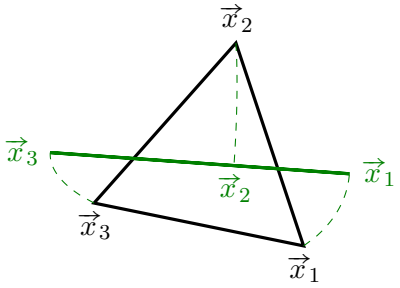

(d) Effect of the parameter z, going from 1 (equilateral triangle) to 0 (flat triangle) at fixed $\phi = \pi/4$.

Figure 3.1 – Definitions and effects of the parameters $\vec{u}_i$, χ, ϕ and z. Initial triangles are black, and the ones obtained after transformation are green.

The matrix $\mathbf{u}$ lives in the "pre shape" space of the triangle (see figure 3.1a). Then, we perform a *singular value decomposition* [WRR03] of the matrix $\mathbf{u}$, in the form of a product of three matrices:

$$\mathbf{u} = \mathbf{R}(\chi) \cdot \mathrm{diag}(\lambda_1, \lambda_2) \cdot \mathbf{R}(\phi/2) \tag{3.5}$$

where $\mathrm{diag}(\lambda_1, \lambda_2)$ a diagonal matrix, and

$$\mathbf{R}(\vartheta) = \begin{pmatrix} \cos\vartheta & -\sin\vartheta \\ \sin\vartheta & \cos\vartheta \end{pmatrix} \tag{3.6}$$

is a rotation matrix, of angle ϑ. By convention $\lambda_1 \leq |\lambda_2|$. As the matrix $\mathbf{R}(\chi)$ acts on the right, the angle $\chi \in [0, 2\pi]$ describes the global rotation of the triangle (see figure 3.1b). We then need an estimator of the size of the triangles. One can choose its area $\mathcal{A}$, but such a definition is spurious because a triangle can become flat without really reducing its size. One introduces the radius of gyration R of the triangle, defined as

$$R^2 = \frac{1}{6} \sum_{i=1}^{3} \sum_{j=1}^{3} |\vec{x}_i - \vec{x}_j|^2. \tag{3.7}$$

The parameters λ_1 and λ_2 are linked to the area and the radius of gyration via

$$R^2 = \vec{u}_1^2 + \vec{u}_2^2 = \mathrm{tr}(\mathbf{u} \cdot {}^T\mathbf{u}) = \lambda_1^2 + \lambda_2^2 \quad \text{and} \quad \mathcal{A} = \frac{\sqrt{3}}{2} \det(\mathbf{u}) = \frac{\sqrt{3}}{2} \lambda_1 \lambda_2. \tag{3.8}$$

We note $\zeta = \lambda_1 \lambda_2$. The last parameter we define must be independent of the size of the triangle; it is then natural to introduce

$$z = \frac{2\lambda_1 \lambda_2}{\lambda_1^2 + \lambda_2^2} \tag{3.9}$$

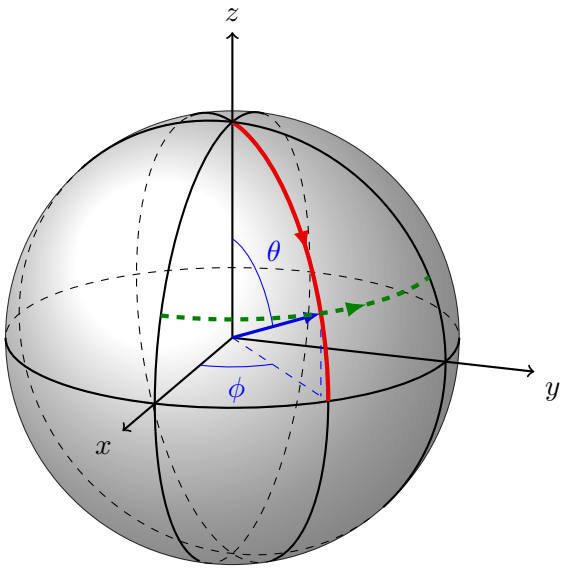

Figure 3.2 – The Kendall sphere. In red, the evolution described in figure 3.1c, with fixed z and ϕ going from 0 to π. In green dotted line, the evolution described in figure 3.1d, with fixed $\phi = \pi/4$ and z going from 1 to 0.

which represents the area of triangle compared to its size squared. One has $z \in [-1, 1]$ and $\phi \in [0, 2\pi]$, so that the representative point of the shape of the triangle lives on the surface of a sphere, and is labelled by its azimuthal angle ϕ and its polar angle θ, related to z by $z = \cos\theta$. The equilateral triangles are represented by the poles of the sphere, while the flat triangles of area equal to zero are located on the equator at $z = 0$ (see figure 3.1d). The two hemispheres represent the two possible topologies for a triangle: in the south (negative algebraic area) the vertices $\{1, 2, 3\}$ are labelled clockwise, while in the north (positive algebraic area) they are labelled counter-clockwise.

The signification of the angle ϕ is a little more difficult to see geometrically. For a given set of parameters λ_1, λ_2 and χ, the vertices of the triangle run through the same ellipse (see figure 3.1c). The transformation $\phi/2 \to \phi/2 + 2\pi/3$ (respectively $\phi/2 \to \phi/2 + 4\pi/3$) amounts to a cyclic permutation of the vertices $\vec{x}_i$: $(1, 2, 3) \to (2, 3, 1)$ (resp. $(1, 2, 3) \to (3, 1, 2)$). Typically, when a triangle is almost flat, the value of ϕ is related to the point where the angle is maximal, which is then the one about to cross the line formed by the two others. On the equator at $\phi = 0$ (resp. $\phi = 2\pi/3$, resp. $\phi = 4\pi/3$), $\vec{x}_1$ and $\vec{x}_2$ coincide (resp. $\vec{x}_2$ and $\vec{x}_3$, resp. $\vec{x}_3$ and $\vec{x}_1$).

The shape space is represented figure 3.2, and the effects of the transformations previously mentioned are shown in the form of paths on the Kendall sphere.

3.1.2 Diffusion on the surface of a sphere

Due to the action of the turbulent flow on the triangle, the motion of its shape representative point can be expected to be a random motion on the Kendall sphere. As the simplest random process for this geometry is the homogeneous Brownian motion, we will use it as a reference case. Consider a diffusion process on a sphere of radius R. In general the diffusion process may be inhomogeneous, and it may have anisotropic diffusion coefficients or drift terms.

The first way to characterize the spherical Brownian diffusion is to compute the drift velocities and the diffusion coefficients linked to the temporal evolution of z and ϕ. During a time δt the stochastic increments reads

$$\langle \delta z \rangle = v_z(z, \phi)\delta t, \quad \langle \delta z^2 \rangle = 2D_z(z, \phi)\delta t, \quad \langle \delta \phi \rangle = v_\phi(z, \phi)\delta t \quad \text{and} \quad \langle \delta \phi^2 \rangle = 2D_\phi(z, \phi)\delta t. \tag{3.10}$$

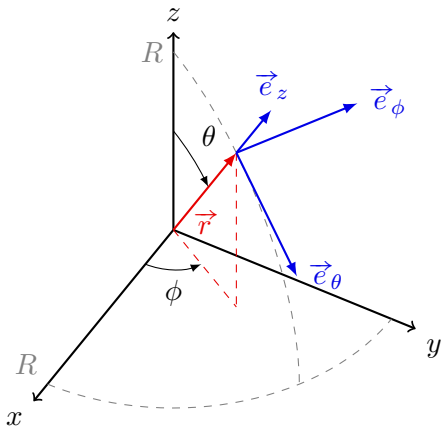

Figure 3.3 – Definition of the spherical coordinates. One has $\vec{r} = R\vec{e}_r = x\vec{e}_x + y\vec{e}_y + z\vec{e}_z$.

Consider a system of standard Cartesian coordinates in the three dimensional space: $(x, y, z) = (R\sin\theta\cos\phi, R\sin\theta\sin\phi, R\cos\theta)$. Due to the invariance with respect to the azimuthal angle ϕ, we can consider a point where $y = 0$ without loss of generality. Define an orthonormal basis $(\vec{e}_r, \vec{e}_\theta, \vec{e}_\phi)$ at the point $(\sin\theta, 0, \cos\theta)$:

$$\begin{aligned} \vec{e}_r &= (x, 0, z)/R, \\ \vec{e}_\theta &= (-z, 0, x)/R, \\ \vec{e}_\phi &= (0, 1, 0). \end{aligned} \tag{3.11}$$

The diffusion of a point $\vec{r} = R\vec{e}_r$ on the surface reads

$$\delta\vec{r} = \delta X\,\vec{e}_\theta + \delta Y\,\vec{e}_\phi + \delta Z\,\vec{e}_r. \tag{3.12}$$

The angular increments δX and δY are non-biased Brownian motion with statistics

$$\langle\delta X\rangle = \langle\delta Y\rangle = 0, \quad \langle\delta X\delta Y\rangle = 0 \quad \text{and} \quad \langle\delta X^2\rangle = \langle\delta Y^2\rangle = 2D\delta t, \tag{3.13}$$

and the increment δZ is determined from the constraint to stay on the sphere, implying $|\vec{r}+\delta\vec{r}| = R$, so that

$$\delta Z = -\frac{1}{2R}(\delta X^2 + \delta Y^2). \tag{3.14}$$

Using the expressions of $\delta\phi$ and δz in terms of δX, δY and δZ:

$$\begin{cases} \delta\phi = \dfrac{1}{\sqrt{R^2 - z^2}}\delta Y, \\ \delta z = -\sqrt{1 - \left(\dfrac{z}{R}\right)^2}\,\delta X - \dfrac{1}{2}\dfrac{z}{R^2}(\delta X^2 + \delta Y^2), \end{cases} \tag{3.15}$$

one obtains

$$\begin{cases} v_z = -\dfrac{2zD}{R^2}, \\ D_z = D\left(1 - \dfrac{z^2}{R^2}\right), \\ v_\phi = 0, \\ D_\phi = \dfrac{D}{R^2 - z^2}. \end{cases} \tag{3.16}$$

At this point a few remarks must be made. First, the motion is unbiased in ϕ, and the expression of D_ϕ is logically divergent at the poles. Secondly, due to the non-zero drift velocity v_z, the

geometry of the sphere acts as a restoring force directed towards the equator. In fact, near the equator the Langevin equation for $z(t)$ reduces to the Ornstein-Uhlenbeck process

$$\dot{z} = -kz + \sqrt{2D}\eta_z(t) \tag{3.17}$$

with η_z a standard white noise process and $k = 2D/R^2$.

Another more formal way to characterize a Brownian motion on a sphere is to consider the Laplace-Beltrami operator associated with the spherical geometry. The Fokker-Planck equation for the density of probability $P(\theta, \phi, t)$ is

$$\frac{\partial P}{\partial t} = D\hat{L}_{\theta,\phi}P(\theta, \phi, t) \tag{3.18}$$

where D is the diffusion coefficient, and $\hat{L}_{\theta,\phi}$ is the Laplace-Beltrami operator:

$$\hat{L}_{\theta,\phi} = \frac{1}{\sqrt{\det \mathbf{g}}}\frac{\partial}{\partial x_i}\left(\sqrt{\det \mathbf{g}}\, g^{ij}\frac{\partial}{\partial x_j}\right) \quad \text{with } x_1 = \theta \text{ and } x_2 = \phi. \tag{3.19}$$

Here

$$\mathbf{g} = R^2\begin{pmatrix}1 & 0\\ 0 & \sin^2\theta\end{pmatrix} \tag{3.20}$$

is the metric of the sphere of radius R, and g^{ij} must be understood as the matrix element of the inverse of $\mathbf{g}$: $g^{ij} = [\mathbf{g}^{-1}]_{ij}$. Explicitly, one obtains

$$\begin{aligned}\hat{L}_{\theta,\phi}P &= \frac{1}{R^2\sin\theta}\frac{\partial}{\partial\theta}\left(\sin\theta\frac{\partial P}{\partial\theta}\right) + \frac{1}{R^2\sin^2\theta}\frac{\partial^2 P}{\partial\phi^2}\\ &= \frac{\partial}{\partial z}\left[\frac{2z}{R^2}P\right] + \frac{\partial^2}{\partial z^2}\left[\left(1-\frac{z^2}{R^2}\right)P\right] + \frac{1}{(R^2-z^2)}\frac{\partial^2 P}{\partial\phi^2}\end{aligned} \tag{3.21}$$

as $z = R\cos\theta$, so that one recovers the expressions of the drift velocities and diffusion coefficients obtained in (3.16).

Starting with a set of points arbitrarily positioned on the sphere, one expects that after a suitable amount of time the repartition will be uniform. Solving the Fokker-Planck equation (3.18) in the stationary case $\partial_t P = 0$ for $P(z, \theta) = P(z)$ (as the diffusion is invariant in ϕ), one obtains the only normalizable solution

$$P(z) = \frac{1}{4\pi R^2}, \tag{3.22}$$

so that $\mathrm{d}P = R\mathrm{d}z\mathrm{d}\phi P(z) = \mathrm{d}z\mathrm{d}\phi/(4\pi R) = \text{cte.}$ and

$$\int_{-R}^{R}\mathrm{d}z\int_0^{2\pi}\mathrm{d}\phi\, P(z) = 1. \tag{3.23}$$

3.2 Advection by a turbulent flow

The phenomenological model presented here was first introduced in [SS95] as a simple description of the actions of the flow. The idea is to decompose arbitrarily the velocity field in three contributions acting on different scales. Velocities with large wave number – or conveniently speaking the large scales eddies – produce only a global advection of the triangle without changing its shape, and are therefore not taken into account by the model. We model the effect of the like-scale eddies as a strain matrix acting globally on the triangle, while the small-scale eddies are supposed to act independently on the three vertices.

We begin by introducing a simple stochastic model were all the eddies are temporally uncorrelated, and present the explicit computation obtained in [PW13] of the Langevin equation on the Kendall sphere.

3.2.1 Phenomenological model with white noise increments

The equation of dynamics for one vertex $\vec{x}_i$ of the triangle is

$$\frac{\mathrm{d}\vec{x}_i}{\mathrm{d}t} = \mathbf{M}\vec{x}_i + R\vec{\xi}_i(t) \tag{3.24}$$

where R is the radius of gyration of the triangle. The matrix $\mathbf{M}$ is a traceless, symmetric matrix in the form

$$\mathbf{M}(t) = \begin{pmatrix} a(t) & b(t) \\ b(t) & -a(t) \end{pmatrix}. \tag{3.25}$$

The matrix elements $a(t)$ and $b(t)$ are independent Gaussian white noise processes, with statistics

$$\langle a(t)\rangle = \langle b(t)\rangle = 0\,,\ \langle a^2(t)\rangle = \langle b^2(t)\rangle = 2D_\mathrm{s} \quad \text{and} \quad \langle a(t)b(t)\rangle = 0, \tag{3.26}$$

and the random vectors $\vec{\xi}_i(t)$ are also Gaussian white noise processes, independent of $a(t)$ and $b(t)$, with statistics

$$\langle \xi_i^{(k)}\rangle = 0 \quad \text{and} \quad \langle \xi_i^{(k)}\xi_j^{(\ell)}\rangle = 2D_\mathrm{d}\delta_{ij}\delta_{k\ell}\delta(t) \tag{3.27}$$

where $\xi_i^{(k)}$ is the k-component ($k \in \{1,2\}$) of $\vec{\xi}_i$.

The evolution equation (3.24) does not depend on the size of the triangle R, because it keeps the same form after dividing by the factor R. Thus, we are describing a self-similar regime which is independent of the size of the triangle.

The action of the matrix $\mathbf{M}$ consists in setting two orthogonal directions, one being contracting and the other dilating. It can be understood as follows: for a short duration of time, the increment of $\vec{x}_i$ reads

$$\begin{aligned} \vec{x}_i(t+\delta t) &= \vec{x}_i(t) + \delta\vec{x}_i(t) \\ &= \left[\mathbf{Id} + \begin{pmatrix} \delta a(t) & \delta b(t) \\ \delta b(t) & -\delta a(t) \end{pmatrix}\right]\vec{x}_i \\ &= \mathbf{B}(t)\,\vec{x}_i. \end{aligned} \tag{3.28}$$

The matrix $\mathbf{B}$ is symmetric, so it can be diagonalised in an orthogonal basis [Lan02]. In this basis, the matrix is symmetric and has as eigenvalues $\lambda_1 = 1 + \sqrt{\delta a^2 + \delta b^2}$ (dilatation) and $\lambda_2 = 1 - \sqrt{\delta a^2 + \delta b^2}$ (contraction).

The term $R\vec{x}_i$ acts as an homogeneous diffusion of the three vertices of the triangle in the physical space. As a consequence, we will refer to it later as the *diffusion term*, even if the strain matrix $\mathbf{M}$ also derives from a diffusion process.

3.2.2 Explicit resolution

In the case of the white noise model, the explicit Langevin equations describing the motion on the sphere were obtained in [PW13]. Being markovian in the physical space, the process is shown to be also markovian in the shape space. The strain term and the diffusion process feature two different motions. As for the spherical Brownian motion, it is sufficient to compute the drift velocities v_z and v_ϕ, and the diffusion coefficients D_z and D_ϕ as functions of z and ϕ.

For both the strain term and the diffusion process, the drift velocity for ϕ, v_ϕ, is found to be equal to zero. Explicitly, one obtains [PW13]

$$v_z^\mathrm{strain} = -8D_\mathrm{s}z^3\,,\ D_z^\mathrm{strain} = 4z^2(1-z^2)D_\mathrm{s} \quad \text{and} \quad D_\phi^\mathrm{strain} = \frac{4z^2}{(1-z^2)}D_\mathrm{s} \tag{3.29}$$

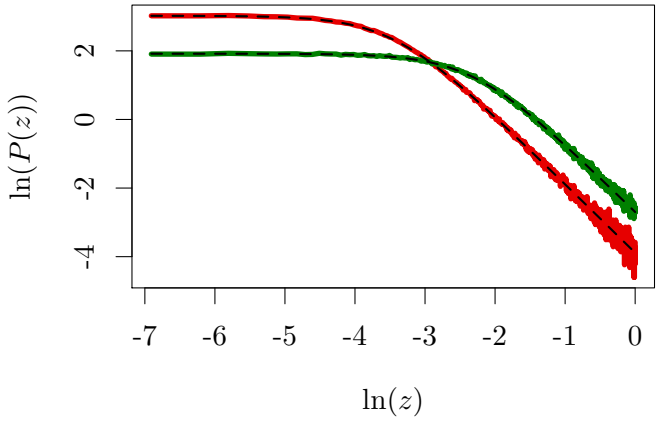

Figure 3.4 – Stationary density of probability $P(z)$, in logarithmic coordinates and for $z > 0$, obtained from numerical simulation of the white noise model (3.24). In green $\epsilon = 10^{-2}$, in red $\epsilon = 10^{-3}$. The analytic predictions for both values of ϵ are shown in dashed lines, and fit well with the data.

for the the action of the shear matrix, and

$$v_z^{\text{diff.}} = -8D_{\text{d}}z\,,\ D_z^{\text{diff.}} = 4(1-z^2)D_{\text{d}} \quad \text{and} \quad D_\phi^{\text{diff.}} = \frac{4}{(1-z^2)}D_{\text{d}} \tag{3.30}$$

for the diffusion process. Note that the expressions of the drift velocity and the diffusion coefficient obtained from the action only the shear matrix only differ to the corresponding coefficients derived from the action of the shear matrix by a factor z^2 , and that the drift velocities and diffusion coefficients obtained for the diffusion term are the same as the ones computed for the Brownian motion on a sphere (3.16), up to a factor 4. Thus, a homogeneous diffusion in the physical space leads to a homogeneous diffusion on the Kendall sphere. This result was not presented in the original work of Kendall [Ken77], but derived in later works using computer algebra packages [Ken+98] or through a quite abstract machinery [Ken84]. The factor 4 between the two set of coefficients comes from the actual radius of the Kendall sphere, which is formally set to 1/2 instead of 1.

To describe the joint effect of the strain and the diffusion, one simply adds the drift velocities and the diffusion coefficients, leading to the mix coefficients $v_z = v_z^{\text{strain}} + v_z^{\text{diff.}}$, $D_z = D_z^{\text{strain}} + D_z^{\text{diff.}}$ and $D_\phi = D_\phi^{\text{strain}} + D_\phi^{\text{diff.}}$. Consequentially, the Fokker-Planck equation for the density of probability $P(z, \phi, t)$ is

$$\frac{\partial P}{\partial t} = -\frac{\partial}{\partial z}[v_z P] + \frac{\partial^2}{\partial z^2}[D_z P] + \frac{\partial^2}{\partial \phi^2}[D_\phi P]. \tag{3.31}$$

This equation has a steady-state solution which does not depend on ϕ. The stationary marginal distribution for z, $P(z) = \int \mathrm{d}\phi P(z,\phi)/(2\pi)$, satisfies

$$2z(\epsilon + z^2)P + \frac{\partial}{\partial z}[(\epsilon + z^2)(1-z^2)P] = \text{cte} \tag{3.32}$$

where the constant must be taken equal to zero in order to find a normalizable solution. The parameter ε is defined as the ratio of diffusion coefficients:

$$\epsilon = \frac{D_{\text{d}}}{D_{\text{s}}}. \tag{3.33}$$

Thus, this parameter quantifies the relative importance of the two terms acting on the triangle, and the stationary distribution only depends on its value. From (3.32), one obtains

$$P(z) = \frac{\sqrt{\epsilon}}{2\arctan(1/\sqrt{\epsilon})}\,\frac{1}{\epsilon + z^2}, \tag{3.34}$$

where the multiplier normalize $P(z)$ on the interval $[-1, 1]$. The parameter ϵ defines two regions of different dynamics. For $z \ll \sqrt{\epsilon}$ the diffusion term dominates and the distribution tends to be flat, as the representative point is diffused homogeneously on the sphere. On the contrary for $z \gg \sqrt{\epsilon}$ the shear term is prominent, resulting in a global drift towards the equator and a power-law distribution for the density of probability in the form $P(z) \propto z^{-2}$. In the limit $\epsilon \to 0$ the density of probability (3.34) tends to a Dirac distribution, as all the trajectories will converge to the equator. The diffusion process resulting from the small-scale eddies prevents this collapsing.

The prediction (3.34) was checked numerically (see figure 3.4). We start from a set of equilateral triangles, so at one of the poles of the Kendall sphere. As the evolution is independent of the size R of the triangle, at each step we project the matrix $\mathbf{u}$ on the surface of the 3-sphere of radius $R = 1$. Moreover, in order to obtain a strict conservation of the area under the action of the strain matrix $\mathbf{M}$, the approximate evolution equation $\vec{x}_i(t + \delta t) = (\mathbf{Id} + \delta\mathbf{M})\vec{x}_i(t)$ is replaced by

$$\vec{x}_i(t + \delta t) = \exp(\delta\mathbf{M})\vec{x}_i(t). \tag{3.35}$$

As $\det(\exp(\delta\mathbf{M})) = \exp(\mathrm{tr}(\delta\mathbf{M})) = 1$, the area is conserved by the strain term.

The model studied in this section only involves uncorrelated eddies, because the increments of the strain matrix $\mathbf{M}$ and the diffusion process $R\vec{\xi}_i(t)$ are all Gaussian white noise processes, with a correlation time formally equal to zero. It is natural to wonder how the dynamics is affected if we introduce finite correlation times, related to the turnover times for the corresponding eddies. In particular, one can expect the correlation time $\tau(R)$ for an eddy of size R in the inertial regime to be determined by the Kolmogorov scaling:

$$\tau(R) = \epsilon^{-1/3} R^{2/3}, \tag{3.36}$$

where ϵ is the rate of energy dissipation. As the descriptions in the following sections are made for a scale invariant model, we implicitly assume that during the typical time to reach stationary dynamics for the model, the size of the triangle does not appreciably change due to the Richardson diffusion.

First we examine the effect of correlated small-scale eddies on the rate of topological changes, then we consider the influence of a finite correlation time for the strain matrix on the stationary distribution on the surface of the sphere.

3.3 Statistics of crossing

It is of interest to consider the topological changes induced by the flow, as it is related to the mixing properties of the fluid. The mixing in fluid flows is facilitated by the stretching and folding of material lines, which amplifies concentration gradients and allows diffusion effects to occur. A topological change is linked to a change of sign of the algebraic area of the triangle, resulting to a crossing of the equator of the Kendall sphere. The strain matrix conserves the area, so its action on the triangle cannot make the representative point on the Kendall sphere cross the equator. Nevertheless under this term the dynamics make the representative point converge towards the equator, where the diffusion term $\vec{\xi}_i(t)$ is prominent. In this section, we will then consider only the independent diffusion of the vertices in the physical space, and not the influence of the strain matrix. The equation of motion for the vertices $\vec{x}_i$ is then

$$\frac{\mathrm{d}\vec{x}_i(t)}{\mathrm{d}t} = R\vec{\xi}_i(t) \tag{3.37}$$

where the statistics of the stochastic vectors $\vec{\xi}_i(t)$ are given by (3.27).

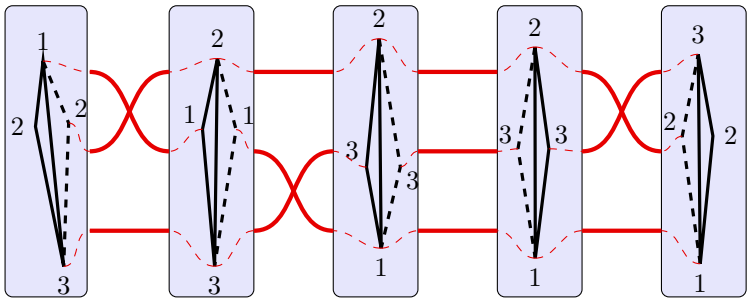

Figure 3.5 – Braids of topological changes of the triangle. In this typical case the word describing the topological changes is 21332.

3.3.1 Braids

Singularities of the shape of the triangles arise when the three points are collinear. These singularities divide into three classes, according to which one of the three vertices is in the middle position. One then can divide the equator in three equal zones, $[0, \pi/3]$, $[\pi/3, 2\pi/3]$ and $[2\pi/3, 4\pi/3]$, corresponding respectively to a passage of $\vec{x}_2$, $\vec{x}_3$ and $\vec{x}_1$. Thus, we label a crossing of the equator by 1, 2, or 3, depending on which vertices crosses the line formed by the two others. A list of the labels of the crossings is sufficient to define the topology of the particle trajectories. Such a list can take the form of a "word" from a three-number alphabet $\{1, 2, 3\}$, such as 11232111321. If a particle, say 1, cross the line dividing 2 and 3 and then immediately takes it back again, then the topology remains the same. This implies that our word can be "pruned" by deleting repeated letters. The previous example 11232111321 then becomes 2321321 and still gives the same information about the topological changes. The topology of the trajectory is consequentially described by a *braid* with three strands. The singularities where one point crosses the line dividing the other are associated with the generators of the braid group B_3 [TF06].

In the absence of the shear term, the coupled Langevin equations for the variables z and ϕ are

$$\dot{z} = -8D_{\mathrm{d}} z + 2\sqrt{2(1-z^2)D_{\mathrm{d}}}\,\eta_z(t) \quad \text{and} \quad \dot{\phi} = 2\sqrt{\frac{2D_{\mathrm{d}}}{1-z^2}}\,\eta_\phi(t)\,, \tag{3.38}$$

where $\eta_z(t)$ and $\eta_\phi(t)$ are two independent Gaussian white noise processes. Consider the equation on $z(t)$, as the motion for $\phi(t)$ is a simple diffusion. Close to the equator ($|z| \ll 1$), one can neglect the z-dependence of D_z and one obtains

$$\dot{z} = -kz + \sqrt{2D_{\text{eff.}}}\,\eta_z(t) \quad \text{with} \quad k = 2D_{\mathrm{d}} \quad \text{and} \quad D_{\text{eff.}} = 4D_{\mathrm{d}}. \tag{3.39}$$

Due to the presence of the non-differentiable term $\eta_z(t)$, the average number of crossing per unit of time diverges. Explicitly, let $\Pi(\Delta t)$ the steady-state probability for the area of the triangle to change between t and $t + \Delta t$ when t is sufficiently large, so that the process is stationary. Let

$$\varpi(\Delta t) = \frac{\Pi(\Delta t)}{\Delta t}\,. \tag{3.40}$$

The average number of crossings occurring per unit of time is then defined as the limit of $\varpi(\Delta t)$ when Δt tends to zero. This limit does not exists in the case of the process defined in (3.39), and one has $\varpi(\Delta t) \propto \Delta t^{-1/2}$ for small Δt. Note that when performing numerical simulations, a natural cut-off is induced by the discrete-time dynamics needed in the simulations. Nevertheless one needs to introduce a more realistic model where at least the limit $\lim_{\Delta t \to 0} \varpi(\Delta t)$ exists, which consists in considering a finite correlation time for the small scale eddies.

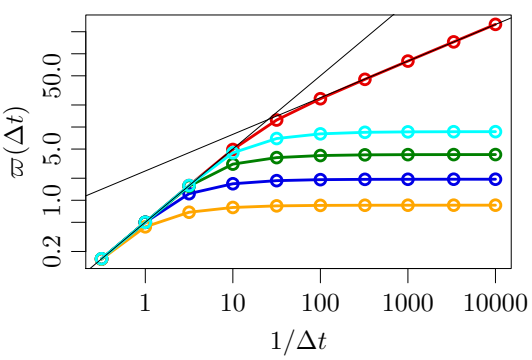

(a) Plot of $\varpi(\Delta t)$ with respect to Δt, in the case of the white noise process (3.39) (red), and for a time-correlated process (from top to the bottom: $\tau = 10^{-3/2}$, 10^{-1}, $10^{-1/2}$, 1; $c\tau^2$ is fixed to 1).

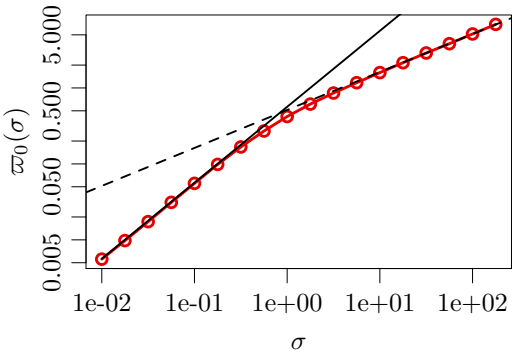

(b) Plot of $\varpi_0(\sigma)$ as a function of σ in logarithmic coordinates. At small σ the prediction (3.55), $\varpi_0(\sigma) = \sigma/\sqrt{\pi}$, is plotted (black line). At large σ one observes a regime where $\varpi_0 \propto \sqrt{\sigma}$.

Figure 3.6 – Statistics of crossing for triangles driven by time-correlated eddies, for which the average number of crossings per unit of time is defined. **(a)** comparison with the white noise model, **(b)** dependence of ϖ_0 with the dimensionless parameter σ.

3.3.2 Time-correlated small-scales eddies

We introduce a correlation-time for the processes of diffusion $\vec{\xi}_i(t)$, which can be seen as the turnover time of the small-scale eddies. The simplest time-correlated random process a the velocity field is the *Ornstein-Uhlenbeck process* [Van92; Gar+85] defined by the Langevin equation

$$\dot{v} = -\frac{v - v_0}{\tau} + \sqrt{c}\,\eta(t) \tag{3.41}$$

where v_0 is the mean drift, τ the correlation time, c a constant and as usual $\eta(t)$ a Gaussian white noise. The density of probability $P(y, z)$ for the variable v satisfies a Fokker-Planck equation:

$$\frac{\partial P}{\partial t} = -\frac{\partial}{\partial v}[(v - v_0)] + \frac{c}{2}\frac{\partial^2 P}{\partial v^2}. \tag{3.42}$$

As the Langevin equation is linear, the Ornstein-Uhlenbeck process is Gaussian. Its transition probability $P(v_2, t_2|v_1, t_1)$ reads

$$P(v_2, t_2|v_1, t_1) = \frac{1}{\sqrt{\pi c\tau(1 - \mathrm{e}^{-2t/\tau})}} \exp\left(-\frac{(v_2 - v_0 - (v_1 - v_0)\,\mathrm{e}^{-t/\tau})^2}{c\tau(1 - \mathrm{e}^{-2t/\tau})}\right), \tag{3.43}$$

and its steady-state density of probability $P(v)$ reads

$$P(v) = \frac{1}{\sqrt{\pi c\tau}} \exp\left(-\frac{(v - v_0)^2}{c\tau}\right). \tag{3.44}$$

In the limit $\tau \to 0$ with the coefficient $c\tau^2$ fixed, the correlation time tends to zero and the Ornstein-Uhlenbeck process tends to a Gaussian white noise process: $v(t) \to \sqrt{2D}\eta(t)$ with $2D = c\tau^2$. Such a process is the prototype of *coloured noise processes*, in contrast with the Gaussian white noise process which has a flat power density spectrum.

As a more realistic model for the homogeneous diffusion in the physical space, we suppose that the vertices of the triangles are driven by an Ornstein-Uhlenbeck process. For simplicity we set $R = 1$, so that one has

$$\frac{\mathrm{d}\vec{x}_i}{\mathrm{d}t} = \vec{\xi}_i(t) \tag{3.45}$$

with

$$\frac{\mathrm{d}\vec{\xi}}{\mathrm{d}t} = -\frac{\vec{\xi}_i}{\tau} + \sqrt{c}\vec{\eta}_i\,, \tag{3.46}$$

where the $\vec{\eta}_i$ are uncorrelated Gaussian white noise processes. It is straightforward to show[(2)] that such a process for the vertices $\vec{x}_i$ leads to a similar process for the matrix elements of $\mathbf{u}$ defined in (3.4):

$$\begin{cases} \dfrac{\mathrm{d}u_{ij}}{\mathrm{d}t} = y_{ij}\,, \\ \dfrac{\mathrm{d}y_{ij}}{\mathrm{d}t} = -\dfrac{y_{ij}}{\tau} + \sqrt{c}\,\eta_{ij}\,, \end{cases} \tag{3.47}$$

where the statistics of the Gaussian white noises $\eta_{ij}(t)$ are given by:

$$\langle \eta_{ij}(t)\rangle = 0 \qquad \text{and} \qquad \langle \eta_{ij}(t)\eta_{k\ell}(0)\rangle = \delta_{ik}\delta_{j\ell}\delta(t)\,. \tag{3.48}$$

With this regularized process, the ratio $\varpi(\Delta t)/\Delta t$ tends to a finite value when Δt tends to 0 (see figure 3.6a).

To proceed, we first determine the relevant dimensionless parameters of the dynamics. Define $\theta = t/\tau$, $\omega_{ij} = \tau y_{ij}$ and $\xi(\theta(t)) = \sqrt{\tau}\eta(t)$, so that

$$\begin{cases} \dfrac{\mathrm{d}u_{ij}}{\mathrm{d}\theta} = \omega_{ij} \\ \dfrac{\mathrm{d}\omega_{ij}}{\mathrm{d}\theta} = -\omega_{ij} + \sigma\,\xi_{ij}(\theta) \end{cases} \tag{3.49}$$

with the following statistics for $\xi_{ij}(\theta)$:

$$\langle \xi_{ij}(\theta)\rangle = 0 \qquad \text{and} \qquad \langle \xi_{ij}(\theta)\xi_{kl}(0)\rangle = \delta_{ik}\delta_{j\ell}\delta(\theta)\,. \tag{3.50}$$

and the dimensionless parameter

$$\sigma^2 = c\tau^3\,. \tag{3.51}$$

All the dynamics of the evolution is linked to this parameter. In particular, the limit for a white noise process, $\tau \to 0$ and $c\tau^2$ fixed, corresponds to the limit $\sigma \to 0$. We define

$$\varpi_0 = \lim_{\Delta t \to 0} \frac{\Pi(\Delta t)}{\Delta t/\tau} \tag{3.52}$$

which is a dimensionless function of σ. We computed numerically the evolution of $\varpi_0(\sigma)$ with respect to σ (see figure 3.6b). One observes two different regimes: for small values of σ one has $\varpi_0(\sigma) \propto \sigma$, while for large values of σ one obtains a different power-law, $\varpi_0(\sigma) \propto \sqrt{\sigma}$.

As seen previously, a Brownian motion in the physical space is associated with a Brownian motion on the Kendall sphere. It is then tempting to say that an Ornstein-Uhlenbeck process in the physical space leads to an Ornstein-Uhlenbeck process on the Kendall sphere, but it is not that simple, mostly because a spherical Ornstein-Uhlenbeck is not well defined (see for example [WP11]). As a consequence, it is quite challenging to describe exactly the dynamics resulting from the time-correlated motion. Yet, one can still explain the power-law dependence of ϖ_0 in σ for small values of σ. In this limited regime, the Ornstein-Uhlenbeck process is close to a Gaussian white noise, so it seems reasonable to estimate the dynamics near the equator from (3.39) by writing

$$\begin{cases} \dot{z} = -kz + 2y(t) \\ \dot{y} = -y/\tau + \sqrt{c}\,\eta(t) \end{cases} \tag{3.53}$$

with $k = 2D_\mathrm{d}$, $c\tau^2 = 2D_\mathrm{d}$ and $\eta(t)$ a Gaussian white noise. The equations describe the motion of an harmonic oscillator driven by an Ornstein-Uhlenbeck process. As the dynamics is Gaussian,

[(2)] This is due to the orthogonality of the transformation (3.3).

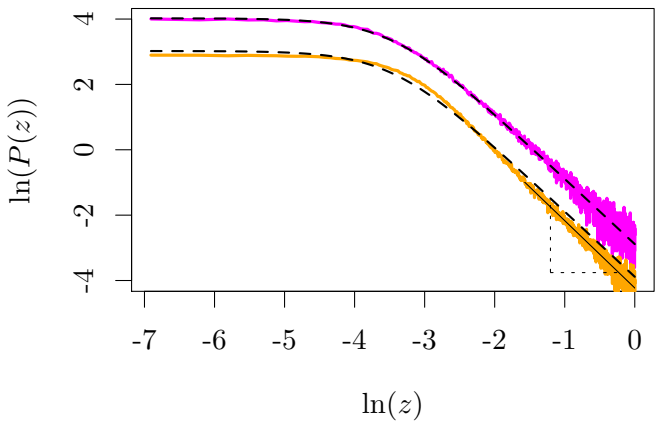

Figure 3.7 – Stationary density of probability $P(z)$, in logarithmic coordinates and for $z > 0$, obtained from numerical simulation of the coloured noise model (3.56). From both simulations $\epsilon = 10^{-3}$. In magenta $\sigma^2 = 0.01$, in orange $\sigma^2 = 0.5$ with a linear regression in black lines for large z of slope -2. The first plot is vertically translated for clarity. The analytic prediction for the white noise model is shown in dashed lines, and still fits well for $\sigma^2 = 0.01$. The regime of $z \gg \sqrt{\epsilon}$ exhibits a power-law dependence in the form $P(z) \propto z^{-2}$, for both values of σ.

one can explicitly compute the average number of crossings per unit of time. One obtains after a long but straightforward calculation

$$\lim_{\Delta t \to 0} \frac{\Pi(\Delta t)}{\Delta t} = \sqrt{\frac{k}{\pi \tau}} \tag{3.54}$$

so that for $\sigma \ll 1$

$$\varpi_0(\sigma) = \frac{\sigma}{\sqrt{\pi}}. \tag{3.55}$$

This prediction was compared with the numerical results, see figure 3.6b, and seems to correctly describe the evolution of ϖ_0 with σ in the limit $\sigma \to 0$.

3.4 Influence of temporal correlation of like-scale eddies

In this section we concentrate on the action of the strain matrix $\mathbf{M}$. Without the diffusive term all the trajectories on the sphere will converge towards the equator without crossing it, because the algebraic area is conserved through the evolution. The action of the small-scale eddies will prevent the collapsing of all the particles to the equator of the Kendall sphere ($z = 0$).

3.4.1 Model definition and qualitative results

We suppose that the eddies of scale comparable to that of the triangle have a finite correlation time, and consequentially introduce a model of correlated noise for the strain matrix. We have in the physical space

$$\begin{cases} \dfrac{\mathrm{d}\vec{x}_i}{\mathrm{d}t} = \mathbf{M} \cdot \vec{x}_i(t) \\ \dfrac{\mathrm{d}\mathbf{M}}{\mathrm{d}t} = -\dfrac{\mathbf{M}}{\tau} + \sqrt{c}\,\boldsymbol{\eta} \end{cases} \tag{3.56}$$

where $\boldsymbol{\eta}$ is a symmetric traceless matrix of Gaussian white noises coefficients, characterized by the following statistics

$$\langle \eta_{ij} \rangle = 0 \quad \text{and} \quad \langle \eta_{ij}(0)\eta_{k\ell}(t) \rangle = (\delta_{ik}\delta_{j\ell} + \delta_{i\ell}\delta_{jk} - \delta_{ij}\delta_{k\ell})\delta(t). \tag{3.57}$$

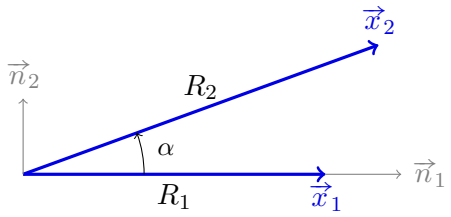

Figure 3.8 – Notation for the triangle. For simplicity we set $\vec{x}_3$ to $\vec{0}$.

The parameter τ is the correlation time of the Ornstein-Uhlenbeck process. We define the parameter ϵ, which compares the strain and diffusive terms, by the relation

$$\epsilon \overset{\text{def.}}{=} \frac{2D_\text{b}}{c\tau^2}. \tag{3.58}$$

If $\tau \to 0$ with $D_\text{s} \overset{\text{def.}}{=} c\tau^2$ fixed, $\mathbf{M}$ evolves into a Gaussian white noise process, and the model defines above tends to the previous model. In this case, the parameter ϵ is equal to the one defined in (3.33), but in general it will quantify the size of the influence zone of each term. The dimensionless parameter which quantifies the gap between the white noise and the coloured noise model is introduced as in the previous section, but this time for the strain term,

$$\sigma^2 = c\tau^3. \tag{3.59}$$

As expected, the limit

$$\tau \to 0\,, \quad D_\text{d} = \text{cte} \quad \text{and} \quad c\tau^2 = \text{cte} \tag{3.60}$$

corresponds in terms of the dimensionless variables to the limit

$$\sigma \to 0 \qquad \text{and} \qquad \epsilon = \text{cte}. \tag{3.61}$$

Two densities of probability obtained from this coloured noise model are shown figure 3.7. In the zone of influence of the shear term, for $z \gg \sqrt{\epsilon}$, one still observe a power-law dependence of $P(z)$ in z: $P(z) \propto z^\alpha$. Surprisingly, the exponent α, equal to -2 in the case of a white noise process, seems to not depend on the value of σ. While the transition zone for $z \sim \sqrt{\varepsilon}$ is not well described by the density of probability (3.34), the behaviour at large z remains unchanged.

3.4.2 Dynamics near the equator

We consider flat triangles, that is triangles with z small in absolute value. For such triangles it exists at least one very acute angle. Up to a change of the labels of the vertices, one obtains generically a situation as shown figure 3.8, where without a loss of generality $\vec{x}_3 = \vec{0}$ and the $\vec{n}_i$ are orthogonal vectors. We note α the angle between $\vec{x}_1$ and $\vec{x}_2$, and we suppose $|\alpha| \ll 1$. In this configuration, we have

$$\begin{cases} \vec{x}_1 = R_1 \vec{n}_1, \\ \vec{x}_2 = R_2(\vec{n}_1 + \alpha \vec{n}_2) + \mathcal{O}(\alpha^2). \end{cases} \tag{3.62}$$

The evolutions of $\vec{x}_1$ and $\vec{x}_2$ are given by

$$\frac{\mathrm{d}\vec{x}_i}{\mathrm{d}t} = \mathbf{M}\vec{x}_i \tag{3.63}$$

which leads to

$$\begin{cases} \dot{R}_1 \vec{n}_1 + R_1 \dot{\vec{n}}_1 = R_1 \mathbf{M} \vec{x}_1, \\ \dot{R}_2(\vec{n}_1 + \alpha \vec{n}_2) + R_2(\dot{\vec{n}}_1 + \dot{\alpha}\vec{x}_2 + \alpha \dot{\vec{x}}_2) = R_2(\mathbf{M}\vec{n}_1 + \alpha \mathbf{M}\vec{n}_2). \end{cases} \tag{3.64}$$

Let

$$F_{ij} = \vec{n}_i \cdot \mathbf{M}\vec{n}_j \tag{3.65}$$

the element of matrix of $\mathbf{M}$ in the basis $(\vec{n}_1, \vec{n}_2)$. The vectors $\vec{n}_i$ are orthogonal, so that one has

$$\vec{n}_1\dot{\vec{n}}_1 = \vec{n}_2\dot{\vec{n}}_2 = 0 \quad \text{and} \quad \vec{n}_1\dot{\vec{n}}_2 + \vec{n}_2\dot{\vec{n}}_1 = 0. \tag{3.66}$$

After multiplying (3.64) by the vectors $\vec{n}_i$, one gets eventually four equations:

$$\frac{\dot{R}_1}{R_1} = \frac{\dot{R}_2}{R_2} = F_{11} + \mathcal{O}(\alpha)\,, \quad \vec{n}_2\dot{\vec{n}}_1 = F_{21} \tag{3.67}$$

and

$$\dot{\alpha} = \alpha(t)y_1(t) + \mathcal{O}(\alpha) \quad \text{where} \quad y_1(t) = F_{22} - F_{11} \tag{3.68}$$

In order to close the equations of motion, we need to compute the temporal evolution of the function $y_1(t)$. In the orthogonal basis $(\vec{n}_1, \vec{n}_2)$ the matrix $\mathbf{M}$ remains symmetric and traceless, so that $F_{22} = -F_{11}$ and $F_{12} = F_{21}$. We have[3]

$$\dot{F}_{22} = \dot{n}_2\mathbf{M}n_2 - \omega F_{22} + n_2\mathbf{M}\dot{n}_2 + \sqrt{c}\, n_2\boldsymbol{\eta}n_2 \tag{3.69}$$

where $\omega = \tau^{-1}$, so that

$$\dot{y}_1 = -\omega y_1 + 2\dot{n}_2\mathbf{M}n_2 - 2\dot{n}_1\mathbf{M}n_1 + 2\sqrt{c}\, n_2\boldsymbol{\eta}n_2 \tag{3.70}$$

At this point we use the relations $F_{21} = n_2\dot{n}_1 = -n_1\dot{n}_2$ to obtain

$$\dot{n}_1 = F_{21}n_2 \quad \text{and} \quad \dot{n}_2 = -F_{21}n_1 \tag{3.71}$$

and finally

$$\dot{y}_1 = -\omega y_1 - 4F_{21} + 2\sqrt{c}\, n_2\boldsymbol{\eta}n_2 \tag{3.72}$$

Let $y_2 = F_{21}$. We have

$$\dot{F}_{21} = -\omega F_{21} + \dot{n}_2\mathbf{M}n_2 + n_2\mathbf{M}\dot{n}_1 + n_2\boldsymbol{\eta}n_1 \tag{3.73}$$

so that

$$\dot{y}_2 = -\omega y_2 + F_{21}(F_{22} - F_{11}) + \sqrt{c}\, n_2\boldsymbol{\eta}n_1\,. \tag{3.74}$$

The factor $n_i\boldsymbol{\eta}n_j$ is the expression of the (i,j) coefficient of the matrix $\boldsymbol{\eta}$ in the basis $(\vec{n}_1, \vec{n}_2)$. In this basis $\boldsymbol{\eta}$ remains a stochastic strain matrix, so that we finally get the two coupled Langevin equations

$$\begin{cases} \dot{y}_1 = -\omega y_1 - 4y_2^2 + 2\sqrt{c}\,\eta_1 \\ \dot{y}_2 = -\omega y_2 + y_1 y_2 + \sqrt{c}\,\eta_2 \end{cases} \tag{3.75}$$

where η_1 and η_2 are uncorrelated Gaussian white noises :

$$\langle \eta_i \rangle = 0 \quad \text{and} \quad \langle \eta_i(t)\eta_j(0)\rangle = \delta_{ij}\delta(t). \tag{3.76}$$

We have to make explicit the relation between α and z. With the notation of the section 3.1.1, one has

$$R^2 = R_1^2 + R_2^2 \quad \text{and} \quad \xi = \frac{1}{\sqrt{3}} R_1 R_2\, \alpha + \mathcal{O}(\alpha^2) \tag{3.77}$$

so that

$$z = \frac{1}{\sqrt{3}} \frac{R_1 R_2}{R_1^2 + R_2^2}\alpha. \tag{3.78}$$

[3] The arrows above the vectors are omitted.

Thus, z is the product between α and a function which only depends on the ratio R_1/R_2: $z = g(R_1/R_2)\alpha$. From the first equation in (3.67), one has, in first orders in α,

$$\frac{\mathrm{d}}{\mathrm{d}t}\left[g\left(\frac{R_1}{R_2}\right)\right] = \left(\frac{\dot{R}_1}{R_2} - \frac{\dot{R}_2 R_1}{R_2^2}\right) g'\left(\frac{R_1}{R_2}\right) = 0 \tag{3.79}$$

so that $z(t)$ and $\alpha(t)$ have the same logarithmic derivative:

$$\frac{\dot{z}}{z} = \frac{\dot{\alpha}}{\alpha}. \tag{3.80}$$

It means that for flat triangles the action of the strain matrix consists in a fast motion along a meridian of the Kendall sphere at $\phi = \mathrm{cte}$ (because the ratio R_1/R_2 is directly linked to the value of ϕ), and a slow motion along a circle of latitude near the equator.

We introduce the variable y, defined as $y = \ln(z)$. One redefines the time: $t' = \omega t$, and one notes

$$x_1 = \frac{y_1}{2\sigma\omega} \quad \text{and} \quad x_2 = \frac{y_2}{\sigma\omega}, \tag{3.81}$$

so that finally

$$\begin{cases} \dot{y} = 2\sigma x_1 \\ \dot{x}_1 = -x_1 - 2\sigma x_2^2 + \xi_1(t) \\ \dot{x}_2 = -x_2 + 2\sigma x_1 x_2 + \xi_2(t) \end{cases} \tag{3.82}$$

where X' is the derivative of X with respect to the dimensionless time t', σ is introduced previously, and $\xi_1(t)$, $\xi_2(t)$ are Gaussian white noise processes with respect to the time t':

$$\langle \xi_i(t') \rangle = 0 \quad \text{and} \quad \langle \xi_i(t')\xi_j(0) \rangle = \delta_{ij}\delta(t'). \tag{3.83}$$

The functions $x_1(t')$ and $x_2(t')$ should not be confused with some positions in the physical space; they are linked to the dynamics of the shear matrix $\mathbf{M}$. The equations (3.82) describe the motion of a particle advected by the random process x_1, which dynamics is given by a set of two coupled Langevin equations. The parameter σ quantifies the gap between the coloured noise process and the corresponding white noise process. As the Langevin equations involve non-linear terms, the process in non-Gaussian. Note that we defined the variables $x_i(t)$ in order to have σ appearing as a factor of the non-linear terms, rather than in front of the Gaussian white noises $\xi_i(t)$. When performing perturbations methods for small values of σ, the system of coupled Langevin equations will be seen as a non-linear perturbed Ornstein-Uhlenbeck process, and not as a deterministic dynamical system involving small additive noises.

3.4.3 Perturbation expansion for the stationary distribution of non-linear Langevin equations

One of the first quantity that we can compute in order to characterize the dynamics of the collapsing towards the equator is the mean value of $x_1(t)$, which gives the speed at which this collapsing occurs. More precisely, $x_1(t)$ can be seen, up to a pre-factor, as an instantaneous Lyapunov exponent for the dynamical variable $z(t)$, and the equator of the Kendall sphere ($z = 0$) is then an attractor of the dynamics.

As the variable y only appears in the first equation of the system (3.82), the dynamics of x_1 can be understood just by considering the reduced system

$$\begin{cases} \dot{x}_1 = -x_1 - 2\sigma x_2^2 + \xi_1(t) \\ \dot{x}_2 = -x_2 + 2\sigma x_1 x_2 + \xi_2(t) \end{cases} \tag{3.84}$$

consisting in two coupled Langevin equations.

The joint probability density for x_1 and x_2, $P(x_1, x_2, t)$, satisfies the Fokker-Planck equation

$$\begin{aligned}\frac{\partial P}{\partial t'} &= \frac{\partial}{\partial x_1}[(x_1 + 2\sigma x_2^2)P] + \frac{\partial}{\partial x_2}[(x_2 - 2\sigma x_1 x_2)P] + \frac{1}{2}\frac{\partial^2 P}{\partial x_1^2} + \frac{1}{2}\frac{\partial^2 P}{\partial x_2^2} \\ &= (\hat{\mathcal{F}}_0 + \sigma\hat{\mathcal{F}}_1)P,\end{aligned} \tag{3.85}$$

where

$$\begin{cases} \hat{\mathcal{F}}_0 = \dfrac{\partial}{\partial x_1}(x_1 \cdot) + \dfrac{\partial}{\partial x_2}(x_2 \cdot) + \dfrac{1}{2}\dfrac{\partial^2}{\partial x_1^2} + \dfrac{1}{2}\dfrac{\partial^2}{\partial x_2^2}, \\ \hat{\mathcal{F}}_1 = 2x_2^2\dfrac{\partial}{\partial x_1} - 2x_1\dfrac{\partial}{\partial x_2}(x_2 \cdot). \end{cases} \tag{3.86}$$

Perturbative expansion of the joint density of probability

We are looking for a stationary solution of the Fokker-Planck equation, in the form of a power series

$$P(x_1, x_2) = \sum_{j=0}^{\infty} \sigma^j P_j(x_1, x_2). \tag{3.87}$$

Injecting this form into the equation (3.85), one obtains the recursion relation:

$$\hat{\mathcal{F}}_0 P_{j+1} = -\hat{\mathcal{F}}_1 P_j \quad \text{and} \quad \hat{\mathcal{F}}_0 P_0 = 0. \tag{3.88}$$

The motivation of the following is to find the spectrum of the operator $\hat{\mathcal{F}}_0$. We follow the method shown in [MW04; Meh+05] based on [Ris84]. To proceed, we find the stationary probability density function of the unperturbed system ($\sigma = 0$):

$$P_0(x_1, x_2) = \frac{1}{\pi}\exp(-x_1^2 - x_2^2). \tag{3.89}$$

The operator $\hat{\mathcal{F}}_0$ is not hermitian. We perform the following transformation using the stationary pdf:

$$\hat{\mathcal{H}}_0 = \exp\left(\frac{x_1^2}{2} + \frac{x_2^2}{2}\right)\hat{\mathcal{F}}_0 \exp\left(-\frac{x_1^2}{2} - \frac{x_2^2}{2}\right) \tag{3.90}$$

and find the hermitian "hamiltonian":

$$\hat{\mathcal{H}}_0 = 1 - \frac{x_1^2}{2} - \frac{x_2^2}{2} + \frac{1}{2}\partial_{x_1 x_1}^2 + \frac{1}{2}\partial_{x_2 x_2}^2. \tag{3.91}$$

This is almost the hamiltonian of the two-dimensional quantum harmonic oscillator, up to some constants and signs. Coherently, we use notation from the quantum formalism, with bras and kets. The eigenvalues of $\hat{\mathcal{H}}_0$ are expressed in the form

$$\lambda_{n_1 n_2} = -(n_1 + n_2) \quad \text{where} \quad n_1, n_2 \in \mathbf{N}. \tag{3.92}$$

The corresponding eigenvectors form a orthogonal basis of the Hilbert space:

$$\hat{\mathcal{H}}_0 \left|\phi_{n_1 n_2}\right\rangle = \lambda_{n_1 n_2} \quad \text{and} \quad \langle\phi_{n_1 n_2}|\phi_{n_1' n_2'}\rangle = \delta_{n_1 n_1'}\delta_{n_2 n_2'}. \tag{3.93}$$

The ground state of $\hat{\mathcal{H}}_0$ is then $|\phi_{00}\rangle$, and we have

$$\langle\vec{x}|\phi_{00}\rangle = \frac{1}{\sqrt{\pi}}\exp\left(-\frac{x_1^2}{2} - \frac{x_2^2}{2}\right). \tag{3.94}$$

One then defines the creation and annihilation operators :

$$\hat{a}_i^\dagger = \frac{1}{\sqrt{2}}(x_i - \partial_i) \quad \text{and} \quad \hat{a}_i = \frac{1}{\sqrt{2}}(x_i + \partial_i) \tag{3.95}$$

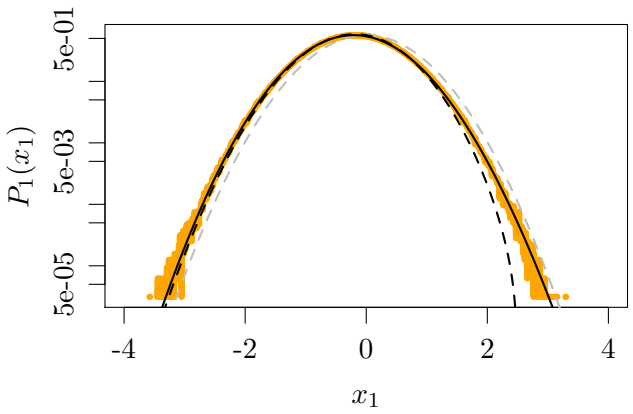

Figure 3.9 – Stationary density of probability $P_1(x_1) = \int \mathrm{d}x_2 P(x_1, x_2)$, in logarithmic coordinates, obtained from numerical simulation of the model (3.84). In grey doted lines, the zero-order analytic prediction, in black doted lines, the first-order analytic prediction and in black lines, the third-order analytic prediction.

which verifies the following commutation relations

$$\left[\mathcal{H}_0, \hat{a}_i^\dagger\right] = -\hat{a}_i^\dagger \quad , \quad [\mathcal{H}_0, \hat{a}_i] = \hat{a}_i \quad \text{and} \quad \left[\hat{a}_i \hat{a}_j^\dagger\right] = \delta_{ij}, \tag{3.96}$$

so that:

$$\hat{x}_i = \frac{1}{\sqrt{2}}(\hat{a}_i + \hat{a}_i^\dagger). \tag{3.97}$$

The actions of the creation and annihilation operators on the eigenfunctions are classic:

$$\begin{cases} \hat{a}_1 \left|\phi_{n_1 n_2}\right\rangle = \sqrt{n_1}\left|\phi_{n_1 - 1\, n_2}\right\rangle \\ \hat{a}_1^\dagger \left|\phi_{n_1 n_2}\right\rangle = \sqrt{n_1 + 1}\left|\phi_{n_1 + 1\, n_2}\right\rangle \end{cases} \text{and} \quad \begin{cases} \hat{a}_2 \left|\phi_{n_1 n_2}\right\rangle = \sqrt{n_2}\left|\phi_{n_1\, n_2 - 1}\right\rangle \\ \hat{a}_2^\dagger \left|\phi_{n_1 n_2}\right\rangle = \sqrt{n_2 + 1}\left|\phi_{n_1\, n_2 + 1}\right\rangle \end{cases} \tag{3.98}$$

and one defines the counting operator $\hat{N}_i$ as $\hat{N}_i = \hat{a}_i^\dagger \hat{a}_i$ so that $\hat{N}_1 \left|\phi_{n_1 n_2}\right\rangle = n_1 \left|\phi_{n_1 n_2}\right\rangle$ and $\hat{N}_2 \left|\phi_{n_1 n_2}\right\rangle = n_2 \left|\phi_{n_1 n_2}\right\rangle$.

Consider the operator $\mathcal{F}_1$, which contains the non-linear of the dynamics. We note

$$\hat{\mathcal{H}}_1 = \exp\left(\frac{x_1^2}{2} + \frac{x_2^2}{2}\right) \hat{\mathcal{F}}_1 \exp\left(-\frac{x_1^2}{2} - \frac{x_2^2}{2}\right) \tag{3.99}$$

and we can express $\hat{\mathcal{H}}_1$ in terms of the creation and annihilation operators:

$$\hat{\mathcal{H}}_1 = -2\sqrt{2}\hat{a}_1^\dagger \hat{x}_2^2 + 2\sqrt{2}\hat{a}_2^\dagger \hat{x}_1 \hat{x}_2. \tag{3.100}$$

In order to compute the stationary joint density of probability $P(x_1, x_2)$, we are looking for an null-eigenvector of the operator $\hat{\mathcal{H}} = \hat{\mathcal{H}}_0 + \sigma \hat{\mathcal{H}}_1$:

$$(\hat{\mathcal{H}}_0 + \sigma \hat{\mathcal{H}}_1)\left|\Psi_{00}\right\rangle, \tag{3.101}$$

in the form of a power series:

$$\left|\Psi_{00}\right\rangle = \sum_{j=0}^{\infty} \sigma^j \left|Q_j\right\rangle. \tag{3.102}$$

We already have $\left|Q_0\right\rangle = \left|\phi_{00}\right\rangle$, and the recursion relation reads:

$$\hat{\mathcal{H}}_0 \left|Q_{j+1}\right\rangle + \hat{\mathcal{H}}_1 \left|Q_j\right\rangle = 0. \tag{3.103}$$

In order to solve this equation for $|Q_{j+1}\rangle$ knowing $|Q_j\rangle$, one has to inverse the operator $\hat{\mathcal{H}}_0$. As $\hat{\mathcal{H}}_1^* |\phi_{00}\rangle = 0$ (where $\mathcal{A}^*$ denotes the adjoint of the operator $\mathcal{A}$), the image of $\hat{\mathcal{H}}_1$ is orthogonal to the kernel of $\hat{\mathcal{H}}_0$, so that one can legitimately writes

$$|Q_{j+1}\rangle = -\hat{\mathcal{H}}_0^{-1}\hat{\mathcal{H}}_1 |Q_j\rangle . \tag{3.104}$$

Rigorously, we should add to the expression of $|Q_{j+1}\rangle$ an element of the kernel of $\hat{\mathcal{H}}_0$, say $\kappa |\phi_0\rangle$. However, the normalisation condition of the density of probability $P(x_1, x_2)$ reads in the space of the kets

$$\langle\phi_{00}|\Psi_{00}\rangle = 1, \tag{3.105}$$

so that as $|Q_0\rangle = |\phi_{00}\rangle$, $|Q_j\rangle$ for $j > 0$ is orthogonal to $|\phi_{00}\rangle$: $\langle\phi_{00}|Q_j\rangle = 0$. Note that we have two different normalisation conditions: first, the eigenvectors of $\hat{\mathcal{H}}_0$ form an orthogonal basis, so that $\langle\phi_{n_1n_2}|\phi_{n_1'n_2'}\rangle = \delta_{n_1n_1'}\delta_{n_2n_2'}$; second, the density of probability must be normalised, which corresponds to the equation (3.105). In particular, there is no reason to have $\langle\Psi_{00}|\Psi_{00}\rangle = 1$, and for this type of perturbation development it is in general not the case.

We decompose the $|Q_j\rangle$ in term of the eigenfunctions:

$$|Q_j\rangle = c_{nm}^{(j)} |\phi_{nm}\rangle . \tag{3.106}$$

One finds immediately

$$\begin{aligned} |Q_1\rangle &= -\hat{\mathcal{H}}_0^{-1}\hat{\mathcal{H}}_1 |Q_0\rangle \\ &= \sqrt{2}\hat{\mathcal{H}}_0^{-1} |\phi_{10}\rangle \\ &= -\sqrt{2} |\phi_{10}\rangle . \end{aligned} \tag{3.107}$$

Thus, the first order expression of $|\Psi_{00}\rangle$ reads

$$|\Psi_{00}\rangle = |\phi_{00}\rangle - \sqrt{2}\sigma |\phi_{10}\rangle + \mathcal{O}(\sigma^2) \tag{3.108}$$

and so

$$P(x_1, x_2) = \frac{1}{\sqrt{\pi}} \exp\left(-\frac{x_i^2}{2}\right) \left[\langle\vec{x}|\phi_{00}\rangle - \sqrt{2}\sigma \langle\vec{x}|\phi_{10}\rangle + \mathcal{O}(\sigma^2)\right] . \tag{3.109}$$

As

$$\langle\vec{x}|\phi_{10}\rangle = \sqrt{\frac{2}{\pi}} x_1 \exp\left(-\frac{x_1^2}{2} - \frac{x_2^2}{2}\right), \tag{3.110}$$

the marginal density of probability for x_1, $P_1(x_1) = \int \mathrm{d}x_2 P(x_1, x_2)$, reads explicitly at the first order:

$$P_1(x_1) = \frac{1}{\sqrt{\pi}} \left[1 - 2\sigma x_1 + \mathcal{O}(\sigma^2)\right] \exp(-x_1^2). \tag{3.111}$$

Figure 3.9 shows the first orders of the perturbation expansion, compared with the stationary density of probability obtained numerically.

First moment of the distribution

In order to compute the first moments of the stationary distribution, and particularly the mean $\langle x_1\rangle$, we can use the following formula:

$$\langle x_1\rangle = \frac{\langle\phi_{00}|\hat{x}_1|\Psi_{00}\rangle}{\langle\phi_{00}|\Psi_{00}\rangle} = \langle\phi_{00}|\hat{x}_1|\Psi_{00}\rangle . \tag{3.112}$$

By using the expression of x_1 in term of $\hat{a}_1$ and $\hat{a}_1^\dagger$, one finds

$$\langle x_1\rangle = \frac{1}{\sqrt{2}} \langle\phi_{00}|\hat{a}_1|\Psi_{00}\rangle , \tag{3.113}$$

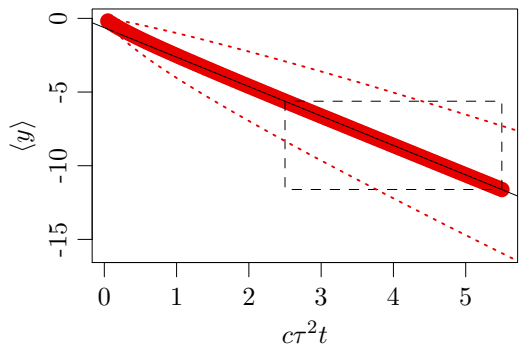

(a) In red, plot of $\langle y(t)\rangle$ with respect to $c\tau^2 t = 2D_s$ in the case of the white noise process (3.24). The standard deviation is shown in red dotted lines. In black dotted lines, the domain where the linear regression is performed, giving $\langle y(t)\rangle \approx 2c\tau^2 t$.

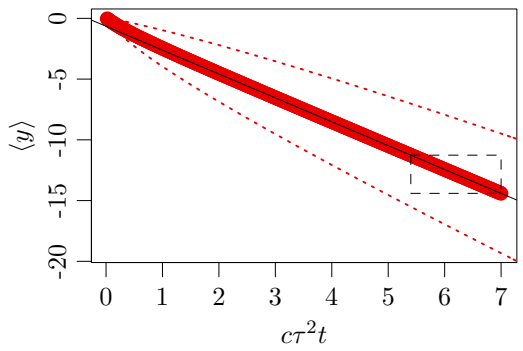

(b) In red, plot of $\langle y(t)\rangle$ with respect to $c\tau^2 t = 2D_s$ in the case of the correlated noise process (3.56) with $\sigma = 0.1$. The linear regression gives $\langle y(t)\rangle \approx -1.965\, c\tau^2 t$, while the development of $\langle x_1\rangle$ up to the fifth order in σ gives $\langle y(t)\rangle \approx -1.962\, c\tau^2 t$.

Figure 3.10 – Numerical computations of the rate of collapsing toward the equator of the Kendall sphere. One obtains a linear evolution of $y = \ln z$ with respect to the time, and the slope is linked to $\langle x_1\rangle$.

and so immediately

$$\langle x_1\rangle = -\sigma + \mathcal{O}(\sigma^2). \tag{3.114}$$

More generally, the series expansion of $\langle x_1\rangle$ reads

$$\langle x_1\rangle = \frac{1}{\sqrt{2}}\sigma^j c_{10}^{(j)} \quad \text{with} \quad c_{nm}^{(j)} = \langle \phi_{nm}|Q_j\rangle\,. \tag{3.115}$$

One can compute the recursion relation for the coefficients $c_{nm}^{(j)}$ following the expression of $\hat{\mathcal{H}}_1$:

$$\begin{aligned}\frac{c_{k\ell}^{(j+1)}}{\sqrt{2}} = \frac{1}{k+\ell}\Bigg(&-\sqrt{k}(\ell+1)c_{k-1\,\ell}^{(j)} - \sqrt{k(\ell+1)(\ell+2)}c_{k-1\,\ell+2}^{(j)} \\ &+ \sqrt{(k+1)\ell(\ell-1)}c_{k+1\,\ell-2}^{(j)} + \sqrt{k+1}\ell c_{k+1\,\ell}^{(j)}\Bigg).\end{aligned} \tag{3.116}$$

One finds that the even powers in σ in the series expansion of $\langle x_1\rangle$ are zero. One obtains up to the 5th order

$$\langle x_1\rangle = -\sigma + 2\sigma^3 - \frac{32}{3}\sigma^5 + \mathcal{O}(\sigma^7). \tag{3.117}$$

It is natural to wonder whether this series expansion has a finite radius of convergence, and how accurate it is. One can simulate the dynamics of triangles only under the action of the shear matrix. Eventually all the particles will converge towards the equator, and one can compute the behaviour of $\langle y(t)\rangle = \langle \ln z(t)\rangle$ as a function of the dimensional time t. One predicts that after a relaxation time larger than τ, and as soon as the particles are sufficiently close to the equator,

$$\begin{aligned}\langle y(t)\rangle &= 2\sigma\,\langle x_1\rangle\,\omega t \\ &= -2c\tau^2 t\left[1 - 2\sigma^2 + \frac{32}{3}\sigma^4 + \mathcal{O}(\sigma^6)\right].\end{aligned} \tag{3.118}$$

In particular, for the white noise process ($\sigma = 0$) one has $\langle y(t)\rangle = -4D_s t$. Qualitatively, the finite correlation time of the eddies reduces the rate of convergence towards the equator (see figure 3.10).

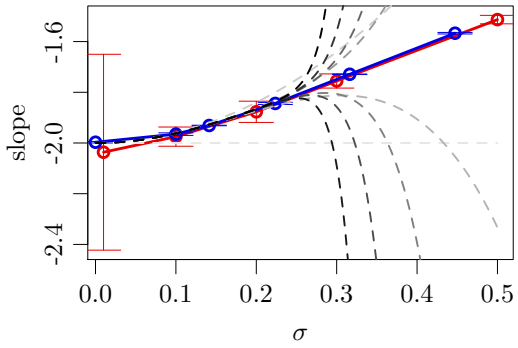

(a) In red, plot of the slope $\mathrm{d}\langle y\rangle/\mathrm{d}t$ with respect to σ, computed from direct simulations of the triangles model. In blue, $2\sigma\langle x_1\rangle/\tau$ obtained from the simulation of (3.84). The ten shades of gray represent the series expansions summed to orders $j/2 = 0, \ldots, 9$ (light gray: low values of j).

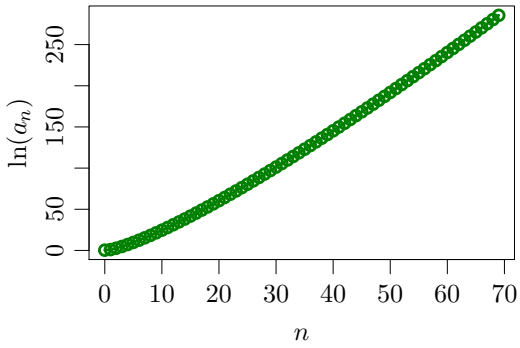

(b) Plot of a_n with respect to n, as defined in (3.119). One observes what seems like a linear growth, but without being able to accurately conclude between a exponential evolution of a_n with n and the presence of a factorial component.

Figure 3.11 – Evolution of the rate of collapsing toward the equator of the Kendall sphere from the model of the triangles and comparison with the results obtained from the reduced system and the perturbative development.

Moreover, it is not difficult to simulate directly the system of Langevin equations (3.84), and to compute the stationary value of $\langle x_1\rangle$, without having to deal with the collapsing of particles towards $y = -\infty$. The comparison between the results obtained from direct simulation of (3.84), numerical simulations of the model of the triangles and the first terms in the perturbative development of $\langle x_1\rangle$ is shown figure 3.11a.

The description of the dynamics near the equator seems accurate, and the perturbative development gives a good description for apparently $\sigma < 0.2$. In order to determine if the series expansion (3.115) of $\langle x_1\rangle$ converges, one can evaluate the evolution of the coefficients a_n with n, where the a_n are defined as

$$\langle x_1\rangle = \sum_{n=0}^{\infty} (-1)^n\, a_n \sigma^{2n+1}. \tag{3.119}$$

It is difficult to conclude that the evolution of a_n is exponential (see figure 3.11b), and it is possible that the coefficients grow as $a_n \propto \alpha^n (n!)^\beta$ with $\alpha > 1$ and $\beta > 0$, which would lead to a radius of convergence formally equal to zero. Nevertheless, the series (3.119) is an asymptotic series: it diverges, but as the sign of the coefficients alternate, one can expect that every partial sum of the series approaches $\langle x_1\rangle(\varepsilon)$ as ε tends to zero [DD73].

3.4.4 Stationary distribution for the global system

Consider now the global system of coupled Langevin equations (3.82). Direct numerical simulations of the dynamical model for triangles shows a power-law dependence of $P(z)$ in z, in regions where the influence of the diffusion term is weak (see figure 3.7), and with apparently a value of the exponent independent of σ: $P(z) \propto z^{-2}$. This power-law dependence can be understood from the analysis of the dynamics for flat triangles: one obtained that $y' = 2\sigma x_1(t')$ where the dynamics of x_1 does not depend on $y = \ln z$. The problem presents then a *translational invariance*. The diffusive term acts on region where z is smaller than $\sqrt{\varepsilon}$; in the space of $y = \ln z$, its influence can be modelled by a impervious wall at a given position, say $y = 0$. If we can define a region "far from the wall", where the dynamics of y is not affected by the presence of the wall, then the stationary density of probability $P(y)$ must also have a translational invariance. In other words,

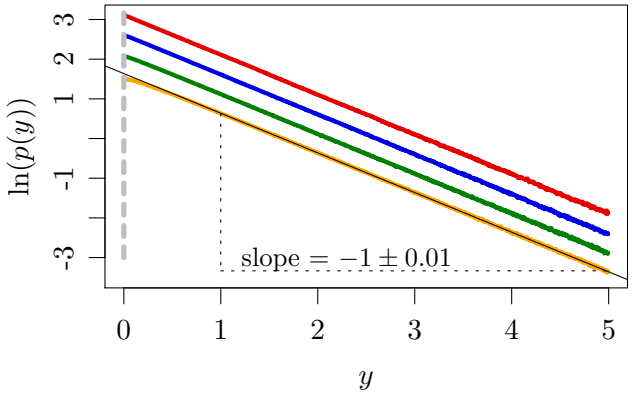

Figure 3.12 – Plot of the logarithm of $P(y) = \int \mathrm{d}x_1 \mathrm{d}x_2\, P(y, x_1, x_2)$ obtained from numerical simulations of the Langevin equations (3.82), for different values of σ. In red $\sigma = 0.1$, in blue $\sigma = 0.2$, in green $\sigma = 0.5$ (these three plots have been vertically translated for better comparison), and in orange $\sigma = 1$. The linear regression (in black for $\sigma = 1$) shows that far enough from the wall (at $y = 0$, represented by a vertical grey dashed line), all slopes are of value -1.

$P(y)$ must be a eigenvector of the translation operator [LL65], so that

$$P(y) = \mathcal{N} \exp(\alpha y) \tag{3.120}$$

where $\mathcal{N}$ is a normalisation constant. As the drift velocity $2\sigma \langle x_1 \rangle$ is negative, one expects to obtain more particle on the left than on the right of the y-axis, so that $\alpha < 0$. Thus, the presence of wall is unavoidable in order to obtain a normalisable solution, just as the diffusion term is needed to avoid all the particles to collapse on the equator of the Kendall sphere. The link with the density of probability of z is straightforward: as $P(z)\mathrm{d}z = P(y)\mathrm{d}y$, one obtains

$$P(z) = \mathcal{N} z^{\alpha - 1}, \tag{3.121}$$

which explains the power-law behaviour observed in numerical simulations.

The joint stationary density of probability $P(y, x_1, x_2)$ verifies the steady-state Fokker-Planck equation

$$0 = -2\sigma x_1 \frac{\partial P}{\partial y} + \frac{\partial}{\partial x_1}[(x_1 + 2x_2^2)P] + \frac{\partial^2 P}{\partial x_1^2} + \frac{\partial}{\partial x_2}[(x_1 - 2x_1 x_2)P] + \frac{\partial^2 P}{\partial x_1^2}. \tag{3.122}$$

We look for a solution in the form $P(y, x_1, x_2) = p(x_1, x_2) \exp(\alpha y)$. While one can expect a complex form for the density of probability of the "speeds" $p(x_1, x_2)$, as the analysis of the reduced system showed, it turns out that the equation (3.122), although involving non-linear terms in $x_2^2, x_1 x_2$, has an exact a simple solution, independent of σ:

$$P(y, x_1, x_2) = \exp(-y - x_1^2 - x_2^2), \tag{3.123}$$

so that in particular $\alpha = -1$ whatever the value of σ. One recovers the power-law $P(z) \propto z^{-2}$ in the case of a white noise process, and more generally this result explains the apparent non-dependence in σ of the tails of the densities of probability computed from the coloured noise model (see figure 3.7).

3.5 Conclusion

In this chapter we presented a simplified model for the dynamics of triplets of points advected by a flow in homogeneous turbulence, using stochastic methods. During the temporal evolution

the three particles spread and explore the scales of the flow. We supposed that the dynamics does not depend on the scale, and sought for a description of the evolution of the shape of the triangle, a quantity independent of the size, global rotation and position in space of the set of points. We introduced the natural home for the shape of triangle: the Kendall sphere.

The action of the velocity field was divided into three contributions: eddies of large, small and medium size compared to that of the triangle, resulting in different effects. In the case of time-correlated processes, an explicit resolution of the dynamics on the Kendall sphere was already obtained [PW13]. However in real flows the velocity field has a finite correlation time, and the models must be refined. We quantified some effects of a finite correlation time in the shape dynamics: regularisation of the topological changes and influence on the distribution of quasi flat triangles. Under the influence of the shear matrix only, the equator of the Kendall sphere acts as an attractor of the dynamics, and the spatial repartition around it is linked to a sedimentation process. This is a central idea in this thesis, as we will see in the next chapter, where a different physical problem with a different kind of attractor is studied, but formally the same description emerges.

One natural question which often arises in physics is: "What is happening for higher dimensions?" In our case, it will correspond to the study of three-dimensional structures, and as a triangle is the minimal set of points needed to span the space in two dimension, one can consider advected tetrads in three dimensional turbulent flows. Due to the volume preservation, such structures also tend to become flat under the action of the flow, resulting in planar clusters of points [PSC00]. The shape space is however more complicated, because its dimension is then $4\times3-3\,[\text{centre of mass}]-3\,[\text{rotational position in space}]-1\,[\text{global size}]=5$. Thus, it is difficult to find a single parameter corresponding, in the case of the triangles, to z. Nevertheless one can expect to obtain similar distributions of shape, with a balance between shear processes due to the like-scale eddies and homogeneous diffusion of vertices.

Chapter 4

Dynamics of inertial particles

Outline

In this chapter we no longer consider the dynamics of tracers in turbulent flows, as in the previous chapter, but rather the evolution of particles heavier than the carrying fluid. Due to the resulting inertia, the motion of these particles does not follow exactly the pathlines of the underlying flow. As a consequence, the description of the motion does not depend only on the flow velocity. The study of these particles can have numerous applications, already listed in chapter 2. We are interested in a phenomenon known as *preferential concentration*, where the particle concentration field encounters strong inhomogeneities.

In the following, we first recall the equations of the motion of inertial particles in a turbulent flow, and the particular one dimensional model describing the action of the fluid on the particles. This model which exhibits a *path coalescence transition*: the system goes from a regime where the trajectories of the particles fill the whole space, to a regime where all the trajectories merge into a single one. In the first case the particles form cluster having fractal properties, and one can compute an estimate of the dimension of such structures: the correlation dimension. The main result of this chapter is the extension of the notion of fractal dimension to the negative cases, in the regime where, in the absence of any perturbation, the attractor of the dynamics is a point-like structure.

The results of this chapter have been partly published in [Wil+15].

4.1 The model

4.1.1 Equations of motion

We recall here the equations of motion of an inertial particle in a turbulent flow, already derived in chapter 2. We consider particles of size much smaller than the Kolmogorov scale η, meaning that the fluid motion is smooth at the scale of the particle, and suppose that the associated Reynolds number is small. Moreover, we suppose that the flow is incompressible. Assuming that the relative velocity of the particle compared to that of flow is small, [Gat83; MR83] derived the equations of motion, which involves many terms and is quite hard to deal with in the general case. However, for very small particles of density much higher than that of the fluid, we can consider the Stokes drag force as the prominent term in the different contributions acting on the particle, leading to the simplified motion:

$$\ddot{\vec{x}} = -\frac{1}{\tau_{\mathrm{S}}}(\dot{\vec{x}} - \vec{u}(\vec{x}, t)) \tag{4.1}$$

where $\vec{u}(\vec{x}, t)$ is the velocity field and

$$\tau_{\mathrm{S}} = \frac{2}{9}\frac{a^2}{\nu}\frac{\rho_{\mathrm{particle}}}{\rho_{\mathrm{fluid}}} \tag{4.2}$$

is the particle relaxation time or Stokes time (ρ_{A} is the mass density of A).

4.1.2 One dimensional dynamical system

In the following we study a one dimensional model based on the motion equations (4.1). Moreover, we add a noise term in the equation on $\dot{x}$. This term represents the diffusion motion of the particles in the flow and the resultant of the neglected forces in the description (4.1). Thus, one has

$$\begin{cases} \dot{x} = v + \sqrt{2\mathcal{D}}\,\eta(t)\,, \\ \dot{v} = -\gamma[v - u(x,t)]. \end{cases} \tag{4.3}$$

where we defined

$$\gamma = \tau_{\mathrm{S}}^{-1} \tag{4.4}$$

and where $\eta(t)$ is a standard Gaussian white noise with statistics

$$\langle \eta(t) \rangle = 0 \quad \text{and} \quad \langle \eta(t)\eta(t') \rangle = \delta(t - t'). \tag{4.5}$$

The underlying fluid $u(x, t)$ is modelled by a stochastic process whose statistics have a translational invariance both in time and space:

$$\langle u(x,t) \rangle = 0 \quad \text{and} \quad \langle u(x,t)u(x',t') \rangle = c(x - x', t - t')\,. \tag{4.6}$$

The specific form of the correlation function $c(x - x', t - t')$ makes the process correlated in space but uncorrelated in time:

$$c(x - x', t - t') = A^2 \exp\left(-\frac{(x - x')^2}{\ell_{\mathrm{c}}^2}\right)\delta(t - t') \tag{4.7}$$

where ℓ_{c} is the correlation length of the fluid and A a constant. The flow is the same for all the particles, but the realisations of the noise $\sqrt{2\mathcal{D}}\,\eta(t)$ differ for each particle.

Considering clustering processes, we are interested in the motion of particles in the *physical space*, so that we consider attractors embedded in the one dimensional space of the variable x.

Later in this chapter, we will obtain an evolution equation for the separation δx of two nearby trajectories in the form

$$\delta\dot{x} = Z(t)\delta x, \tag{4.8}$$

where we will explicitly show that the fluctuating variable $Z(t)$ satisfies his own equation of motion, which does not depend on the separation δx or on the spatial position x. Thus, it is sufficient to consider only the motion along the x axis.

For the particular one-dimensional model, one can observe in numerical simulations a phenomenon known as a *path coalescence transition* [WM03]: when varying the physical parameters of the model, the qualitative behavior of the solutions transits from a phase where two nearby trajectories diverge with probability one as time increases, to a regime where all the trajectories eventually merge. The transition in the model (4.3) is reminiscent of the phenomenon of preferential concentration, although it does show several important differences. In particular, the clustering of particles is, in the model (4.3), *not* due to inertial effects. As we show below, the clustering processes occurs for *decreasing values* of the Stokes time τ_{S}, so that the one dimensional model proposed here does not faithfully describe the motion of inertial particles.

As a consequence, the following must not be seen as a physically accurate description of the dynamics of inertial particles in one dimension, but rather as the study of a particular dynamical system inspired by the dynamics of inertial particles. However, the tools developed here can be used for more realistic models describing the dynamics of inertial particles [GMW15]. Moreover, qualitative information can be gained by studying the solution of (4.3), in particular concerning the caustics formations (see equation (4.48) below).

4.1.3 Numerical simulations

The objective of this section is to present the methods used to simulate the Eulerian flow $u(x,t)$, whose statistics are given in (4.7). In the following, we consider the motion to occur in a periodical space of size ℓ, thus identify x and $x+\ell$. A realisation of the random function $u(x,t)$ can be generated as a periodic function of period L, taken to be sufficiently large for the periodicity to be irrelevant, combined with a Gaussian white noise process: $u(x,t) = f(x)\xi(t)$ where $\xi(t)$ is a standard Gaussian white noise process and

$$f(x,t) = \sum_{n=1}^{N} a_n \cos\left(\frac{2\pi n x}{L}\right) + b_n \sin\left(\frac{2\pi n x}{L}\right) \tag{4.9}$$

where a_n and b_n are random variables, satisfying

$$\langle a_n\rangle = \langle b_n\rangle = \langle a_n b_{n'}\rangle = 0 \quad \text{and} \quad \langle a_n a_{n'}\rangle = \langle b_n b_{n'}\rangle = \delta_{nn'} K_L(n). \tag{4.10}$$

It leaves us with two variable parameters, L and N, and each must be chosen sufficiently large. The parameter $k_{\min} = 1/L$ is the lowest wave number generated by the flow, which must be much larger than the typical length scale ℓ_{c}, so that one has $L \gg \ell_{\mathrm{c}}$. We set

$$K_L(n) = B_L \exp(-n^2\Lambda_L^2/2). \tag{4.11}$$

The spatial correlations of the function f are then

$$\begin{aligned}
\langle f(x)f(x')\rangle &= \sum_{n=1}^{N} \langle a_n^2\rangle \cos\left(\frac{2\pi n x}{L}\right)\cos\left(\frac{2\pi n x'}{L}\right) + \langle b_n^2\rangle \sin\left(\frac{2\pi n x}{L}\right)\sin\left(\frac{2\pi n x'}{L}\right) \\
&= \sum_{n=1}^{N} K_L(n)\cos\left(\frac{2\pi n(x-x')}{L}\right) \\
&= B_L \sum_{n=1}^{N} \exp\left[-\frac{(L\Lambda_L)^2}{2}\left(\frac{n}{L}\right)^2\right]\cos\left(2\pi(x-x')\frac{n}{L}\right).
\end{aligned} \tag{4.12}$$

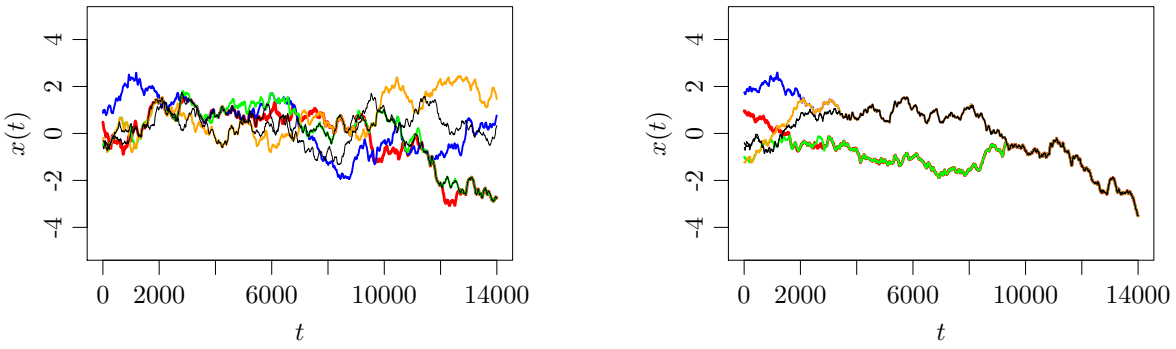

(a) Set of trajectories with a positive λ.

(b) Set of trajectories with a negative λ.

Figure 4.1 – Two sets of trajectories for the model (4.3) with $\mathcal{D} = 0$. One observes two different behaviours, depending on the sign of the average of the instantaneous Lyapunov exponent, $\lambda = \langle Z(t) \rangle$. **a)** $\lambda > 0$, the trajectories fill all the space; **b)** $\lambda > 0$, all trajectories collapse on a single one, the attractor is a random walk.

For large L, one has

$$\begin{aligned} \langle f(x) f(x') \rangle &\simeq L B_L \int_0^{N/L} \mathrm{d}y \exp\left[-\frac{(L\Lambda_L)^2}{2} y^2 \right] \cos(2\pi(x - x')y) \\ &\approx \sqrt{\frac{\pi}{2}} \frac{B_L}{\Lambda_L} \exp\left(-\frac{2\pi^2 (x - x')^2}{\lambda^2} \right) \end{aligned} \tag{4.13}$$

where $\lambda = L\Lambda_L$. The latter equation is valid as long as the upper limit of the integral, N/L, is much larger than λ^{-1}. Thus, one recovers the statistics (4.7) if we choose λ, B_L and Λ_L such as

$$\lambda = \sqrt{2}\pi \ell_c, \ \Lambda_L = \lambda / L \quad \text{and} \quad B_L = A^2 \Lambda_L \sqrt{\frac{2}{\pi}}. \tag{4.14}$$

and with

$$\frac{L}{N} \ll \ell_c \ll L. \tag{4.15}$$

For a sufficiently small time interval Δt the motion equations

$$\begin{cases} \dot{x} = v + \sqrt{2\mathcal{D}}\, \eta(t) \\ \dot{v} = \gamma(u(x,t) - v) \end{cases} \tag{4.16}$$

give

$$\begin{cases} x(t + \Delta t) = x(t) + v(t)\Delta t + n_1 \sqrt{2\mathcal{D}\Delta t} \\ v(t + \Delta t) = v(t) - \gamma v(t) \Delta t + \gamma n_2(t) \sqrt{\Delta t} f(x) \end{cases} \tag{4.17}$$

where $n_1(t)$, $n_2(t)$ are temporally uncorrelated normal random variables with mean 0 and variance 1.

4.2 Path coalescence transition and negative fractal dimension

4.2.1 Phenomenology

We analyse the separation between two nearby trajectories. To this end, we consider a linearisation of the equations of motion (4.3) and obtain

$$\begin{cases} \delta\dot{x} = \delta v + 2\sqrt{\mathcal{D}}\,\eta(t), \\ \delta\dot{v} = \gamma\left(\dfrac{\partial u}{\partial x}(x(t),t) - \delta v\right). \end{cases} \tag{4.18}$$

For the unperturbed process ($\mathcal{D} = 0$), we introduce the *instantaneous Lyapunov exponent* $Z(t)$, defined as

$$Z(t) = \frac{\partial v}{\partial x}(x(t),t) \tag{4.19}$$

so that for the equation on $\delta\dot{x}$ only one has

$$\delta\dot{x} = Z(t)\delta x. \tag{4.20}$$

The exponent $Z(t)$ is then the logarithmic derivative of the separation $\delta x(t)$ with respect to time. Its expectation value is in fact the Lyapunov exponent λ of the unperturbed process:

$$\lambda = \lim_{t\to\infty} \frac{1}{t}\int_0^t \mathrm{d}t' Z(t') = \langle Z(t)\rangle\,. \tag{4.21}$$

In the case of an autonomous system with an attractor, the attractor must be a fixed point in phase space, and $Z(t)$ approaches a constant as $t \to \infty$. In our case however the dynamical system is non-autonomous, and $Z(t)$ is in fact a *fluctuating* quantity. Depending on the sign of λ, two different behaviours emerge. First, if $\lambda > 0$ two nearby trajectories separate with probability unity during the dynamics, and the system is therefore unstable (see figure 4.1a). The trajectories cluster on a strange attractor which exhibits a fractal measure. Second, when $\lambda < 0$ the system is stable, in the sense that two trajectories tend to stay very close, and eventually all trajectories converge on a attractor which is not a fixed point (see figure 4.1b). Note that the coalescence of all the trajectories on a single path might take extremely long times. However, if we assume that the trajectories have the properties of random paths, then as in one dimension two random paths cross with probability one as the time goes to infinity, one can expect that two trajectories will cross with probability one, so that the local dynamics happens to stick them, resulting eventually in the coalescence of all the trajectories.

This description was made for the unperturbed system, with $\mathcal{D} = 0$. However, when we add the random noise ($\mathcal{D} \neq 0$) in the equation of motion, the system is expected to behave differently. Note that (4.20) generalizes to:

$$\delta\dot{x} = Z(t)\delta x + 2\sqrt{\mathcal{D}\,\eta(t)}, \tag{4.22}$$

so that the random noise term is dominant for small δx, when the two trajectories are very close, and tends to prevent clustering. When the dynamics is unstable ($\lambda > 0$), the phenomenology of the trajectories does not appreciably change, because both terms contribute to separate the particles. However, for the stable regime ($\lambda < 0$), there is a competition between the diffusion and the compression due to the negative Lyapunov exponent. As a consequence, the separation of two close trajectories, Δx, can have large excursions away from zero (see figure 4.2a). Those large excursions are a manifestation of the phenomenon of intermittency, as illustrated figure 4.2b. In fact, when computing the distribution of waiting times near the transition around $\lambda = 0$, one obtains power-law in the form

$$P(T) \sim T^{-3/2}, \tag{4.23}$$

as expected for an intermittency behaviour.

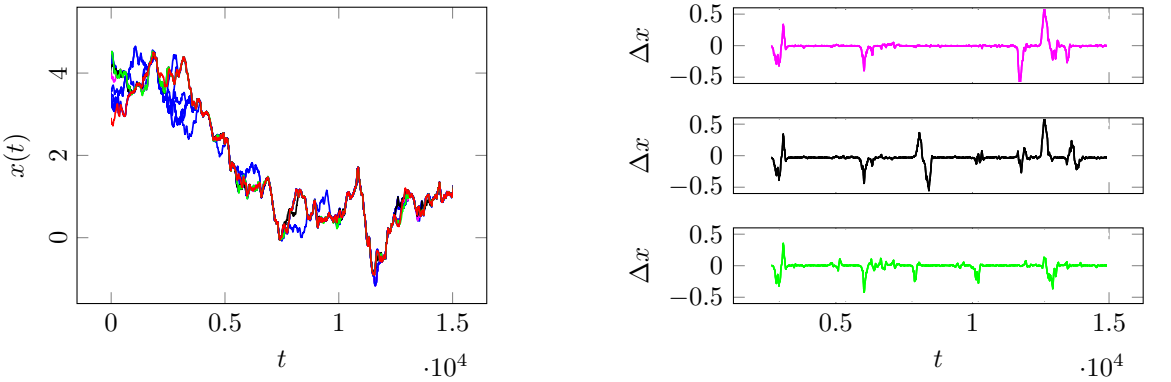

(a) Set of trajectories for $\lambda < 0$, with $\mathcal{D} \neq 0$. Different trajectories separate and recombine.

(b) Intermittent separation of pairs of trajectories $\Delta x(t)$.

Figure 4.2 – Set of trajectories for the model (4.3) with $\lambda < 0$ and $\mathcal{D} \neq 0$. The parameters are $\gamma = 0.05$, $\ell_c = 0.08$, $A = 0.02$ and $\mathcal{D} = 1 \times 10^{-8}$. The master trajectory, from which the separations Δx are computed, is in red.

4.2.2 Power-law distributions

In this section we characterize the fractal structures by analysing the distribution of nearby trajectories, and compute an estimator of the non-integer fractal dimension. There exist many definitions of fractal dimensions; for dynamical system, we use the correlation dimension [GP83; GP84; Ott02]. We briefly recall the definition: pick a particle at random and determine the number $\mathcal{N}(\epsilon)$ of other particles within a ball of radius centred on this particle. One considers the mean of this quantity, $\langle \mathcal{N}(\epsilon) \rangle$. If the attractor as a fractal measure, then $\langle \mathcal{N}(\epsilon) \rangle$ is expected to have a power-law dependence in the form:

$$\langle \mathcal{N}(\epsilon) \rangle \sim \epsilon^{D_2}, \tag{4.24}$$

and the exponent D_2 is the fractal dimension. It is sometimes easyer to deal with probability density function for separation of trajectories, $P(\Delta x)$. The two quantities are linked by an integral equation:

$$\langle \mathcal{N}(\epsilon) \rangle = \int_0^{\varepsilon} \mathrm{d}\Delta x P(\Delta x), \tag{4.25}$$

so that one expects also a power-law for $P(\Delta x)$ in the form

$$P(\Delta x) \sim |\Delta x|^{D_2 - 1}. \tag{4.26}$$

Unstable case

In the non-stable case (for $\lambda > 0$) and in the absence of noise ($\mathcal{D} = 0$), it has already been observed that the attractor presents a fractal structure, leading to a power-law behaviour for the density of probability of two close trajectories $P(\Delta x)$. If we turn on the noise ($\mathcal{D} \neq 0$), we still obtain power-law distribution, as presented figure 4.3a. The exponent of the power-law is linked to the correlation dimension D_2 of the attractor. One has

$$P(\Delta x) \sim |\Delta x|^{\alpha - 1} \tag{4.27}$$

so that $D_2 = \alpha$, where D_2 is between 0 and 1. Note that the value of the exponent does not depend on the intensity $\mathcal{D}$ of the noise. In particular, we obtain we same value in the absence of noise $\mathcal{D} = 0$. In the absence of the noise term, the distribution is still normalisable for $\Delta x \to 0$. In other terms, and as expected, the average number of trajectories inside a ball of radius ϵ, $\mathcal{N}(\epsilon)$, effectively decreases with decreasing ϵ, because the scaling is

$$\mathcal{N}(\epsilon) \sim \epsilon^{D_2}. \tag{4.28}$$

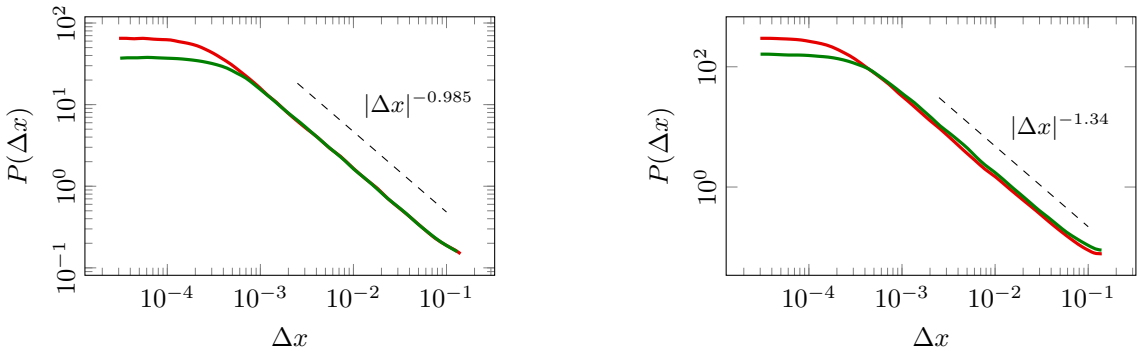

(a) Unstable regime, $\lambda > 0$.

(b) Stable regime, $\lambda < 0$.

Figure 4.3 – Probability distribution of the separation of trajectories, $P(\Delta x)$, for two values of $\mathcal{D}$ ($\mathcal{D} = 3 \times 10^{-10}$, red lines, and $\mathcal{D} = 1 \times 10^{-9}$, green lines). **(a)**: $\gamma = 0.0375$, $\ell_c = 0.08$, $A = 0.02$ so that $\lambda > 0$; **(b)**: $\gamma = 0.075$, $\ell_c = 0.08$, $A = 0.02$ so that $\lambda < 0$. The distributions are fitted by a power-law (dotted lines).

Stable case

In the stable regime, when $\langle Z(t) \rangle < 0$, and in the absence of diffusion, all trajectories merge into a single path, so that $P(\Delta x)$ is a Dirac distribution. In the presence of diffusion term, one may expect the density of probability of the separation of trajectories $P(\Delta x)$ to be well approximated by a Gaussian distribution. This is because, in the case of a stable autonomous system, the motion equation in the vicinity of the attractor with Lyapunov exponent $\lambda < 0$ can be written as

$$\dot{x} = \lambda x + \sqrt{2\mathcal{D}}\,\eta(t) \tag{4.29}$$

which is an Ornstein-Uhlenbeck process. In this case the deviations from the attractor do have a Gaussian distribution with a variance $\mathcal{D}/|\lambda|$, so that $P(\Delta x)$ is also Gaussian with a variance $2\mathcal{D}/|\lambda|$. We show here that the distribution $P(\Delta x)$ is in fact *non-Gaussian*, and has power-law tails when Δx tends to 0 (see figure 4.3b), in the form of (4.27), but with α negative. For very small values of Δx, the diffusion term becomes prominent and the distribution is flat in the limit $\Delta x \to 0$. Note that a distribution in the form $P(\Delta x) \sim |\Delta x|^{\alpha - 1}$ with $\alpha < 0$ is non-normalizable for $\Delta x \to 0$. Without the diffusion ($\mathcal{D} = 0$), the resulting distribution is a Dirac function centred around $\Delta x = 0$.

One of the main results is that the value of the exponent α does *not* depend on the diffusion coefficient $\mathcal{D}$, and is therefore intrinsic to the unperturbed dynamical system. The role of the diffusion is to sustain a non-zero separation between close trajectories, enabling positive fluctuations of the instantaneous Lyapunov exponent $Z(t)$ to produce intermittent bursts, which lead to power-law distributions. Thus, the mechanism for producing large excursions – the fluctuations of $Z(t)$ – is independent of the mechanism which seeds them – the diffusion term $\sqrt{2\mathcal{D}}\,\eta(t)$.

Origin of the power-law distributions

The origin of power-law distributions can be explained by characterizing the motion of nearby trajectories. Let us consider the dynamics of the fluctuations in a logarithmic variable:

$$y = \ln(\Delta x). \tag{4.30}$$

In the tail of $P(\Delta x)$, the fluctuations are much larger than the driving noise, so that the term $2\sqrt{D}\eta(t)$ in (4.18) can be neglected. In this limit the equation of motion for $y(t)$ is simply

$$\dot{y} = Z(t). \tag{4.31}$$

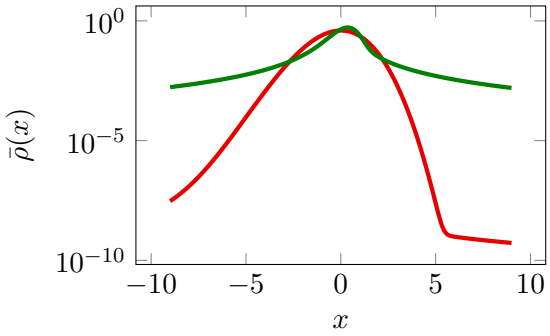

(a) Plot of the stationary density of probability for the unconditional process, $\bar{\rho}(x)$, as a function of x, for two values of ε: in red $\varepsilon = 0.1$ and in green $\varepsilon = 3$.

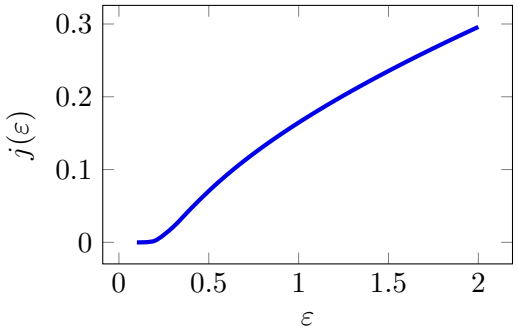

(b) Plot of the flux $j(\varepsilon)$ as a function of the dimensionless parameter ϵ. One observes an apparent non-analytic behaviour at $\varepsilon = 0$.

Figure 4.4 – Analytical predictions for the stationary density of probability $\bar{\rho}(x)$ and the flux $j(\varepsilon)$, related to the rate of formation of caustics.

The main point is that the statistics of the fluctuating quantity $Z(t)$ are independent of y, so that the stationary density of probability of y is expected to be invariant under a translation in the form: $y \to y + \delta y$. Thus, the only possible functional form for $p(y)$, the density of probability of y, is:

$$p(y) \sim \exp(\alpha y). \tag{4.32}$$

Therefore, by using the change of variables

$$\mathrm{d}P = p(y)\mathrm{d}y = P(\Delta x)\mathrm{d}\Delta x \tag{4.33}$$

one obtains a power-law dependence for $P(\Delta x)$, in the form

$$P(\Delta x) \sim |\Delta x|^{\alpha - 1}, \tag{4.34}$$

thus retrieving the form (4.27). Note that when $y \to -\infty$, or alternatively, $\Delta x \to 0$, the noise term dominates in (4.22), so the power-law does not hold. This prevents any difficulty with the divergence of $p(y)$; the noise term provides a natural cut-off at small separations ($\Delta x \to 0$), thus preventing potential normalisation problems. The equation (4.31) is the prototype of a sedimentation process, with a negative drift velocity $\langle Z(t) \rangle = \lambda$, so that the noise term acts as a "wall" in the space of the variable y.

For the distribution $P(\Delta x)$, the transition from the unstable to the stable regime acts as follows. For $\lambda > 0$ the system as a strange attractor and $P(\Delta x)$ is described by (4.27). As λ approaches zero from below, so does α. The power-law tails exhibited for $\lambda < 0$ correspond $\alpha < 0$. If we extend the identity $D_2 = \alpha$ to negative values of α, the equation (4.27) gives a physical meaning to a *negative* fractal dimension. This intrinsic property of the unperturbed dynamical system emerges due to the diffusion process in the physical space.

In the next section we present numerical results of the determination of the exponent α for the specific model of inertial particles, along with two perturbation approaches for its explicit computation.

4.3 Computation of the fractal dimension

4.3.1 Formulation in terms of a Fokker-Planck equation

In this section we determine the evolution of the instantaneous Lyapunov exponent $Z(t)$. To proceed, consider again the linearised equations of the dynamics (4.18). Let $S(t)$ be the velocity

gradient at the position of a particle:

$$S(t) = \frac{\partial u}{\partial x}(x(t), t). \tag{4.35}$$

This variable is a Gaussian white noise with coefficient D, such that

$$S(t) = \sqrt{2D}\xi(t) \quad \text{with} \quad D = \frac{A^2}{\ell_c^2}, \tag{4.36}$$

where $\xi(t)$ is independent of $\eta(t)$ but with the same statistics (4.5). When $\mathcal{D} = 0$, we obtain the following stochastic differential equation of motion for $Z(t)$ (previously derived in [WM03]):

$$\dot{Z} = -\gamma Z - Z^2 + \sqrt{2D}\,\gamma\,\xi(t), \tag{4.37}$$

which must be consider along with $\dot{y} = Z(t)$. It is convenient to replace Z by a scaled variable x, and introduce a dimensionless parameter ε:

$$x(t) = \frac{1}{\gamma}\sqrt{\frac{\gamma}{D}}Z(t), \quad \varepsilon = \sqrt{\frac{D}{\gamma}}, \tag{4.38}$$

so that after a natural rescaling of the time $t \to \tau = \gamma t$ one obtains

$$\begin{cases} y' = \varepsilon x \\ x' = -x - \varepsilon x^2 + \sqrt{2}\,\bar{\xi}(\tau) \end{cases} \tag{4.39}$$

with $\bar{\xi}(\tau)$ a standard Gaussian white noise, and where $z'(\tau) = \partial_\tau z$. The joint density of probability for y and x, $P(x, y, \tau)$, verifies a Fokker-Planck equation:

$$\frac{\partial P}{\partial \tau} = -\varepsilon x \frac{\partial P}{\partial y} + \frac{\partial}{\partial x}[(x + \varepsilon x^2)P] + \frac{\partial^2 P}{\partial x^2}. \tag{4.40}$$

One looks for a stationary solution in the form

$$P(x, y) = \rho(x)\exp(\alpha y) \tag{4.41}$$

so that

$$[-\alpha\varepsilon x + \partial_x \hat{J}_\varepsilon]\rho(x) = 0 \quad \text{where} \quad \hat{J}_\varepsilon = \partial_x + x + \varepsilon x^2. \tag{4.42}$$

Because ∂_x is a left-factor of $\hat{J}_\varepsilon$, any normalisable solution of (4.42) with a non-zero α must satisfy

$$\int_{-\infty}^{\infty} \mathrm{d}x\, x\, \rho(x) = 0. \tag{4.43}$$

The physical meaning of (4.43) is that in order to find a stationary distribution for the sedimentation variable y, the flux must be constant and equal to zero. Moreover, it gives us an implicit method to find α. Note that the integral (4.43) is *distinct* from the Lyapunov exponent $\lambda = \varepsilon\gamma\,\langle x \rangle$, because $\rho(x)$ is a distribution of x which is conditional upon the value of y, even if this variable does not appear explicitly.

To compute the Lyapunov exponent λ as a function of the dimensionless parameter ε, one has to consider the Fokker-Planck equation for the stationary distribution of the variable x unconditional upon the value of y, which we note $\bar{\rho}(x)$. One has simply

$$\partial_x \hat{J}_\varepsilon \bar{\rho}(x) = 0. \tag{4.44}$$

One particularity of the Langevin equation (4.37) is the existence of solutions consisting in divergent trajectories in finite time. One to see it is to write the potential from which the Langevin equation derives,

$$\phi_\varepsilon(x) = \frac{x^2}{2} + \varepsilon\frac{x^3}{3}, \tag{4.45}$$

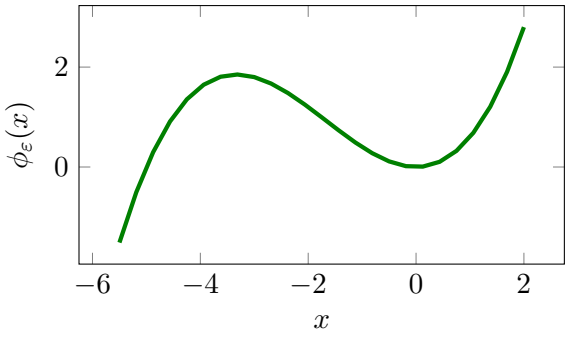

Figure 4.5 – Potential associated to the Langevin equation (4.39): $\phi_\varepsilon(x) = x^2/2 + \varepsilon x^3/3$, here plotted for $\varepsilon = 0.3$.

which diverges to $-\infty$ as $x \to -\infty$ (see figure 4.5). As a consequence, the stationary solution must have a non-zero flux $j(\varepsilon)$. The solution of the Fokker-Planck equation with non-zero flux is

$$\bar{\rho}(x) = j(\varepsilon) \exp\left(-\phi_\varepsilon(x)\right) \int_{-\infty}^{x} \mathrm{d}x' \exp\left(\phi_\varepsilon(x')\right). \tag{4.46}$$

The value of the flux $j(\varepsilon)$ is determined by the normalisation:

$$\int_{-\infty}^{\infty} \mathrm{d}x\, \bar{\rho}(x) = 1. \tag{4.47}$$

The finite value of $j(\varepsilon)$ is linked to the rate of formation of the caustics, because those singularities correspond to points where $\delta x = 0$ and δv is finite, which leads to a divergence of $Z(t) = \delta v/\delta x$. The figure 4.4 shows $\bar{\rho}(x)$ for two values of ε, and the dependence of $j(\varepsilon)$ in ε. One can show that the dimensional rate of formation $J(\varepsilon) = \gamma j(\varepsilon)$ in the limit $\varepsilon \to 0$ reads

$$J = \frac{\gamma}{2\pi} \exp\left(-\frac{1}{6\varepsilon^2}\right). \tag{4.48}$$

Considering the expression of $\varepsilon = \sqrt{\mathcal{D}\tau_\mathrm{S}}$, it supports the hypothesis that the rate of caustic formation has a non-analytic behaviour as the Stokes time τ_S approaches zero [WMB06; FP07].

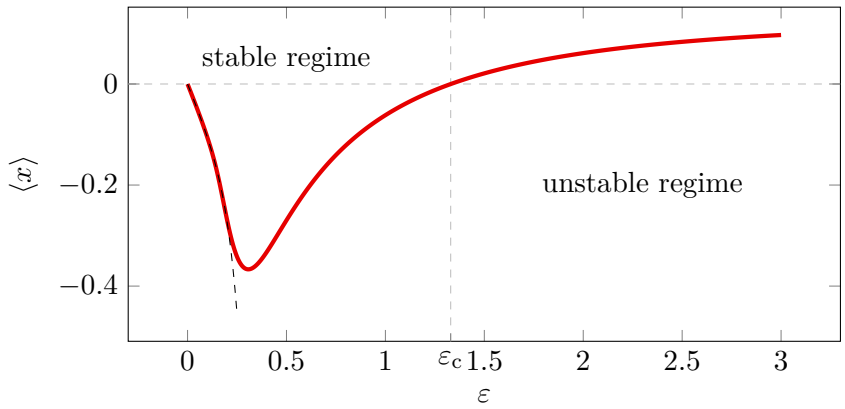

Figure 4.6 – Mean $\langle x \rangle$ as a function of the dimensionless parameter ε. The Lyapunov exponent λ is proportional to $\langle x \rangle$: $\lambda = \varepsilon\gamma \langle x \rangle$. The transition between the two regimes occurs at $\varepsilon_\mathrm{c} \approx 1.33$. In dashed black lines, the expansion up to the 7th power of ε.

The transition between the stable and the unstable linear dynamics occurs when the Lyapunov exponent λ changes sign. One can compute the evolution of $\langle x \rangle$ as a function of ε, where

$$\langle x \rangle = \int_{-\infty}^{\infty} \mathrm{d}x\, x\, j(\varepsilon) \exp\left(-\phi_\varepsilon(x)\right) \int_{-\infty}^{x} \mathrm{d}x' \exp\left(\phi_\varepsilon(x')\right). \tag{4.49}$$

The result is show figure 4.6. For large values of ϵ the dynamics is unstable and the trajectories converge on a strange attractor with positive fractal measure. The Lyapunov exponent changes sign at $\varepsilon_c \approx 1.33$, so that for $\varepsilon < \varepsilon_c$ the dynamics is stable and paths coalesce. Remark that small values of ϵ correspond to large values of γ, which denotes an overdamped dynamics.

The exponent α defined in (4.27) is a function of the dimensionless parameter ε only. We determined this exponent via numerical simulations of the model (4.3). The results are shown figure 4.7. As expected, α is negative for $\varepsilon < \varepsilon_c$, leading to non-normalisable distributions (see also figure 4.3) in the absence of the noise $\sqrt{2D}\,\eta(t)$. As the transition between the two regimes is smooth, it is appealing to extend the notion of fractal dimension to the negative cases.

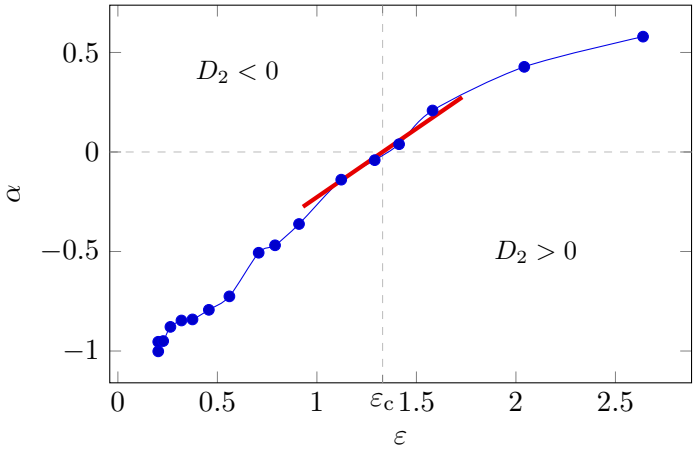

Figure 4.7 – Exponent α as a function of the dimensionless parameter ε. One observes a possible non-analytical behaviour at $\varepsilon \to 0$. At the transition for $\varepsilon = \varepsilon_c$, the linear dependence of α in $\varepsilon - \varepsilon_c$ computed in (4.81) is drawn in red lines.

We now consider two different perturbative approaches of (4.42) in order to determine the coefficient α as a function of ε. First we look for an expansion around $\varepsilon = 0$, which correspond to the limit where the non-linear term vanishes; the tools that we use are similar to the ones developed in the previous chapter. Then, we sketch the first steps of a perturbation expansion about the critical point ε_c where the fractal dimension changes sign.

4.3.2 Perturbation theory in the Gaussian noise limit

We consider the dynamics in the limit $\varepsilon \to 0$, which we call the Gaussian noise limit, because for $\epsilon = 0$ the Langevin equation for x in (4.39) is linear, so that its solution $\bar{\rho}(x)$ is Gaussian.

Perturbative expansion of the Lyapunov exponent

The Langevin equation for x is and Ornstein-Uhlenbeck process perturbed by a non-linear term:

$$\dot{x} = -x - \varepsilon x^2 + \sqrt{2}\,\bar{\xi}(\tau). \tag{4.50}$$

In order to compute a perturbative expansion in powers of ε of the Lyapunov exponent defined as $\lambda = \varepsilon\gamma\,\langle x\rangle$, we can use the tools developed in the previous chapter. One formally searches an expansion of $\langle x\rangle$ in the form

$$\langle x\rangle = \sum_{n=0}^{\infty} a_n \varepsilon^n. \tag{4.51}$$

For convenience, we define

$$x_1 = \frac{x}{\sqrt{2}} \quad \text{and} \quad \sigma = \sqrt{2}\,\varepsilon \tag{4.52}$$

so that

$$\dot{x}_1 = -x_1 - \sigma x_1^2 + \xi(\tau). \tag{4.53}$$

The density of probability for x_1 verifies a Fokker-Planck equation, which can be turn into an "hamiltonian" form:

$$(\hat{\mathcal{H}}_0 + \sigma\hat{\mathcal{H}}_1)\,|\Psi_0\rangle = 0 \tag{4.54}$$

Here $\mathcal{H}_0$ is an hermitian operator corresponding to the dynamics for $\varepsilon = 0$ and reads

$$\mathcal{H}_0 = \frac{1}{2} - \frac{x_1^2}{2} + \frac{1}{2}\partial^2_{x_1x_1} \tag{4.55}$$

where $\hat{a}^\dagger$ and $\hat{a}$ are the classical creation and annihilation operators whose actions on the orthogonal set of eigenvectors $\{|\phi_n\rangle\}_{n\in\mathbf{N}}$ of $\mathcal{H}_0$ are

$$a\,|\phi_n\rangle = \sqrt{n}\,|\phi_{n-1}\rangle\,, \quad a^\dagger\,|\phi_n\rangle = \sqrt{n+1}\,|\phi_{n+1}\rangle \quad \text{so that} \quad \hat{\mathcal{H}}_0\,|\phi_n\rangle = -n\,|\phi_n\rangle\,. \tag{4.56}$$

The operator $\hat{\mathcal{H}}_1$ corresponds to the non-linear part of the Langevin equation (4.52) and reads in terms of the creation and annihilation operators

$$\hat{\mathcal{H}}_1 = -\frac{1}{\sqrt{2}}\left(\hat{a}^\dagger\hat{a}^\dagger\hat{a}^\dagger + \hat{N}\hat{a} + \hat{a}^\dagger(2\hat{N}+1)\right) \quad \text{with} \quad \hat{N} = \hat{a}^\dagger\hat{a}\,. \tag{4.57}$$

One can show that $\langle x_1\rangle$ reads

$$\langle x_1\rangle = \frac{1}{\sqrt{2}}\,\langle\phi_1\,|\,\Psi_0\rangle\,. \tag{4.58}$$

Finally, one finds for $\langle x\rangle$ that all the even orders in ε are zero, and that the orders in the expansion read

$$\langle x\rangle = -\varepsilon - 5\varepsilon^3 - 60\varepsilon^5 - 1105\varepsilon^7 + \mathcal{O}(\varepsilon^9). \tag{4.59}$$

The coefficients a_n grow with n like ${\beta_1}^n(n!)^{\beta_2}$ with $\beta_1 > 1$ and $\beta_2 > 0$. As they are all of the same sign, contrarily to the expansion in chapter 3, one cannot expect the series to converge towards the function $\langle x\rangle\,(\varepsilon)$, which is likely non-analytic near $\varepsilon = 0$. Nevertheless, the first terms give a first approximation of the behaviour of the Lyapunov exponent near $\varepsilon = 0$ (see figure 4.6).

Computation of the fractal dimension

To determine the dependence of the coefficient α in ε in the Gaussian limit, we need to solve the equation (4.42) for both α and $\rho(x)$. We explicitly expand both $\rho(x)$ and α in powers of ε:

$$\alpha = \sum_{j=0}^{\infty}\alpha_j\,\varepsilon^j \quad \text{and} \quad \rho(x) = \sum_{j=0}^{\infty}\rho_j(x)\,\varepsilon^j. \tag{4.60}$$

To proceed, we do not look for a transformation in order to use an orthonormal basis of function, as in the previous paragraph. We follow a method discussed in [WMG10], where we consider non-hermitian operators, thus expanding each of the functions $\rho_j(x)$ in terms of a basis set:

$$\rho_j(x) = \sum_{n=0}^{\infty}\varrho_n^{(j)}\,\phi_n(x). \tag{4.61}$$

Here the basis functions $\{\phi_j(x)\}_{n=0}$ are un-normalised harmonic oscillator states, generated by raising and lowering operators:

$$\hat{b}^\dagger = -\partial_x, \quad \hat{b} = \partial_x + x \tag{4.62}$$

with explicitly

$$\phi_0(x) = \mathcal{N}_0\exp\left(-\frac{x^2}{2}\right), \quad \hat{b}^\dagger\,\phi_n(x) = \phi_{n+1}(x), \quad \text{and} \quad \hat{b}\,\phi_n(x) = n\phi_{n-1}(x). \tag{4.63}$$

The exact expression of the normalisation constant $\mathcal{N}_0$ is not needed. The Fokker-Planck equation (4.42) reads

$$\left[-\alpha\varepsilon(\hat{b}+\hat{b}^\dagger) - \hat{b}^\dagger\hat{b} - \varepsilon\hat{b}^\dagger(\hat{b}^\dagger+\hat{b})^2\right]\rho = 0. \tag{4.64}$$

By substituting the expressions of $\rho(x)$ and α defined in (4.60), one finds the recursion

$$-\alpha_{n-1}\,\phi_1(x) - \hat{b}^\dagger\hat{b}\,\rho_n(x) + Q_n(x) = 0 \tag{4.65}$$

where $Q_n(x)$ is explicitly expressed in terms of the solutions $\rho_m(x)$ obtained at lower orders ($m < n$):

$$Q_n(x) = -\sum_{m=1}^{n-2}\alpha_m(\hat{b}^\dagger+\hat{b})\,\rho_{n-m-1}(x) + \left[\hat{b} - \hat{b}^\dagger\hat{b}^2 - (\hat{b}^\dagger)^3 - 2(\hat{b}^\dagger)^2\hat{b}\right]\,\rho_{n-1}(x) \tag{4.66}$$

$$= \sum_{k=0}^{\infty} Q_{n,k}\,\phi_k(x). \tag{4.67}$$

In addition, we use the zero flux condition for the conditional distribution (4.43). One can show the following orthogonality condition

$$\int_{-\infty}^{\infty} x\,\phi_k(x)\,\mathrm{d}x = \delta_{k1} \tag{4.68}$$

which immediately implies

$$\varrho_1^{(j)} = 0 \quad \text{for all } j. \tag{4.69}$$

As a consequence, the recursion (4.65) is solved if we set $\alpha_{n-1} = Q_{n,1}$ for all n.

We start the iteration with $\rho_0(x) = \phi_0(x)$, which leads to

$$-\alpha_0\,\phi_1 - \hat{b}^\dagger\hat{b}\,\rho_1 + \phi_1 + \phi_3 \tag{4.70}$$

so that $\alpha_0 = -1$ and $\rho_1(x) = \phi_3(x)/3$. Solving recursively the system of perturbation equations therefore yields $\alpha_0 = -1$, and then, $\alpha_j = 0$ for all values of $j > 0$, so that the development of α has only one non-zero term[(1)]. This can be shown with the following induction. Assume that $\alpha_j = 0$ up to order $j = n-2$; then all of the terms in the summation in (4.66) are zero. The coefficient $Q_{n,1} = \alpha_{n-1}$ results from the application of the operator $\hat{b} - \hat{b}^\dagger\hat{b}^2$ to the component $\varrho_2^{(n-1)}\,\phi_2(x)$ of $\rho_{n-1}(x)$, and this is automatically zero.

The implication is that, as the Lyapunov exponent λ or the flux $j(\varepsilon)$, α has a non-analytic dependence upon ε, such as $\alpha \sim -1 + c\exp(-S/\epsilon^2)$ (where c and S are constants). Yet, our data showed figure 4.7 are not sufficiently precise to determine the non-analytic term reliably.

4.3.3 Behaviour at the transition

We perform here a perturbative expansion about the critical point, where the Lyapunov exponent changes sign. For the model studied here, this occurs at $\varepsilon_\mathrm{c} \approx 1.33$. The parameter of the perturbation is then α, which is in first approximation (see figure 4.7) proportional to $\varepsilon - \varepsilon_\mathrm{c}$:

$$\alpha = K(\varepsilon - \varepsilon_\mathrm{c}) + \mathcal{O}((\varepsilon-\varepsilon_\mathrm{c})^2). \tag{4.71}$$

We want to find the coefficient K. To proceed, we consider the Fokker-Planck equation for the conditional density of probability $\rho(x)$:

$$(-\alpha\varepsilon x + \partial_x\hat{J}_\varepsilon)\,\rho \quad \text{with} \quad \hat{J}_\varepsilon = \partial_x + x + \varepsilon x^2. \tag{4.72}$$

[(1)] This was previously noted by B. Mehlig and K. Gustafsson in an unpublished work.

We search $\rho(x)$ in the form of a development in powers of $(\varepsilon - \varepsilon_c)$:

$$\rho(x) = \rho_0(x) + (\varepsilon - \varepsilon_c)\rho_1(x) + \mathcal{O}((\varepsilon - \varepsilon_c)^2). \tag{4.73}$$

Note that the functions $\rho_i(x)$ are distinct from the ones of the previous development around $\varepsilon = 0$. We substitute this expression into the equation (4.72) and find at the lowest order in $(\varepsilon - \varepsilon_c)$

$$\partial_x \hat{J}_{\varepsilon_c} \rho_0 = 0. \tag{4.74}$$

so that one has explicitly

$$\rho_0(x) = j(\varepsilon_c) \exp\left(-\phi_{\varepsilon_c}(x)\right) \int_{-\infty}^{x} \mathrm{d}x' \exp\left(\phi_{\varepsilon_c}(x')\right). \tag{4.75}$$

In the first order in $(\varepsilon - \varepsilon_c)$, one obtains

$$\partial_x \hat{J}_{\varepsilon_c} \rho_1 - K\varepsilon_c x\, \rho_0 + \partial_x(x^2\rho_0) = 0, \tag{4.76}$$

The function $\rho_1(x)$ must be determined under two constraints. First the distribution $\rho(x)$ must stay normalised, and second it must verify the zero flux condition (4.43). It leads us to

$$\int_{-\infty}^{\infty} \mathrm{d}x \rho_1(x) = 0 \quad \text{and} \quad \int_{-\infty}^{\infty} \mathrm{d}x\, x\rho_1(x) = 0. \tag{4.77}$$

As the operator $\partial_x \hat{J}_{\varepsilon_c}$ is linear, one can decompose the solution ρ_1 into the sum of two functions: $\rho_1(x) = \rho_1'(x) + \rho_1''(x)$, satisfying the equations

$$\partial_x \hat{J}_{\varepsilon_c} \rho_1(x) + \partial_x(x^2\rho_0) = 0, \tag{4.78}$$

$$\partial_x \hat{J}_{\varepsilon_c} \rho_1'(x) - K\varepsilon_c x\, \rho_0 = 0. \tag{4.79}$$

The goal is to compute the values $\langle x' \rangle$ and $\langle x'' \rangle$, defined as the first moments of the partial distributions $\rho_1'(x)$ and $\rho''(x)$, so that the zero flux condition reads

$$\langle x' \rangle + \langle x'' \rangle = 0. \tag{4.80}$$

The solution of equation (4.78) is easy to find. Consider the normalised solution of the Fokker-Planck equation (4.72) with $\alpha = 0$, which we denote by $\varrho(x, \varepsilon)$. It is straightforward to notice that the function $\partial_\varepsilon \varrho(x, \varepsilon)|_{\varepsilon=\varepsilon_c}$ is the proper solution of (4.78). As a result, $\langle x' \rangle$ is simply equal to $\partial_\varepsilon \langle x \rangle |_{\varepsilon=\varepsilon_c}$, where $\langle x \rangle$ is the first moment of the unconditional distribution $\bar{\rho}(x)$ defined in (4.46). In particular, one can express explicitly $\langle x' \rangle$ in terms of a combination of single integrals. One finds $\langle x' \rangle \approx 0.141$.

The equation (4.79) is more difficult to solve, and one must use numerical approaches in order to compute the multiple integrals involved. One finds $\langle x'' \rangle \approx 0.205\, K$, so that finally

$$K \approx 0.688. \tag{4.81}$$

This value is in good accordance with the numerical results shown figure 4.7.

4.4 Generalisations and conclusion

4.4.1 Noisy dynamical systems

We claim that power-law distributions for the departure of an attractor may occur in dynamical systems which are *non-autonomous*, and *stable*, in the sense that in the absence of noise, solutions converge to a point attractor. It is the interaction between the noise and the fluctuating environment which generates intermittency, via a stochastic mechanism of amplification. The

particular physical situation studied here is the prototype of more general processes, which in one dimension can be written in the form

$$\dot{x} = v(x,t) + \sqrt{2\mathcal{D}}\,\eta(t) \tag{4.82}$$

where the velocity field $v(x,t)$ satisfies its own equation of motion, and fluctuates in space and time. The instantaneous Lyapunov exponent can be readily defined from the noise-free dynamics:

$$Z(t) = \frac{\partial v}{\partial x}, \tag{4.83}$$

and the system is stable when $Z(t)$ is negative in average: $\lambda = \langle Z(t) \rangle < 0$. The main point is that the statistics of the fluctuating quantity $Z(t)$ should not depend on the trajectory.

4.4.2 Power-law distribution and negative fractal dimension

It has already been pointed out (see [Wil+12]) that fluctuating instantaneous Lyapunov exponents can lead to clustering of trajectories, even if the Lyapunov exponent λ is positive, implying an exponential growth of small separations. For such systems, a set of trajectories forms a dynamical fractal structure in the physical space, which can be characterised by its correlation dimension D_2. The probability density function for the separation of trajectories then follows a power-law:

$$P(\Delta x) \sim |\Delta x|^{D_2 - 1}. \tag{4.84}$$

In this chapter we showed that we can find power-law distributions even in the case of a stable dynamical system, with $\lambda < 0$. These distributions arise if we add a noise in the equation of motion which prevents all trajectories to merge. Typically, two random processes are involved in the dynamics: the noise $\sqrt{2\mathcal{D}}\,\eta(t)$ avoids two nearby trajectories to merge, while the positive fluctuations of $Z(t)$ might lead to large excursions, which are a signature of intermittency, and eventually lead to power-law distribution.

Numerical evidences and analytical results exhibited for our particular model the following functional form for $P(\Delta x)$:

$$P(\Delta x) \sim |\Delta x|^{\alpha - 1}. \tag{4.85}$$

where α is negative for $\lambda < 0$, so that $P(\Delta x)$ is non-normalisable for $\Delta x \to 0$. This is expected, because in the absence of noise all trajectories merge into a single one, and the attractor is a point-like structure. The noise term causes a regularisation of the density of probability in the limit of small separations $\Delta x \to 0$.

The similarities between (4.84) and (4.85), the independence of α in the noise term and its smooth variation at the transition between the stable and the unstable regime drive us to extend the notion of correlation dimension to negative values, setting $D_2 = \alpha < 0$. When the system is stable ($\lambda < 0$), the point-like attractor still has a fractal dimension, which is negative. We claim that this results are generic for non-autonomous dynamical systems, so that the addition of the noise term in the equation of motion allows the emergence of a property of the underlying dynamical system alone.

4.4.3 Link to other definitions of the fractal dimension

It is of interest to see if the analysis presented here can be extended to other definitions of fractal dimensions. In the chapter 2 we presented the case of a vanishing Cantor set where the box-counting dimension appeared to be negative. However, if we try to compute the box-counting dimension for the model presented in this chapter, we will not obtain a negative fractal dimension. The main issue is the presence of the noise term, which is prominent for small separations Δx.

Thus, by decreasing the size of the box, we will characterize the diffusion induced by the noise term, and not the properties of the unperturbed system.

We can also compare the notion of negative fractal dimension to an other estimate of the fractal dimension, the Lyapunov dimension D_{KY} [KY79], defined as follows. Considering an ordered Lyapunov spectrum $\lambda_1 \geq \lambda_2 \geq \cdots \geq \lambda_n$, and let j be the largest integer for which $\lambda_1 + \lambda_2 + \cdots + \lambda_j \geq 0$. Then, the Kaplan-Yorke formula reads

$$D_{\mathrm{KY}} = j + \frac{\sum_{i=1}^{j} \lambda_i}{|\lambda_{j+1}|}. \tag{4.86}$$

The Lyapunov dimension is generally an upper bound for fractal dimensions. For the one dimensional system studied in this chapter, the application of this formula is straightforward. In the unstable case ($\lambda > 0$) one obtains $D_{\mathrm{KY}} = 1$, which does not faithfully describe the behaviour of the system, while in the stable case ($\lambda < 0$) one obtains $D_{\mathrm{KY}} = 0$. In both cases, the Lyapunov dimension fails to give us supplementary information on the system, because it does not consider *fluctuations* of the Lyapunov exponent. For $\lambda > 0$ the negative fluctuations of the instantaneous Lyapunov exponent drive the formation of clusters and dynamical attractors with correlation dimension smaller than 1. On the contrary for $\lambda > 0$ the positive fluctuations of the instantaneous Lyapunov exponent coupled with the action of the diffusion term lead to negative fractal dimensions.

It is interesting to note that the effects on fluctuating Lyapunov exponents were already analysed by Grassberger and Procaccia [GP84], in particular in order to compare the correlation dimension with the Kaplan-Yorke formula (4.86). They also obtained a sedimentation description for the dynamics of the separation of trajectories. For a stable direction with a negative Lyapunov exponent, the contribution to the correlation dimension was arbitrary set to 0, and the correlation function along this particular direction were a Dirac function. In this chapter we extended this prescription.

Here we should stress out that the negative fractal dimension lacks certain basic properties expected for dimension estimators. In particular, consider a fractal attractor along the axis x_1 with correlation dimension $\nu_1 > 0$, and another one along the axis x_2 with correlation dimension $\nu_2 > 0$. For a trajectory in the plane (x_1, x_2), the expected number of trajectories on the plane in a ball of radius ϵ scales as

$$\mathcal{N}(\epsilon) \sim \epsilon^{\nu_1 + \nu_2} \tag{4.87}$$

so that the dimensions of the two decoupled attractors add up. Now, if the attractor in space x_1 has a negative fractal dimension, so a point-like structure if the absence of the noise sustaining term, the number of trajectories in a ball of radius ϵ is ill-defined, because of the noise term needed to obtain power-law distributions. Turning off the noise and setting the value of the correlation dimension to zero gives a resulting correlation dimension of value ν_2 for the attractor in the space (x_1, x_2), as expected, so that if we want to add the two values of fractal dimension, one must take the dimension of the attractor in the space x_1 to be 0, rather than the negative value linked to the fluctuations of the Lyapunov exponent (see figure 4.8 and below for a typical example obtained from the chapter 3).

4.4.4 Sedimentation description

The mapping $y = \ln \Delta x$ is widely used in intermittency problems [PST93; PHH94]. In our case it leads to a sedimentation problem, where in the absence of the noise the variable y follows an equation of motion in the form

$$\dot{y} = Z(t). \tag{4.88}$$

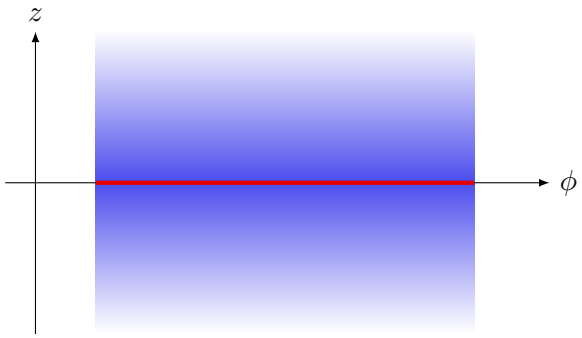

Figure 4.8 – Schematic description of the attractor at the equator of the Kendall sphere. For the dynamics without the homogeneous diffusion, the attractor is the equator of the Kendall sphere (in red), of dimension 1. With the diffusion, we obtains an attractor of dimension -1 in the z direction (in blue).

As the statistics of $Z(t)$ are independent of y, we can show that the only functional form for the density of probability $p(y)$ is exponential:

$$p(y) \sim \exp(\alpha y), \tag{4.89}$$

so that the density of probability for the separation of trajectories $P(\Delta x)$ has a power-law dependence:

$$P(\Delta x) \sim |\Delta x|^{\alpha-1}. \tag{4.90}$$

The average Lyapunov exponent $\lambda = \langle Z(t) \rangle$ can be seen as a drift velocity in the space of the variable $y(t)$. In order to prevent all the particles from going toward $y \to -\infty$, a bouncing or re-injection process is needed at some position y. Such a role is played by the noise term which becomes prominent at small Δx, i.e. for $y \to -\infty$.

It is interesting to note that in the unstable case $\lambda > 0$, the positive drift velocity drives the particles towards $y \to \infty$, so that a re-injection process seems also to be needed. However, the sedimentation description is valid only for small separation of trajectories, and the dynamics for large y is not accurately described by (4.88). Though, if we know the dynamical equations describing $Z(t)$, one can still use the sedimentation equation to compute the fractal dimension, which is positive in that case.

Note that we obtained the same description for the model introduced in the previous chapter, about the dynamics of triangles in turbulent flows. The non-autonomous dynamical system was linked to the action of the like-scale eddies on the tracers, while the noise term was related to the homogeneous diffusion process caused by small-scales eddies. We showed that the equator of the Kendall sphere was an attractor of the dynamics. In terms of the correlation dimension, the fractal dimension of the attractor at $z = 0$ in the space of the variable z was of value -1, because we obtained power-laws in the form

$$P(z) \sim z^{-2}. \tag{4.91}$$

In the space space of the dynamics, which is the Kendall sphere, we need to consider the ϕ direction (see figure 4.8). For the dynamics without a diffusion process in the physical space, all the particles converge towards the equator, so that the attractor is the equator, which has a dimension 1. The addition of the noise breeds the fluctuations, and thus a new structure emerges in the z direction.

In the final chapter of this thesis, we focus on the particular problem (4.88). Using tools from the large deviation theory, we derive a systematic method to find α, the exponent of the sedimentation equilibrium (4.89).

Chapter 5

Non-thermal Einstein relations

Outline

This chapter, more formal than the others, deals with a classic problem of statistical physics. In the two previous chapters of this thesis, we encountered equations in the form

$$\dot{y} = \kappa\, x(t) \tag{5.1}$$

where $x(t)$ is a fluctuating function, whose statistics are independent of y, and κ a constant.

In both chapter 3 and 4 the variable y describes a clustering process. For the triangle model, it is linked to $z = \cos\theta$ via

$$y = \ln z, \tag{5.2}$$

where θ is the polar angle of the shape representative point of the triangle on the Kendall sphere (see section 3.1.1). Due to the action of the strain matrix, the triangles are driven towards the equator of the Kendall sphere, so that $z \to 0$ and consequentially $y \to -\infty$. The presence of

a diffusion term in the equations of motion of the triangle vertices prevents a collapse on the equator, and effectively acts as a re-injection process in the space of the variable z, leading to a normalisable distribution $p(z)$. For the inertial particles, y is linked to the separation of two particles Δx, via

$$y = \ln \Delta x. \tag{5.3}$$

In the path coalescence regime, all the trajectories merge into a single one, so that $\Delta x \to 0$ and thus $y \to \infty$.

In both cases, the equation of motion for y in the limit where z or Δx are small is in the form (5.1), with

$$\langle x \rangle < 0, \tag{5.4}$$

so that on average all the particles go towards $y \to -\infty$. This equation then describes a *sedimentation process* (see section 2.6.1).

The stationary density of probability of y, $P(y)$, is linked to the stationary distribution of z and Δx. In particular, for inertial particles we extended the notion of fractal dimension to the negative cases, and the value of the dimension was determined using various perturbative methods. It is then natural to analyse the equation (5.1) in a more general case.

We begin by setting the problem of sedimentation; in particular, we explain the importance of the boundary conditions in the y-space. Then, we present the determination of the stationary distribution $P(y)$ in terms of a large deviation problem. We study in detail on a process driven by a telegraphic noise, and compute explicitly the form of the distribution $P(y)$. Lastly, we present some perturbative tools in the case where $x(t)$ is generated by non-linear Langevin equations.

The results of this chapter have been partly published in [GPW16].

5.1 Position of the problem

Throughout this chapter we consider stochastic processes in the form (5.1), where the statistics of the "speed" $x(t)$ do not depend on the "position" y, and where we set $\kappa = 1$ without any loss of generality, so that

$$\dot{y} = x. \tag{5.5}$$

One can consider the equation (5.5) as the equation of motion of a particle in a one dimensional axis and whose position is $y(t)$, and whose velocity is $x(t)$. We also consider that the velocity statistics become stationary quickly, in a sense that will be explained later. Thus, unless otherwise stated, the average of a quantity $A(t)$, $\langle A(t) \rangle$, is taken in the stationary limit.

Moreover, we suppose that the process has a *non-zero mean drift velocity*:

$$\langle x \rangle \neq 0. \tag{5.6}$$

If the mean drift velocity is positive (resp. negative), the particle will go toward $y \to \infty$ (resp. $y \to -\infty$) in average. We may also study the case of discrete time processes in the form

$$y_{n+1} = y_n + x_n, \tag{5.7}$$

and we show here that the two types of processes do not not fundamentally differ.

5.1.1 Boundaries and exponential decay

In order to obtain a stationary density of probability $P(y)$ for the position y, we restrict ourselves to problems where space is limited by an impervious barrier (or "wall"), placed at y_{wall}. If the

mean drift is positive, the accessible space is then the half-line $]-\infty, y_{\text{wall}}]$. As a result, the probability distribution is expected to have its maximum close to the wall, and to decay away from it.

We are not interested in describing precisely what happens at the wall. We only suppose that a process of re-injection occurs, allowing the particles to form a structure away from it. In other words, we suppose that we can define a region of the space where the dynamics is not influenced by the presence of the wall. In this region, the problem (5.5) presents a translational invariance. Specifically, the structure of the stationary distribution of the particle position $P(y)$ at a distance $y - y_{\text{wall}}$ to the wall is expected to be independent of y, provided $y - y_{\text{wall}}$ is large compared to a characteristic length scale over which particles lose memory about the wall. This length scale, which corresponds to a *mean free path* for the particle, is assumed to be finite. This excludes from the present study a class of systems where particles can travel arbitrarily far from the wall over a characteristic time scale of the noise (see section 5.2.4 for an explicit examples of such a process).

The translational invariance of the problem leads to a particular structure of the distribution $P(y)$. To proceed, we define a translation operator $\hat{T}_{\Delta y}$ which shifts the origin by Δy by its action on an arbitrary function $f(y)$:

$$\hat{T}_{\Delta y} f(y) = f(y - \Delta y). \tag{5.8}$$

The distribution $P(y)$ must be an eigenfunction of the translation operator, which satisfies

$$\hat{T}\Delta y P(y) = \Lambda P(y) \tag{5.9}$$

for some eigenvalue Λ. It follows that the stationary probability density has an *exponential form* [LL65]:

$$P(y) \sim \exp(\alpha y). \tag{5.10}$$

With the function defined by (5.10), the eigenvalue Λ is equal to $\exp(-\alpha \Delta y)$. The main goal of this chapter is to show how to compute the coefficient α, which we call the *coefficient of sedimentation*[(1)].

It is important to note that $\alpha = 0$ is formally always a solution of the problem. It corresponds to the *homogeneous case*, where the distribution $P(y)$ is uniform, and thus, in a (semi-)infinite system, non-normalisable.

5.1.2 An elementary example: sedimentation of Brownian particles

In a homogeneous system, we expect the motion at long time to resemble a biased random walk with drift velocity $\langle x \rangle$ and diffusion coefficient D_x, given by [Tay22]:

$$D_x = \frac{1}{2} \int_{-\infty}^{\infty} \mathrm{d}t \ \left\langle \left(x(t) - \langle x \rangle\right) \left(x(0) - \langle x \rangle\right) \right\rangle . \tag{5.11}$$

Equation (5.11) gives an expression for the diffusion coefficient, provided the noise $x(t)$ has a finite correlation time, and not only in the case of a very short correlation time.

Temporally uncorrelated process

A first example of a biased random walk is the motion of Brownian particles in a thermal bath under the gravity field, which we treated in chapter 2. We note m the mass of the particle, g the acceleration of the gravity, γ the drag coefficient and D the diffusion coefficient associated

[(1)] This term can be confusing, as α^{-1} has the dimension of a length, but the author did not find a better naming.

with the random action of the molecules of the bath on the particle. In the case of overdamped particles, the equation of motion is

$$\dot{y} = v_0 + \sqrt{2D}\,\xi(t) \tag{5.12}$$

with $v_0 = -mg/\gamma$ and $\xi(t)$ a Gaussian white noise. Thus, the Fokker-Planck equation for the density of probability $P(z,t)$ reads

$$\frac{\partial P}{\partial t} = -v_0 \frac{\partial P}{\partial y} + D\frac{\partial^2 P}{\partial y^2}, \tag{5.13}$$

so that the stationary distribution is

$$P_{\text{stat.}}(y) = \mathcal{A}\exp\left(\frac{v_0}{D}y\right) \tag{5.14}$$

where $\mathcal{A}$ is a normalization constant. One has $\alpha = v_0/D$. In this case the wall is simply the bottom of the thermal bath. From the thermal equilibrium, one can derive the Einstein relation [Ein05; Sut05]:

$$D = \mu k_{\text{B}} T \tag{5.15}$$

where $\mu = -v_0/mg$ is the mobility of the particle. This equation is the first example of a fluctuation-dissipation theorem [Kub66]: the linear response of a given system to an external perturbation – here the drag force counterbalancing the macroscopic motion of the particle – is expressed in terms of fluctuation properties of the system in thermal equilibrium, characterized by the diffusion coefficient D.

This example gives a first possible equation for α, in the form

$$\alpha_{\text{E}} = \frac{\langle x\rangle}{D_x}. \tag{5.16}$$

In the remainder of this chapter, a relation implying α and the statistical properties of $x(t)$ is called a *generalized Einstein relation*, and we refer to (5.16) as a *classical Einstein relation*. In the general case we do not introduce a thermal reservoir and α is solely determined from the equation of motion.

Time correlated Gaussian process

The dynamics of y described by (5.12) is a Markov process: the knowledge of the position y of the particle at time t is enough to determine the future evolution $y(t+\Delta t)$, because the noise $\sqrt{2D}\,\xi(t)$ is temporally uncorrelated. Physically, this means that the correlation time of the process $\sqrt{2D}\,\xi(t)$ is much smaller than the variation time of the macroscopic process $y(t)$. In order to properly describe the dynamics of the small degrees of freedom, one can consider an equation of motion in the form

$$\dot{y} = x(t) \quad \text{and} \quad \dot{x} = -\gamma(x - v_0) + \sqrt{2\mathcal{D}}\,\eta(t), \tag{5.17}$$

where η is a standard Gaussian white noise, and γ is the inverse of the correlation time of the velocity. The speed of the Brownian particle is then an Ornstein-Uhlenbeck process; one generally speaks of a Rayleigh particle [Hoa71]. The motion of y only is not Markovian anymore, because we need to know the value of the velocity x at time t to compute the future evolution of $y(t)$, but the *joint* process $(y(t), x(t))$ is. The system of equations (5.17) is a system of coupled Langevin equations, so that one can write a Fokker-Planck equation for the joint density of probability $P(y,x,t)$:

$$\frac{\partial P}{\partial t} = -x\frac{\partial P}{\partial y} + \gamma\frac{\partial}{\partial x}[(x - v_0)P] + \mathcal{D}\frac{\partial^2 P}{\partial x^2}. \tag{5.18}$$

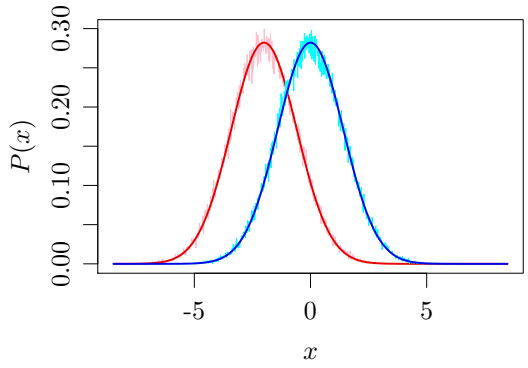

(a) Marginal distribution of x: $P(x) = \int \mathrm{d}y P(y,x)$. In red, the homogeneous case with $\alpha = 0$; in blue, the dynamics in the presence of the wall. Dark lines: theoretical distributions; light lines: numerical simulations.

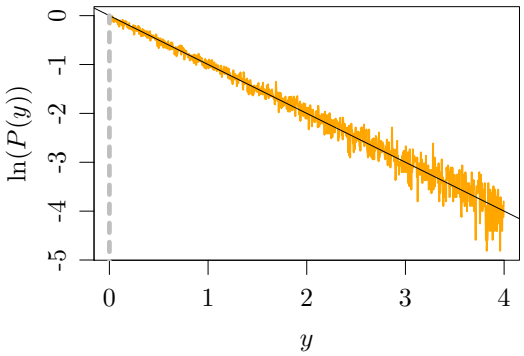

(b) Marginal distribution of y: $P(y) = \int \mathrm{d}x P(y,x)$. The wall is at $y = 0$ (dashed grey line). In orange, numerical computation, in black, analytical prediction. One observes an exponential decrease $P(y) \sim \mathrm{e}^{\alpha y}$ with $\alpha = v_0\gamma^2/\mathcal{D}$.

Figure 5.1 – Analysis of the model (5.17). The parameters are $v_0 = -2$, $\gamma = 1$ and $\mathcal{D} = 2$, so that $\alpha = -1$. Concerning the distribution of the velocities $P(x)$, one obtains a Gaussian distribution of mean v_0 in the homogeneous case, and in the presence of the wall this distribution is shifted, with a zero mean value.

As the Langevin equations are linear, the dynamics is Gaussian, and the stationary density of probability $P(y,x)$ is a Gaussian function:

$$P(y,x) \sim \exp\left(-\frac{\gamma^2}{2\mathcal{D}}x^2\right)\exp\left(\frac{v_0\gamma^2}{\mathcal{D}}y\right). \tag{5.19}$$

After integrating over all the possible values of the speed x, one recovers a sedimentation equilibrium

$$P(y) \sim \exp(\alpha y) \quad \text{with} \quad \alpha = \frac{v_0\gamma^2}{\mathcal{D}}. \tag{5.20}$$

Determining the spatial diffusion coefficient for the process $x(t)$ described by (5.17) gives $D_x = \mathcal{D}/\gamma^2$, so that $\alpha = \alpha_{\mathrm{E}}$, and the classical Einstein relation holds.

5.1.3 First approaches

If the problem (5.5) is Markovian, the density of probability $P(y,t)$ follows in the general case a Master equation:

$$\frac{\partial P(y,t)}{\partial t} = \int \left[W(y|y')P(y',t) - W(y'|y)P(y,t)\right]\mathrm{d}y' \tag{5.21}$$

where $W(y_2|y_1)$ is the transition probability per unit time from y_1 to y_2, which may depend on time. If we know the transition probabilities, we can inject a solution in the form $P(y) = \exp(\alpha y)$ into (5.21), obtaining an implicit equation to find α. However, one generally does not know the transition of probability for y, but rather the statistics of x. Thus, numerous efforts were made to obtain developments in partial differential equations of the Master equation, such as the Kramers-Moyal development [Moy49], or the van Kampen expansion [Kam61].

In general, we process (5.5) is not Markovian, so that one cannot expect to find a partial differential equation for the distribution $P(y,t)$. A variety of different approaches to find approximate equations in the form of a Fokker-Planck equation exists. As a fruitful example, one can cite a method proposed in [SSS86]. Considering the more general problem

$$\dot{y} = f(y) + g(y)x(t) \tag{5.22}$$

where f and g are smooth functions, and $x(t)$ is a random process independent of y. Let $\rho(y,t)$ be the density of trajectories in the space phase, for a given realisation of the noise $x(t)$. This density verifies a Liouville equation

$$\partial_t \rho(y,t) = -\partial_y \left[(f(y) + g(y)x(t))\rho(y,t) \right], \tag{5.23}$$

which can be written, using the terminology of van Kampen [Van92],

$$\dot{u} = \hat{A}\, u \tag{5.24}$$

with $u = \rho(y,t)$ and $\hat{A}$ a stochastic operator:

$$\hat{A} = -\partial_y \left[(f(y) + g(y)x(t))\cdot \right]. \tag{5.25}$$

The density of probability for y, $P(y,t)$, is related to the average of $\rho(y,t)$ over all the realisations of $x(t)$:

$$P(y,t) = \langle \rho(y,t) \rangle . \tag{5.26}$$

One then can use tools developed by van Kampen [Van76] to compute an approximate evolution equation for $\langle u \rangle = P(y,t)$. Usually, the noise $x(t)$ is an Ornstein-Uhlenbeck process, and one can obtain a series expansion for $P(y,t)$ in powers of the correlation time, and involving spatial derivatives of $P(y,t)$.

Our approach however does not make explicit use of a generalisation of a Fokker-Planck equation, but rather uses large deviation theory. In particular, we explicitly show that the classical Einstein relation is not valid in the general case.

5.2 Large deviation formulation

In this section, we first compute an implicit equation for α, without reference to any particular model. Then we show how the formalism of large deviation theory apply in this case. We also give two explicit examples where the prediction of an exponential decay fails.

5.2.1 A general form of the Einstein relation

Discrete time processes

We consider the discrete-time dynamics

$$y_{n+1} = y_n + x_n. \tag{5.27}$$

If the x_n are *non-correlated*, then there exists a simple relation between the probability density for y at time $n+1$, P_{n+1}, and the probability density for y at time n, P_n. Let $\pi(x_n)$ be the probability density of x_n, which does not depend on n. One has

$$P_{n+1}(y) = \int \mathrm{d}x\, P_n(y-x)\pi(x). \tag{5.28}$$

We look for a stationary distribution for y in the form $P_{\text{stat.}}(y) = \exp(\alpha y)$. From (5.28) one obtains

$$1 = \int \mathrm{d}x\ \mathrm{e}^{-\alpha x}\, \pi(x) = \langle \mathrm{e}^{-\alpha x} \rangle . \tag{5.29}$$

Nevertheless, in the general case the velocities are *correlated*, so we cannot use such a simple approach. Let $\pi(x_n, n)$ be the probability density of x_n, which this time depends on n. One has

$$P_{n+1}(y) = \int \mathrm{d}x\, P_n(y-x)\pi(x,n). \tag{5.30}$$

One cannot simply take the stationary limit because, as the speeds are correlated, $P_n(x,n)$ depends explicitly on the "time" n. Thus, we iterate this process to obtain for $m > 1$

$$P_{n+m}(y) = \int \mathrm{d}\left(\sum_{i=1}^{n+m-1} x_i\right) P_n\left(y - \sum_{i=1}^{n+m-1} x_i\right) \Pi\left(\sum_{i=n}^{n+m-1} x_i, n\right). \tag{5.31}$$

where $\Pi\left(\sum_{i=n}^{n+m-1} x_i, n\right)$ is the density of probability of the sum $\sum_{i=n}^{n+m-1} x_i$. Now, if m is much larger than the correlation time of x_n, the latter distribution does not depend on n anymore, so that one can take legitimately the stationary limit. Looking for a stationary distribution $P_{\text{stat.}}$ in the form $\exp(\alpha y)$, one obtains

$$\lim_{m\to\infty} \left\langle \exp\left(-\alpha \sum_{i=0}^{m} x_i\right)\right\rangle = 1. \tag{5.32}$$

The conditions of validity of this approach will be explained later, but we already see that the quantity defined in (5.32) must exist. In particular, we suppose that the noise $x(t)$ has a finite correlation time.

Continuous time processes

We now consider the discrete time process

$$\dot{y} = x \tag{5.33}$$

and define the temporal integral of this equation over a time t:

$$y(T) = y(0) + \Delta y(T) \quad \text{where} \quad \Delta y(T) = \int_0^T \mathrm{d}t\, x(t). \tag{5.34}$$

The analysis is similar to the one made for the discrete time process. Let $\Pi(\Delta y, T)$ be the probability density of Δy at time T. Provided T is much larger than the correlation time of the original process $x(t)$ so that we can assume that $\Delta y(T)$ is independent of the initial time, we express the condition that the distribution $P(y)$ is stationary in the form:

$$P(y) = \int \mathrm{d}\Delta y P(y - \Delta y)\, \Pi(\Delta y, T). \tag{5.35}$$

Using explicitly the exponential form of the PDF $P(y)$, one obtains the expression:

$$\lim_{T\to\infty} \int \mathrm{d}\Delta y\ \exp(-\alpha \Delta y)\, \Pi(\Delta y) = 1, \tag{5.36}$$

which can be interpreted as the average of $\exp(-\alpha\Delta y)$, the variable $\Delta y(T)$ being characterized by its density of probability, $\Pi(\Delta y)$. Finally one has an equation similar to the discrete time case:

$$\lim_{T\to\infty} \left\langle \exp\left(-\alpha \int_0^T \mathrm{d}t\, x(t)\right)\right\rangle = 1. \tag{5.37}$$

Thus, we obtained explicit equations for α, both for discrete time processes and continuous time processes. We now present the formalism needed to analysis such equations.

5.2.2 The large deviation principle

Both equations (5.32) and (5.37) can be simply analysed with the formalism of the large deviation theory, which we introduce here. The goal of the following is not to present the mathematical foundation of the large deviation theory, nor to review all the physics fields in which this theory is at play. Such a work will widely exceed the framework of this thesis, and an excellent review of the applications of the large deviation theory in physics can be found in [Tou09]. We will use the large deviation theory as a generalization of the law of large numbers. We begin by a simple example; then we introduce the basics concepts and show how to express the equations (5.32) and (5.37) with this formalism.

Gaussian sample mean

We consider a sequence of independent random variables $\{x_i\}$, identically distributed according to the Gaussian probability density

$$p(x_i) = \frac{1}{\sqrt{2\pi\sigma^2}} \exp\left(-\frac{(x_i-\mu)^2}{2\sigma^2}\right). \tag{5.38}$$

Define an estimator of the mean value of the variables:

$$m_n = \frac{1}{n}\sum_{i=1}^{n} x_i. \tag{5.39}$$

One naturally expects that $\lim_{n\to\infty} m_n = \langle x_i \rangle = \mu$, but we are interested in the asymptotic form of the probability density $P(m_n)$. It is straightforward to show that

$$P(m_n) = \sqrt{\frac{n}{2\pi\sigma^2}} \exp\left(-\frac{n(m_n-\mu)^2}{2\sigma^2}\right). \tag{5.40}$$

This distribution can be directly calculated, or we can use the fact that a sum of Gaussian variables is also Gaussian-distributed. For large values of n, one can extract a exponential behaviour of this exact result:

$$P(m_n) \underset{n\to\infty}{\asymp} \mathrm{e}^{-nI(m)} \quad \text{where} \quad I(m) = \frac{(m-\mu)^2}{2\sigma^2}. \tag{5.41}$$

The function $I(m)$ is generally called a *rate function*. It gives us the behaviour of the distribution $P(m_n)$ for large n. The notation $\underset{m\to\infty}{\asymp}$ means that we neglect the sub-dominant terms with respect to the decaying exponential, here $\sqrt{n}$ for the density (5.40). In our case $I(m)$ is convex (see figure 5.2a) and possesses a single minimum at $m = \mu$, which is also a zero of the function. As a result, the distribution of the estimator m_n gets more and more concentrated around its expected value μ as n grows.

The Gärtner-Ellis theorem

The random variable m_n then follows a *large deviation principle*, characterized by the existence of a rate function $I(m)$ and an exponential decay of its density of probability as n grows. More generally, a random variable A_n follows a large deviation principle if it verifies the Gärtner-Ellis theorem [Gär77; Ell84]. Define the *scaled cumulant generating function* of A_n by

$$\lambda(k) = \lim_{n\to\infty} \frac{1}{n} \ln \langle \exp(nkA_n) \rangle \tag{5.42}$$

for $k \in \mathbf{R}$. If $\lambda(k)$ exists and is differentiable for all $k \in \mathbf{R}$, then the variable A_n satisfies a large deviation principle:

$$P(A_n) \underset{n\to\infty}{\asymp} \mathrm{e}^{-nI(a)} \tag{5.43}$$

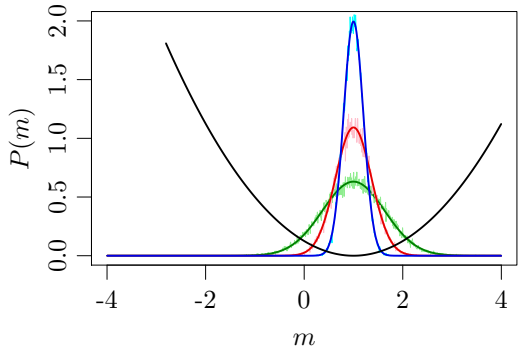

(a) Gaussian sample mean with $\mu = 1$ and $\sigma = 2$, theoretical distributions and numerical simulations, and rate function $I(m)$ in black. In green, $n = 10$, in red, $n = 30$ and in blue $n = 100$.

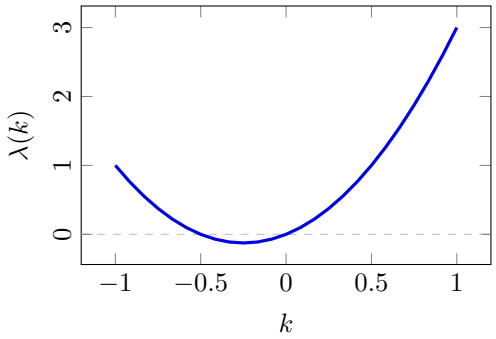

(b) Scaled cumulant generating function for the Gaussian sample mean, $\lambda(k) = \mu k + k^2\sigma^2/2$, with the same values $\mu = 1$ and $\sigma = 2$.

Figure 5.2 – Analytical large deviation results for the Gaussian sample mean. The rate function $I(m)$ and the scaled cumulant generating function $\lambda(k)$ are both quadratic.

with a rate function given by

$$I(a) = \sup_{k\in\mathbf{R}}\{ka - \lambda(k)\}. \tag{5.44}$$

The transform defined above is an extension of the Legendre transform called the *Legendre-Fenchel transform* [Roc70].

For the Gaussian sample mean, or in general for any sample mean of independent and identically distributed random variables, the scaled cumulant generating function as a simple form. One has

$$\lambda(k) = \lim_{n\to\infty} \frac{1}{n} \ln \left\langle \exp\left(k \sum_{i=1}^{n} x_i\right)\right\rangle = \ln \left\langle \mathrm{e}^{kx_i} \right\rangle . \tag{5.45}$$

This result is known as the Cramér's Theorem [Cra38]. For the Gaussian sample mean, $\lambda(k)$ can be explicitly computed:

$$\lambda(k) = \ln \left\langle \mathrm{e}^{kx_i} \right\rangle = \mu k + \frac{1}{2}\sigma^2 k^2. \tag{5.46}$$

Just as the rate function, $\lambda(k)$ is quadratic (see figure 5.2b).

Continuous time processes

The extension to continuous time processes is straightforward. For a stochastic process $x(t)$, we consider the random variable $A_T[x(t)]$ defined as the functional[(2)]:

$$A_T[x(t)] = \frac{1}{T}\int_0^T \mathrm{d}t\, x(t). \tag{5.47}$$

The variable $A_T[x(t)]$ is simply the time integral of $x(t)$. The scaled cumulant generating function is

$$\lambda(k) = \lim_{T\to\infty} \ln \left\langle \exp\left(TkA_T[x(t)]\right)\right\rangle . \tag{5.48}$$

Provided that $\lambda(k)$ exists and is differentiable, the Gärtner-Ellis theorem holds and $A_T[x(t)]$ follows a large deviation principle.

[(2)] More generally, one can define a functional in the form

$$A_T[x(t)] = \frac{1}{T}\int_0^T \mathrm{d}t\, f(x(t))$$

where f is some smooth function. In this text only the case $f = \mathrm{Id}$ is studied.

5.2.3 Implicit equation for the coefficient of sedimentation

Under the formalism of the large deviation principle, the condition (5.32) for discrete time processes, and (5.37) for continuous time processes merely states that $-\alpha$ is a root of the scaled cumulant generating function of the process x:

$$\lambda(-\alpha) = 0, \tag{5.49}$$

where explicitly $\lambda_{\text{dis.}}$ for the discrete time case and $\lambda_{\text{cont.}}$ for the continuous time case read

$$\lambda_{\text{dis.}}(k) = \lim_{n\to\infty} \frac{1}{n} \ln \left\langle \exp k \left(\sum_{i=1}^{n} x_i \right) \right\rangle \quad \text{and} \quad \lambda_{\text{cont.}}(k) = \lim_{T\to\infty} \frac{1}{T} \ln \left\langle \exp k \left(\int_0^T \mathrm{d}t\, x(t) \right) \right\rangle. \tag{5.50}$$

Thus, the determination of α amounts to finding solutions of (5.49). One remarks that, as stated previously, $\alpha = 0$ is always a root of $\lambda(k)$.

The condition for a sedimentation equilibrium corresponds to the existence of the function $\lambda(k)$, so that one can argue that the sedimentation holds if the sample mean of the process x follows a large deviation principle.

As the scaled cumulant generating function is convex [Tou09], it guarantees the existence of at most one other value of α satisfying (5.49). The scaled cumulant generating function is linked to the moments and cumulants of the random process. In particular, one has

$$\left.\frac{\mathrm{d}\lambda(k)}{\mathrm{d}k}\right|_{k=0} = \langle x \rangle\,, \tag{5.51}$$

so that if $\langle x \rangle \neq 0$, this identity ensures that the non-zero value of α and $\langle x \rangle$ have identical signs. These two results, namely the existence of at most one non-zero solution of (5.49) and the sign identity $\alpha \cdot \langle x \rangle > 0$, derive immediately from the large deviation formulation of the sedimentation process.

Lastly, it is interesting to note that the condition (5.49) can be recovered in the case where $x(t)$ derives from infinitesimal stochastic generator, in the generic form[(3)]

$$\dot{x} = b(x) + \sigma(x)\,\eta(t). \tag{5.52}$$

On one hand, from the equation of motion $\dot{y} = x(t)$, the stationary joint density of probability for x and y, $P(x, y) = \rho(x)\,\mathrm{e}^{\alpha y}$, verifies a Fokker-Planck equation:

$$0 = (-\alpha x + \hat{\mathcal{F}})\rho \quad \text{where} \quad \hat{\mathcal{F}} = -\frac{\partial}{\partial x}[b(x)\cdot] + \frac{1}{2}\frac{\partial^2}{\partial x^2}[\sigma^2(x)\cdot]. \tag{5.53}$$

Therefore, the equation (5.53) has a non-zero solution if the operator $-\alpha x + \hat{\mathcal{F}}$ has a non-zero kernel, which gives an explicit expression for α. On the other hand, the scaled cumulant generating function $\lambda(k)$ is then equal to the largest eigenvalue of the operator $\mathcal{L}_k = \mathcal{L} + kx$, where $\mathcal{L}$ is the generator of the stochastic process described in (5.52) (see [DV75]):

$$\mathcal{L} = b(x)\frac{\partial}{\partial x} + \frac{\sigma^2(x)}{2}\frac{\partial^2}{\partial x^2}. \tag{5.54}$$

Thus, as $\mathcal{L}$ is the adjoint of $\mathcal{F}$, they share the same (real) spectrum, so that the condition under α is the same as (5.49).

[(3)] For simplicity we consider a one-dimensional generating process for $x(t)$, but the result can be generalized to higher dimensions.

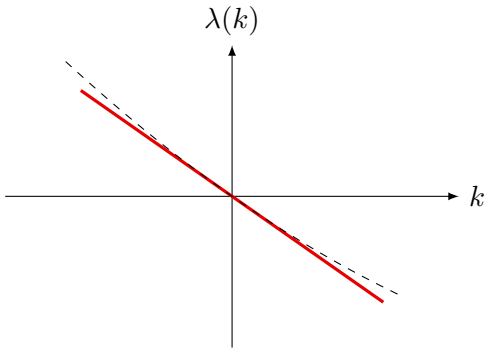

Figure 5.3 – Scaled cumulant generating function $\lambda(k) = x_0 k$ for the non-fluctuating process (5.55) with $x_0 < 0$. In dashed line, we represent the effect of a small fluctuating term on the process: $\dot{y} = x_0 + \sqrt{2D}\,\eta(t)$ with $D \ll 1$ and $\eta(t)$ a Gaussian white noise. As $\lambda(k)$ is a convex function, the non-zero root tends to $+\infty$ as D tends to 0.

5.2.4 Examples where the exponential sedimentation fails

The theory presented here requires the existence of a large deviation principle for the sample mean of the process $\langle x \rangle$, and the existence of a non-zero root of the scaled cumulant generating function. We present here two typical examples where the sedimentation prediction fails.

Non-fluctuating process

This example is very elementary; consider the process

$$\dot{y} = x_0 \tag{5.55}$$

where x_0 is simply a constant. The scaled cumulant generating function has then the simple form $\lambda(k) = x_0 k$, so that λ has only one root, $\alpha = 0$. Physically, the absence of random fluctuations in the process prevents the sedimentation from occurring.

In the light of the previous chapter, such a process can describe the dynamics of a system with a non-fluctuating Lyapunov exponent:

$$\dot{X} = x_0 X \quad \text{with} \quad X = \exp(y). \tag{5.56}$$

To extend the correlation dimension to negative values, we saw that the Lyapunov exponent must experience positive fluctuations in order to produce intermittency bursts and to obtain power-law distributions. Formally, one can set the negative fractal dimension to the value $-\infty$, because the other root of $\lambda(k)$ is at $+\infty$ if x_0 is negative (see figure 5.3).

Long tail distributions

We consider here a discrete time process in the form

$$y_{n+1} = y_n + x_n \tag{5.57}$$

where the x_n are independent and identically distributed random variables according to the so-called Pareto density [Lan73]:

$$P(x) = \frac{A}{(1 + |x - x_0|)^\beta} \tag{5.58}$$

with x_0 a constant, $\beta > 3$ and A a normalization constant. In this case the drift velocity $\langle x \rangle = x_0$ and the diffusion coefficient D_x are finite, but $\lambda(k)$ is undefined, except at $k = 0$. The slowly decaying tails of the distribution $P(x)$ imply that there is no region in space where the particles are not sensitive to the presence of the wall. In a sense, the mean free path of a particle, that is the typical lentgh travel between two jumps, is infinite.

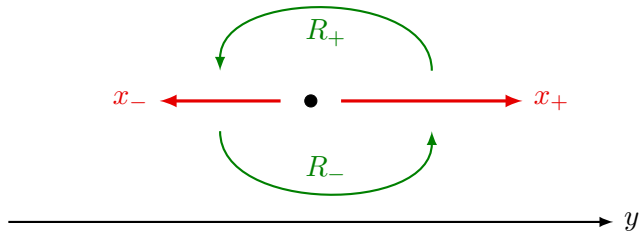

Figure 5.4 – Notation and schematic description of the telegraph noise process.

5.3 A completely solvable problem: telegraphic noise

We consider in this section a continuous time process which is non-Markovian and non-Gaussian, and derive exactly the expression of the scaled cumulant generating function. In particular, we investigate the Gaussian limit, that is the conditions where the sedimentation coefficient α can be approximated by α_{E}, determined by the classical Einstein relation (5.16).

5.3.1 The model

We assume that the process $x(t)$ can only take two values, $x_+ > 0$ or $x_- < 0$. In other words, the particle at position $y(t)$ can have two possible velocities. The velocity switches from x_+ to x_- (resp. x_- to x_+) with transition rates R_+ (resp. R_-); see figure 5.4. In the steady state regime, the probability of the velocity to be x_+ is noted ρ^{s}_+ (resp. ρ^{s}_-), and corresponds to the fraction of time during which the velocity is x_+ (resp. x_-). One has simply

$$\rho^{\mathrm{s}}_+ = \frac{R_-}{R_- + R_+} \quad \text{and} \quad \rho^{\mathrm{s}}_- = \frac{R_+}{R_- + R_+}. \tag{5.59}$$

As a consequence, the mean velocity $\langle x \rangle$ is given by

$$\langle x \rangle = \frac{R_+ x_- + R_- x_+}{R_+ + R_-}. \tag{5.60}$$

As defined, the stochastic process of the speeds $x(t)$ is Markovian; nevertheless, the integrated process $y(t)$ generated by $\dot{y} = x$ is not.

Direct analysis

We introduce the probability distribution of the position y, $P_+(y,t)$ and $P_-(y,t)$, conditioned on the value of x being equal to x_+ and x_-. We expect the stationary distributions P_+ and P_- to decay exponentially as a function of y. The evolution equation for P_+, P_- is given by an advection-diffusion equation:

$$\frac{\partial}{\partial t}\begin{pmatrix} P_+ \\ P_- \end{pmatrix} = -\frac{\partial}{\partial x}\begin{pmatrix} x_+ P_+ \\ x_- P_- \end{pmatrix} + \begin{pmatrix} -R_+ & R_- \\ R_+ & -R_- \end{pmatrix}\begin{pmatrix} P_+ \\ P_- \end{pmatrix}. \tag{5.61}$$

We look for solutions in the form $P_\pm(y) = A_\pm \exp(\alpha y)$. By injecting this form into the equation (5.61), one obtains an eigenvalue equation:

$$0 = \mathbf{M}(\alpha)\begin{pmatrix} A_+ \\ A_- \end{pmatrix} \tag{5.62}$$

where we defined

$$\mathbf{M}(-\alpha) = \begin{pmatrix} -\alpha x_+ - R_+ & R_- \\ R_+ & -\alpha x_- - R_- \end{pmatrix} \tag{5.63}$$

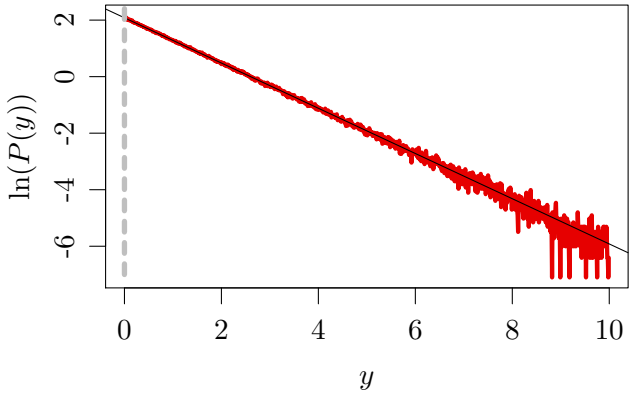

Figure 5.5 – In red, plot of the stationary density of probability $P(y)$ obtained from numerical simulations of the telegraphic model, with parameters $R_+ = 0.6$, $R_- = 0.4$, $x_+ = 0.5$ and $x_- = -1$. The mean speed is $\langle x \rangle = -0.4$. The linear regression shows that away from the wall (at $y = 0$, represented by a vertical grey dashed line), $\ln P(y) \sim \alpha y$ with $\alpha = -0.8$, as expected from (5.65).

so that α is solution of

$$\det \mathbf{M}(-\alpha) = 0. \tag{5.64}$$

This condition leads to a simple algebraic equation, with only one non-zero root:

$$\alpha = -\frac{x_+ R_- + x_- R_+}{x_+ x_-}. \tag{5.65}$$

One immediately sees that as $x_+ x_- < 0$, the coefficient α and $\langle x \rangle$ have the same sign.

Figure 5.5 presents the results of a numerical simulation of the model, with an impervious wall placed at $y = 0$. The elastic rebound condition is the following: if the position $y(t + \Delta t)$ at time $t + \Delta t$ happens to be negative while $y(t)$ is positive, the new position is set to $-y(t + \Delta t)$, and the speed of the particle at x_+. In practice, the re-injection mechanism is of no importance for the sedimentation process away from the wall, as long as it allows the existence of a region in space where the mean flux of particles is zero.

Classical Einstein relation

We show here that the value of α differs from the one given by the classical Einstein relation. To proceed, we consider the telegraphic noise process $x(t)$ unconditional with the position $y(t)$, and note $\rho_\pm(t)$ the distributions of the speeds x_+ and x_-. Their evolution equation is

$$\frac{\partial}{\partial t} \begin{pmatrix} \rho_+ \\ \rho_- \end{pmatrix} = \begin{pmatrix} -R_+ & R_- \\ R_+ & -R_- \end{pmatrix} \begin{pmatrix} \rho_+ \\ \rho_- \end{pmatrix}. \tag{5.66}$$

To compute the diffusion coefficient D_x, let $P_{a|b}(t)$ be the probability that the system is in the state x_a at time t, knowing that it was in the state x_b at time 0 (with $a, b \in \{+, -\}$). It follows that

$$\begin{aligned} \langle x(t)x(0) \rangle &= \sum_{a,b} x_a x_b \rho_{a|b}(t) \rho_b^{\mathrm{s}} \\ &= \Big(x_+ \rho_{+|+}(t) + x_- \rho_{-|+}(t) \Big) x_+ \rho_+^{\mathrm{s}} + \Big(x_+ \rho_{+|-}(t) + x_- \rho_{-|-}(t) \Big) x_- \rho_-^{\mathrm{s}} \end{aligned} \tag{5.67}$$

so that

$$C(t) = \langle x(t)x(0) \rangle - \langle x \rangle^2 = \frac{R_+ R_-}{(R_+ + R_-)^2} (x_+ - x_-)^2 \, \mathrm{e}^{-t/\tau} \tag{5.68}$$

where $\tau = (R_+ + R_-)^{-1}$ is the correlation time of the process. Then, one can compute the expression of the diffusion coefficient

$$D_x = \int_0^\infty \mathrm{d}t\, C(t) = \frac{R_+ R_-}{(R_+ + R_-)^3}(x_+ - x_-)^2, \tag{5.69}$$

so that the classical Einstein relation gives

$$\alpha_\mathrm{E} = \frac{\langle x \rangle}{D_x} = \frac{(R_+ + R_-)^2}{R_+ R_-}\frac{R_+ x_- + R_- x_+}{(x_+ - x_-)^2}. \tag{5.70}$$

As α differs from α_E, this is an example of a simple process that does not follow the classical Einstein relation.

5.3.2 Large deviation formulation

We compute in this section the explicit expression of the scaled cumulant generating function $\lambda(k)$ for the telegraphic noise process, and show that the condition $\lambda(-\alpha) = 0$ indeed corresponds to the equation (5.65). To proceed, we adapt the general approach described in [Tou09].

We begin by discretizing the time and consider $x_n = x(n\Delta t)$ where Δt is a very small time step. As the process $x(t)$ is Markovian, one can write

$$\begin{aligned}\left\langle \exp\left(k\int_0^T \mathrm{d}t\, x(t)\right)\right\rangle &\simeq \left\langle \exp\left(k\sum_{i=1}^n \Delta t\, x_n\right)\right\rangle \\ &= \sum_{x_1,x_2,\ldots,x_n} \rho(x_1)\,\mathrm{e}^{k\Delta t x_i}\,\pi(x_2|x_1)\,\mathrm{e}^{k\Delta t x_2}\cdots\pi(x_n|x_{n-1})\,\mathrm{e}^{k\Delta t x_n}\end{aligned} \tag{5.71}$$

where $\rho(x_1)$ is probability distribution of the initial state x_1, and $\pi(x_{i+1}|x_i)$ is the probability transition from state x_i to state x_{i+1}, that is the conditional probability of x_{i+1}, given x_i. The summation in (5.71) is over all the possible values of x_i, here x_+ or x_-. The probability transition can be written as a 2×2 matrix:

$$\pi(x_a|x_b) = [\boldsymbol{\pi}]_{ab} \quad \text{with} \quad \boldsymbol{\pi} = \begin{pmatrix} 1 - R_+\Delta t & R_-\Delta t \\ R_+\Delta t & 1 - R_-\Delta t \end{pmatrix} \quad \text{and } a, b \in \{+, -\}. \tag{5.72}$$

Now define the "tilted transition matrix" $\boldsymbol{\pi}_k$ as $[\boldsymbol{\pi}_k]_{ab} = \pi_{ab}\,\mathrm{e}^{k\Delta t x_a}$. The right hand term in (5.71) then involves the matrix $\boldsymbol{\pi}$ and the vector $\vec{\rho}_k$ defined as $[\vec{\rho}_k]_a = \rho(x_a)\,\mathrm{e}^{k\Delta t x_a}$. One obtains

$$\left\langle \exp\left(k\sum_{i=1}^n \Delta t\, x_n\right)\right\rangle = \sum_{a\in\{+,-\}} \left[\boldsymbol{\pi}_k^{n-1}\cdot\vec{\rho}_k\right]_a \tag{5.73}$$

For sufficiently small Δt, the matrix $\boldsymbol{\pi}$ is ergodic, because all his coefficients are strictly positive. The Perron–Frobenius theory of positive matrices states that the asymptotic behavior of the product (5.73) does not depend on the initial state, and is dominated by the largest eigenvalue of the matrix $\boldsymbol{\pi}_k$, $\xi(k)$:

$$\left\langle \exp\left(k\sum_{i=1}^n \Delta t\, x_n\right)\right\rangle \sim \xi(k)^n. \tag{5.74}$$

As a consequence, the scaled cumulant generating function $\lambda(k)$ is

$$\lambda(k) = \lim_{\Delta t\to 0}\lim_{n\to\infty}\frac{1}{n\Delta t}\ln\left\langle \exp\left(k\sum_{i=1}^n \Delta t\, x_n\right)\right\rangle \tag{5.75}$$

$$= \lim_{\Delta t\to 0}\frac{1}{\Delta t}\ln\xi(k). \tag{5.76}$$

For small Δt, the matrix $\boldsymbol{\pi}_k$ can be written as

$$\boldsymbol{\pi}_k = \mathbf{Id} + \Delta t\, \mathbf{M}(k) + \mathcal{O}(\Delta t^2), \tag{5.77}$$

where $\mathbf{M}(k)$ is defined in (5.63). Denoting by $\mu(k)$ the largest eigenvalue of $\mathbf{M}(k)$, one has

$$\xi(k) = 1 + \Delta t\, \mu(k) \tag{5.78}$$

so that

$$\lambda(k) = \lim_{\Delta t \to 0} \frac{1}{\Delta t} \ln \xi(k) = \mu(k). \tag{5.79}$$

Thus, the scaled cumulant generating function $\lambda(k)$ is equal to the largest eigenvalue of the matrix $\mathbf{M}(k)$. As a consequence, the condition $\lambda(-\alpha) = 0$ merely states that $\det(\mathbf{M}(-\alpha)) = 0$, so that one recovers the equation (5.65).

5.3.3 Explicit computation of the scaled cumulant generating function

The expression of $\lambda(k)$ is obtained from the matrix $\mathbf{M}(k)$. After a little algebra one has

$$\lambda(k) = \frac{1}{2}(R_+ + R_-)\left[-1 + k\frac{x_+ + x_-}{R_+ + R_-} + \sqrt{1 + \gamma^2 k^2 + 2\frac{\beta - 1}{\beta + 1}\gamma k}\right] \tag{5.80}$$

where we defined the parameters γ and β as follows:

$$\gamma = \frac{v_+ - v_-}{R_+ + R_-} \quad \text{and} \quad \beta = \frac{R_-}{R_+}. \tag{5.81}$$

The parameter γ has a dimension of a length, and is the product of $\tau = (R_+ + R-)^{-1}$, the correlation time of the process, which provides an estimate of how long the particle stays with either velocity x_+ or x_-, and of $x_+ - x_- = (x_+ - \langle x \rangle) - (x_- - \langle x \rangle)$, which is the size of the difference between the mean and the instantaneous velocity. Thus, it is of the order of the size travelled by a particle between two collisions, so that it corresponds to the mean free path of the particle. Note that γ and β are strictly positive.

As expected, the function $\lambda(k)$ is convex (see figure 5.6a). It has two asymptotes in $k \to \pm\infty$, which allows us to recover the two possible values of the speed

$$\lim_{k \to \infty} \lambda(k)/k = x_+ \qquad \text{and} \qquad \lim_{k \to -\infty} \lambda(k)/k = x_-. \tag{5.82}$$

Moreover, the value of the slope at $k = 0$ is the mean of v:

$$\left.\frac{\mathrm{d}\lambda}{\mathrm{d}k}\right|_{k=0} = \frac{R_- x_+ + R_+ x_-}{R_+ + R_-} = \langle v \rangle . \tag{5.83}$$

The rate function $I(x)$ associated with $\lambda(k)$ is given by the Legendre transform of $\lambda(k)$:

$$I(x) = \max_k (xk - \lambda(k)), \tag{5.84}$$

and a plot is proposed figure 5.6b. As the process presents a maximum and a minimum velocity, the rate function is only defined on the interval $[x_-, x_+]$. It has a minimum in $x_{\min} = \langle x \rangle$, for which $I(x_{\min}) = 0$.

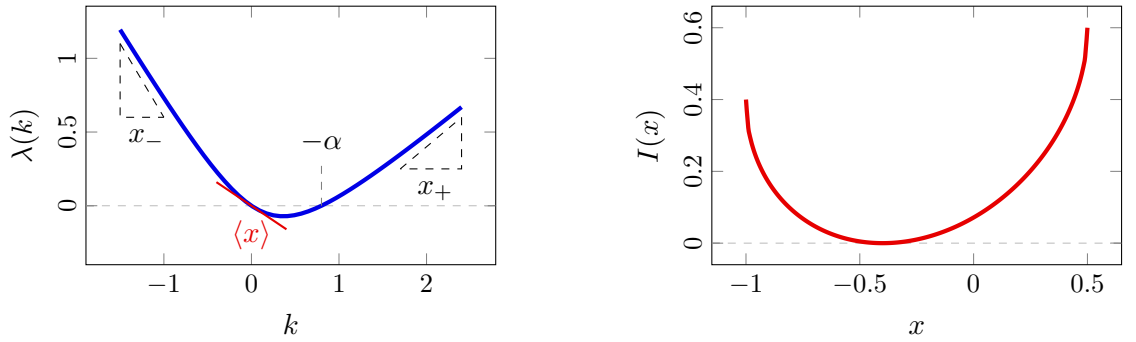

(a) Scaled cumulant generating function $\lambda(k)$.

(b) Rate function $I(x)$.

Figure 5.6 – Analytical large deviation results for the telegraphic process. The rate function $I(x)$ and the scaled cumulant generating function $\lambda(k)$ are both convex. The parameters are $R_+ = 0.6$, $R_- = 0.4$, $x_+ = 0.5$ and $x_- = -1$.

5.3.4 The Gaussian limit

In this section we show in which conditions the coefficient of sedimentation α can be estimated by the result of the classical Einstein relation, α_{E}. To proceed, we notice that in the general case $\lambda(-\alpha)$, as defined in (5.50), can be simply written as a series in powers of α, in the form

$$\lambda(-\alpha) = \lim_{T\to\infty} \frac{1}{T} \ln \left\langle \sum_{n=0}^{\infty} \frac{(-\alpha)^n}{n!} \left(\int_0^T \mathrm{d}t\, x(t) \right)^n \right\rangle = \sum_{n=0}^{\infty} \frac{(-1)^n}{n!} c_n \alpha^n \tag{5.85}$$

where the coefficients c_n are defined as the integrals of the nth order cumulants of the distribution of $x(t)$:

$$c_n = \lim_{T\to\infty} \frac{1}{T} \int_0^T \mathrm{d}t_1 \cdots \int_0^T \mathrm{d}t_n\, \kappa[x(t_1), \ldots, x(t_n)]. \tag{5.86}$$

The first cumulants are simply

$$\begin{aligned} \kappa[x(t_1)] &= \langle x \rangle\,, \\ \kappa[x(t_1), x(t_2)] &= \langle x(t_1)x(t_2) \rangle - \langle x \rangle \\ \kappa[x(t_1), x(t_2), x(t_3)] &= \langle x(t_1)x(t_2)x(t_3) \rangle - \langle x \rangle \langle x(t_2)x(t_3) \rangle\,, \\ &\quad - \langle x \rangle \langle x(t_1)x(t_3) \rangle - \langle x \rangle \langle x(t_1)x(t_2) \rangle + 2 \langle x \rangle^3\,. \end{aligned} \tag{5.87}$$

One can easily check[(4)] that the two first coefficients of the series expansion c_1 and c_2, as defined by (5.86), coincide with $\langle x \rangle$ and $2D_x$, as defined by (5.11). This immediately shows that, whatever the process, the classical Einstein relation predicts the correct value of the coefficient α when the

[(4)] Indeed, one has

$$\begin{aligned} c_2 &= \lim_{T\to\infty} \frac{1}{T} \int_0^T \mathrm{d}t_1 \int_0^T \mathrm{d}t_2\, (\langle x(t_1)x(t_2) \rangle - \langle x \rangle^2) \\ &= \lim_{T\to\infty} \frac{1}{T} \left[\int_0^T \mathrm{d}t_1 \int_0^{t_1} \mathrm{d}t_2\, f(t_1,t_2) + \int_0^T \mathrm{d}t_1 \int_{t_1}^T \mathrm{d}t_2\, f(t_1,t_2) \right] \quad \text{where } f(t_1,t_2) = \langle x(t_1)x(t_2) \rangle - \langle x \rangle^2 \\ &= \lim_{T\to\infty} \frac{1}{T} \left[\int_0^T \mathrm{d}t_2 \int_{t_2}^T \mathrm{d}t_1\, f(t_1,t_2) + \int_0^T \mathrm{d}t_1 \int_{t_1}^T \mathrm{d}t_2\, f(t_1,t_2) \right] \\ &= \lim_{T\to\infty} \frac{2}{T} \int_0^T \mathrm{d}t_1 \int_{t_1}^T \mathrm{d}t_2\, f(t_1,t_2) \quad \text{because } f(t_1,t_2) = f(t_2,t_1), \end{aligned}$$

so that one obtains

$$c_2 = 2D_x.$$

cumulants of order higher than 3 vanish, which is the case when x is given by a Gaussian process. It leads us to the following result: if the noise is a Gaussian process, then the Einstein relation holds. This statement does not depend on whether the process is Markovian or not. Thus, for the time correlated Gaussian process studied in 5.1.2, one immediately recover the classical Einstein relation, without having to solve the joint Fokker-Planck equation.

The telegraphic process is not a Gaussian process; if it was, the scaled cumulant generating function $\lambda(k)$ would be quadratic in k. Thus, the classical Einstein relation holds if $\lambda(k)$ is well approximated by a parabola in the domain $[0, \alpha]$. From the expression (5.50) of $\lambda(k)$, one deduces that such an approximation is valid if

$$\mu = \gamma|\alpha_{\mathrm{E}}| \ll 1. \tag{5.88}$$

The parameter μ compares the mean free path γ to the typical length of the sedimentation α_{E}^{-1}. This condition can be recovered by considering the ratio $\alpha/\alpha_{\mathrm{E}}$. After some algebra, one obtains

$$\frac{\alpha}{\alpha_{\mathrm{E}}} = \left[\left(1+\mu\frac{\beta}{1+\beta}\right)\left(1-\mu\frac{1}{1+\beta}\right)\right]^{-1}, \tag{5.89}$$

Thus, when μ tends to zero, α tends to α_{E}.

Note that this convergence can also be characterized by the evolution of the coefficients c_n. In fact, it is possible to show that for $n > 2$ one has

$$\frac{c_n \alpha_{\mathrm{E}}^n}{n! c_1 \alpha_{\mathrm{E}}} = \mu^{n-2} G_n(y) \tag{5.90}$$

where the G_n are bounded functions. It also seems that $\sup_{y\in\mathbf{R}_+} |G_n(y)| = 1$ for all values of n (this prediction has been checked up to $n = 10$). One can conclude that for μ tending to 0, the coefficients of order strictly higher than 2 in the series expansion (5.85) vanish, so that in the Gaussian limit the scaled cumulant generating function indeed becomes quadratic.

5.4 Processes driven by non-linear Langevin equations

We present in this section some perturbative tools that can be used when the velocity x is generated by a set of non-linear Langevin equations.

5.4.1 Motivations

In both chapters 3 and 4, we obtained equations in the form

$$\begin{aligned} \dot{y} &= [\vec{x}]_1, \\ \dot{\vec{x}} &= -\vec{x} + \varepsilon \vec{g}(\{x_i\}) + \vec{\eta}(t), \end{aligned} \tag{5.91}$$

where the function $\vec{g}(\{x_i\})$ is non-linear in the coordinates of the n-vector $\vec{x}$, $\vec{\eta}(t)$ is a Gaussian white noise vector with statistics

$$\langle \eta_i(t) \rangle = 0 \quad \text{and} \quad \langle \eta_i(t)\eta_j(t') \rangle = \delta_{ij}\delta(t), \tag{5.92}$$

and ε is small parameter which quantifies the non-linearity of the system. It is interesting to note that while studying two different physical systems (advected triangles and inertial particles), the equations describing the separation of trajectories can still be written in the generic form (5.91). We argue that it is the case for many stochastic models (see [MW04; WM03; WG14]).

Considering (5.91), the correlation time of the noise $\vec{x}$ is equal to 1, which can be simply set by rescaling the time with the dimensional correlation time of the process. Note that, as we

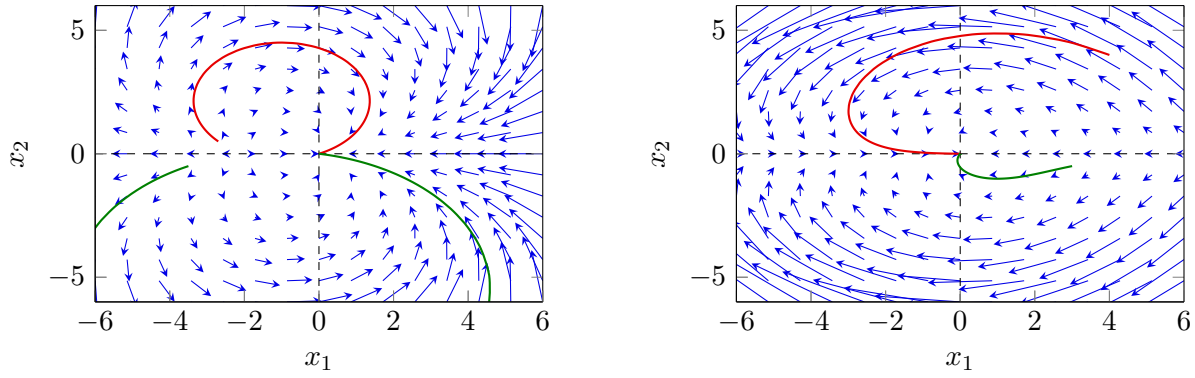

(a) Deterministic vector field for the model (5.95): $(-x_1 + \varepsilon(\Gamma x_2^2 - x_1^2), -x_2 - 2\varepsilon x_1 x_2)$, with $\varepsilon = 0.5$ and $\Gamma = 1$.

(b) Deterministic vector field for the model (5.96) studied in chapter 3: $(-x_1 - 2\varepsilon x_2^2, -x_2 - 2\varepsilon x_1 x_2)$, with $\varepsilon = 0.5$.

Figure 5.7 – Two examples of vector fields. On the left, trajectories with large excursions from the centre $(0, 0)$ can occur.

stated in section 3.4.2, we arbitrarily decided to put the perturbative parameter ε in front of the non-linear terms, rather than in front of the Gaussian white noises. Thus, the system of coupled Langevin equations generating the velocity can be seen as an non-linear perturbed overdamped harmonic oscillator in interaction with a thermostat, and perturbed by non-linear dynamics, rather than as a deterministic dynamical system involving small additive noises.

In the following we present some perturbative methods to characterize the behaviour of the system of equations (5.91).

5.4.2 Validity of the approach

We look for a perturbation expansion of the solution of (5.91) in the form of a power series in ε. However, this perturbative method, in its elementary form, does not permit to derive possible non-analytical behaviours of the solutions. In order to see if we miss potential non-analytical terms, one can study qualitatively the solutions of the Langevin equations

$$\dot{\vec{x}} = -\vec{x} + \varepsilon \vec{g}(\{x_i\}) + \vec{\eta}(t). \tag{5.93}$$

Typically, non-analytical terms are associated to solutions of (5.93) presenting large excursions [MW04]. We already encountered such behaviour. In chapter 4, the Langevin equation studied is

$$\dot{x} = -x - \varepsilon x^2 + \sqrt{2}\eta(t), \tag{5.94}$$

which admits solutions diverging in a finite time. Though, for a one-dimensional Langevin equation, the presence of an even non-linear term κx^{2n} in the Langevin equation always leads to divergences, because the resulting term in the associated potential is in the form $\kappa x^{2n+1}/(2n+1)$, which tends to $-\infty$ for $x \to \infty$ or $x \to -\infty$, depending on the sign of κ. In [MW04], the authors derive a two-dimensional system of Langevin equation, based on a model similar to the one studied in chapter 4:

$$\begin{aligned} \dot{x}_1 &= -x_1 + \varepsilon(\Gamma x_2^2 - x_1^2) + \eta_1(t), \\ \dot{x}_2 &= -x_2 - 2\varepsilon x_1 x_2 + \eta_2(t), \end{aligned} \tag{5.95}$$

where Γ is a dimensionless parameter close to 1, and ε, as in chapter 4, is a measure of the importance of inertial effects. If we plot in the plane (x_1, x_2) the deterministic vector field $(-x_1 + \varepsilon(\Gamma x_1^2 - x_1^2), -x_2 - 2\varepsilon x_1 x_2)$ associated with the model (5.95) (see figure 5.7a), one can qualitatively observe the existence of a non-stable manifold at $x_2 = 0$, which possible large

excursions from the fixed point at $(0,0)$, sustained by the additive noise. On the contrary, the model obtained from the dynamics of triangles in chapter 3:

$$\begin{aligned} \dot{x}_1 &= -x_1 - 2\varepsilon x_2^2 + \eta_1(t), \\ \dot{x}_2 &= -x_2 + 2\varepsilon x_1 x_2 + \eta_2(t), \end{aligned} \tag{5.96}$$

does not present divergent trajectories (see figure 5.7b). Nevertheless, as stated in section 3.4.3, the expansion of $\langle x_1 \rangle$ for the model (5.96) still seems to present a radius of convergence which is equal to 0, but with alternate signs in the development, so that re-summation tools can be applied [DD73].

5.4.3 Direct expansion for the coefficient of sedimentation

We briefly recall the perturbative methods that can be used to obtain a direct expansion of the coefficient of sedimentation α in the form of a power series of the parameter ε. Such methods have already been introduced in chapter 4.

To begin, we write the Fokker-Planck equation that verifies the joint density of probability $P(y, \vec{x}, t)$. One has

$$\frac{\partial P}{\partial t} = x_1 \frac{\partial P}{\partial y} + \hat{\mathcal{F}}_0 P + \varepsilon \hat{\mathcal{F}}_1 P \tag{5.97}$$

where $\hat{\mathcal{F}}_0$ is the Fokker-Planck operator associated with the linear part of the Langevin equation, and $\hat{\mathcal{F}}_1$ is the operator associated with the non-linear part:

$$\hat{\mathcal{F}}_0 = -\frac{\partial}{\partial x_i}[x_i \cdot] + \frac{1}{2}\frac{\partial}{\partial x_i}\left[\frac{\partial}{\partial x_i} \cdot\right] \quad \text{and} \quad \hat{\mathcal{F}}_1 = -\frac{\partial}{\partial x_i}[g_i(\{x_j\}) \cdot]. \tag{5.98}$$

We look for a stationary solution in the form $P(y, \vec{x}) = \rho(\vec{x}) \exp(\alpha y)$. One has

$$0 = [-\alpha x_1 + \hat{\mathcal{F}}_0 + \varepsilon \hat{\mathcal{F}}_1]\rho. \tag{5.99}$$

The idea is to expand α and ρ in the form

$$\alpha = \alpha_i \varepsilon^i \quad \text{and} \quad \rho(\vec{x}) = \rho_i(\vec{x})\varepsilon^i. \tag{5.100}$$

After injecting the expressions in (5.100) into (5.99), one can systematically find the coefficients of the expansion of α, using a set of eigenfunctions of the operator $\hat{\mathcal{F}}_0$.

Note that if we integrate (5.99) over all the coordinates $\{x_i\}$, one obtains

$$0 = \alpha \int_{-\infty}^{\infty} \mathrm{d}x_1 \cdots \int_{-\infty}^{\infty} \mathrm{d}x_n \, x_1 \, \rho(\vec{x}) = \alpha \, \langle x_1 \rangle \, . \tag{5.101}$$

Thus, as we look for a solution with $\alpha \neq 0$, we obtain an implicit equation to find the coefficient of sedimentation:

$$\langle x_1 \rangle = 0. \tag{5.102}$$

The perturbative development presented in section 4.3.3 is based on this equation. Physically, it means that the stationary sedimentation is characterized by a zero-flux condition in the y-space.

5.4.4 Perturbative expansion of the diffusion coefficient

We present here an extension of the method presented in chapter 3, in order to successively compute the expansion of the diffusion coefficient D_{x_1} – defined in (5.11) – in powers of ε. In the following and for simplicity, we treat the one dimensional problem, where the vector $\vec{x}$ has a single component. The extension to higher dimensions is straightforward. The diffusion coefficient

appears in the second term of the expansion (5.85) of the scaled cumulant generating function, and is necessary to compute the classical Einstein relation (5.16). Moreover, from $\dot{y} = x$ one obtains

$$\lim_{T\to\infty} \frac{1}{T} \left\langle \Big(y(t) - y(0) - T \langle x \rangle \Big)^2 \right\rangle = 2D_x, \tag{5.103}$$

so that D_x also quantifies the relative dispersion of $y(t)$ around its expected value $\langle y(t) \rangle = \langle x \rangle t + y(0)$.

The diffusion coefficient (and the mean) are related to the unconditional evolution of x, that is the Langevin equation

$$\dot{x} = -x + \varepsilon g(x) + \eta(t), \tag{5.104}$$

without considering the variable y. Contrarily to the stationary mean of the velocity, $\langle x \rangle$, D_x is related to the correlation function of the process, and consequentially to its temporal evolution.

Hermitian transformation

The Fokker-Planck equation for the density of probability $p(x,t)$ reads

$$\frac{\partial p}{\partial t} = (\hat{\mathcal{F}}_0 + \varepsilon \hat{\mathcal{F}}_1) p. \tag{5.105}$$

We begin by a transformation in order to obtain an hermitian operator from $\hat{\mathcal{F}}_0$. One defines

$$\hat{\mathcal{H}}_i = \exp\left(\frac{x^2}{2}\right) \hat{\mathcal{F}}_i \exp\left(-\frac{x^2}{2}\right) \quad \text{with } i = 1, 2, \tag{5.106}$$

so that the evolution equation of the function $|\psi(x,t)\rangle = p(x,t)\exp(x^2/2)$ is then

$$\frac{\partial |\psi\rangle}{\partial t} = (\hat{\mathcal{H}}_0 + \varepsilon \hat{\mathcal{H}}_1) |\psi\rangle . \tag{5.107}$$

One has a set of eigenvectors of the operator $\hat{\mathcal{H}}_0$: $\hat{\mathcal{H}}_0 |\phi_n\rangle = -n |\phi_n\rangle$. The mean of a quantity related to a ket $|\varphi(t)\rangle$ is simply $\langle \phi_0 | \varphi(t) \rangle$.

Correlation functions

The stationary density of probability for the process $x(t)$ is associated to the ket $|\Psi_0\rangle$, which is an eigenvector of the operator $\hat{\mathcal{H}} = \hat{\mathcal{H}}_0 + \varepsilon \hat{\mathcal{H}}_1$:

$$\left(\hat{\mathcal{H}}_0 + \varepsilon \hat{\mathcal{H}}_1\right) |\Psi_0\rangle = 0 \quad \text{with} \quad \langle \phi_0 | \Psi_0 \rangle = 1. \tag{5.108}$$

Let $\hat{W}(t)$ be the evolution operator associated to the operator $\hat{\mathcal{H}}$:

$$\hat{W}(t) = \exp(t \cdot \hat{\mathcal{H}}). \tag{5.109}$$

As $\hat{\mathcal{H}}$ does not depend on the time, the previous exponential is already ordered. Considering n times $t_1 \geq t_2 \geq \cdots \geq t_n$, one has

$$\langle x(t_1) \cdots x(t_n) \rangle = \left\langle \phi_0 \,\middle|\, \hat{x} \hat{W}(t_1 - t_2) \hat{x} \cdots \hat{x} \hat{W}(t_{n-1} - t_n) \hat{x} \,\middle|\, \Psi_0 \right\rangle . \tag{5.110}$$

For example

$$\langle x(t_1) \rangle = \langle \phi_0 \,|\, \hat{x} \,|\, \Psi_0 \rangle \quad \text{and} \quad \langle x(t_1) x(t_2) \rangle = \left\langle \phi_0 \,\middle|\, \hat{x} \hat{W}(t_1 - t_2) \hat{x} \,\middle|\, \Psi_0 \right\rangle \quad \text{for } t_1 \geq t_2. \tag{5.111}$$

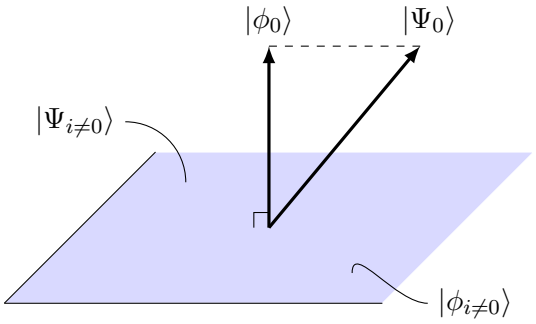

Figure 5.8 – Schematic visualization of the kets $|\phi_i\rangle$ and $|\Psi_i\rangle$. One has $\langle\phi_0|\Psi_0\rangle = 1$, which corresponds to the normalization condition of the distribution p. Moreover, for $n \neq 0$, $|\phi_0\rangle$ is orthogonal to the ket $|\Psi_n\rangle$.

Explicit equation for the diffusion coefficient

Now that we computed the expression of the correlation function, to proceed we introduce a time-dependant quantity:

$$D_x^T = \int_0^T \mathrm{d}t\,[\langle x(0)x(t)\rangle - \langle x\rangle]. \tag{5.112}$$

When T tends to ∞, the coefficient D_x^T tends to D_x. One has

$$\begin{aligned} D_x^T &= \int_0^T \mathrm{d}t \left\langle \phi_0 \right| \hat{x}\hat{W}(t)\hat{x} \left| \Psi_0 \right\rangle - T\,\langle x\rangle \\ &= \left\langle \phi_0 \right| \hat{x}\hat{Y}^T\hat{x} \left| \Psi_0 \right\rangle - T\,\langle x\rangle \quad \text{with} \quad \hat{Y}^T = \int_0^T \mathrm{d}t\,\hat{W}(t). \end{aligned} \tag{5.113}$$

We have to compute the expression of the operator $\hat{Y}^T$. To this end, we suppose that if ε is not too large, we can still diagonalise the operator $\hat{\mathcal{H}}$:

$$\hat{\mathcal{H}} = |\Psi_n\rangle\,\mu_n\,\langle\Psi_n| \quad \text{with } \mu_0 = 0 \text{ and } \mu_{i\neq 0} < 0. \tag{5.114}$$

In other words, we suppose that the spectrum of $\hat{\mathcal{H}}_0$ is not strongly changed by the addition of non-linear terms in the equations of motion. At this point we adopt a matrix representation of the operators, in order to better visualise the calculation. Under this formalism, there is an invertible matrix $\hat{P}$ so that

$$\hat{P}^{-1}\hat{\mathcal{H}}\hat{P} = \begin{pmatrix} \mu_0 & & \\ & \mu_1 & \\ & & \ddots \end{pmatrix} = \hat{D} \tag{5.115}$$

and one has

$$\hat{P}^{-1}\hat{Y}^T\hat{P} = \int_0^T \mathrm{d}t\,\exp(\hat{D}t) = \begin{pmatrix} T & & \\ & -\frac{1}{\mu_1} & \\ & & \ddots \end{pmatrix} + \mathcal{O}(\mathrm{e}^{-T}), \tag{5.116}$$

so that

$$\hat{Y}^T = \hat{P}\left[T\hat{\Pi}_0 + \begin{pmatrix} 0 & & \\ & -\frac{1}{\mu_1} & \\ & & \ddots \end{pmatrix}\right]\hat{P}^{-1} + \mathcal{O}(\mathrm{e}^{-T}), \quad \text{where} \quad \hat{\Pi}_0 = \begin{pmatrix} 1 & & \\ & 0 & \\ & & \ddots \end{pmatrix}. \tag{5.117}$$

One remarks that $\hat{P}\hat{\Pi}_0\hat{P}^{-1}$ is simply the projector of image vect$[\{|\Psi_0\rangle\}]$ and kernel vect$[\{|\phi_0\rangle\}]$ (see figure 5.8)[(5)]:

$$\hat{p} = \hat{P}\hat{\Pi}_0\hat{P}^{-1} = |\Psi_0\rangle\,\langle\phi_0|\,. \tag{5.118}$$

[(5)] Let $\hat{p} = \hat{P}\hat{\Pi}_0\hat{P}^{-1}$. For any vector $|A\rangle$, one gets the unique decomposition $|A\rangle = \sum_{n\in\mathbf{N}} a_n\,|\Psi_n\rangle$, and the action of $\hat{p}$ on $|A\rangle$ reads $\hat{p}\,|A\rangle = a_0\,|\Psi_0\rangle$. One knows that for $n \neq 0$, $\langle\phi_0|\Psi_n\rangle = 0$, because $|\phi_0\rangle \notin \mathrm{im}(\hat{\mathcal{H}})$, and that

Moreover, one has

$$\begin{pmatrix} 0 & & \\ & \frac{1}{\mu_1} & \\ & & \ddots \end{pmatrix} = \begin{pmatrix} 1 & & \\ & \frac{1}{\mu_1} & \\ & & \ddots \end{pmatrix} \begin{pmatrix} 0 & & \\ & 1 & \\ & & \ddots \end{pmatrix} = \begin{pmatrix} 1 & & \\ & \mu_1 & \\ & & \ddots \end{pmatrix}^{-1} \begin{pmatrix} 0 & & \\ & 1 & \\ & & \ddots \end{pmatrix}$$
$$= (\hat{D} + \hat{\Pi}_0)^{-1}(1 - \hat{\Pi}_0). \tag{5.119}$$

It allows us to write

$$\begin{aligned} \hat{Y}^T &= T\hat{p} - \hat{P}\left[(\hat{D} + \hat{\Pi}_0)^{-1}(1 - \hat{\Pi}_0)\right]\hat{P}^{-1} + \mathcal{O}(\mathrm{e}^{-T}) \\ &= T\hat{p} - (\hat{P}\hat{D}\hat{P}^{-1} + \hat{P}\hat{\Pi}_0\hat{P}^{-1})^{-1}(1 - \hat{p}) + \mathcal{O}(\mathrm{e}^{-T}) \\ &= T\hat{p} - (\hat{\mathcal{H}} + \hat{p})(1 - \hat{p}) + \mathcal{O}(\mathrm{e}^{-T}) \end{aligned} \tag{5.120}$$

which leads us to

$$\begin{aligned} D_x^T &= \langle\phi_0\Big|\hat{x}\hat{Y}^T\hat{x}\Big|\Psi_0\rangle - T\langle\phi_0|\hat{x}|\Psi_0\rangle^2 + \mathcal{O}(\mathrm{e}^{-T}) \\ &= T\langle\phi_0|\hat{x}|\Psi_0\rangle^2 - \langle\phi_0\Big|\hat{x}(\hat{\mathcal{H}} + \hat{p})^{-1}(1 - \hat{p})\hat{x}\Big|\Psi_0\rangle - T\langle\phi_0|\hat{x}|\Psi_0\rangle^2 + \mathcal{O}(\mathrm{e}^{-T}). \end{aligned} \tag{5.121}$$

The secular term is cancelled, so that one finally obtains a simple equation for D_x:

$$D_x = -\left\langle \phi_0 \,\middle|\, \hat{x}(\hat{\mathcal{H}} + \hat{p})^{-1}(1 - \hat{p})\hat{x} \,\middle|\, \Psi_0 \right\rangle. \tag{5.122}$$

Application

The equation (5.122) gives us a systematic way to compute the expansion of D_x in powers of ε. The ket $|\Psi_0\rangle$ is computed from (5.108). The operator $(\hat{\mathcal{H}} + \hat{p})^{-1}(1 - \hat{p})$ formally reads

$$(\hat{\mathcal{H}} + \hat{p})^{-1}(1 - \hat{p}) = \hat{\mathcal{H}}_0' \left[\sum_{n=0}^{\infty} \left(-\varepsilon\hat{\mathcal{H}}_1\hat{\mathcal{H}}_0'\right)^n\right](1 - \hat{p}) \tag{5.123}$$

where $\hat{\mathcal{H}}_0'$ is the invertible operator obtained from $\hat{\mathcal{H}}_0$:

$$\hat{\mathcal{H}}_0' = \hat{\mathcal{H}}_0 + |\phi_0\rangle\langle\phi_0|. \tag{5.124}$$

Consider the model obtained in chapter 3, with ε the perturbative parameter (the term 2ε in the evolution equation of y is of no importance):

$$\begin{aligned} \dot{y} &= 2\varepsilon x_1 \\ \dot{x}_1 &= -x_1 - 2x_2^2 + \eta_1(t) \\ \dot{x}_2 &= -x_2 + 2x_1x_2 + \eta_2(t) \end{aligned} \tag{5.125}$$

One knows that the associated stationary Fokker-Planck equation has an exact solution:

$$P(y, x_1, x_2) \propto \exp\left(-x_1^2 - x_2^2 - y\right) \quad \text{so that } \alpha = -1. \tag{5.126}$$

$\langle\phi_0|\Psi_0\rangle = 1$. Thus, $|\Psi_0\rangle\langle\phi_0|A\rangle = a_0|\Psi_0\rangle$ which leads to the identification

$$\hat{p} = |\Psi_0\rangle\langle\phi_0|.$$

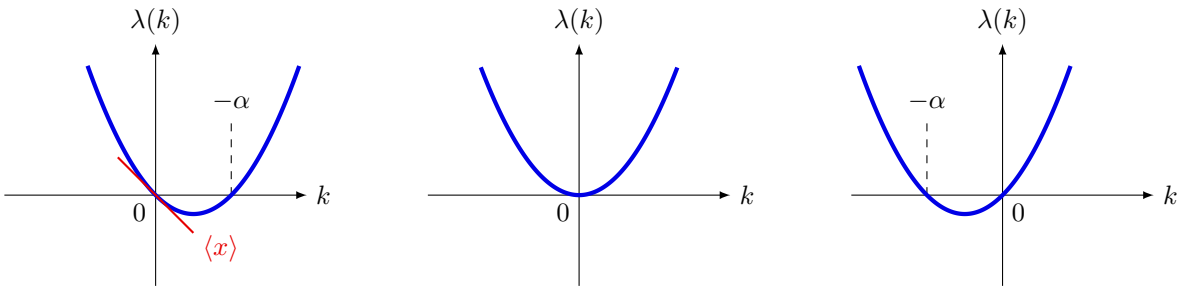

(a) $\langle x \rangle < 0$. **(b)** $\langle x \rangle = 0$. **(c)** $\langle x \rangle > 0$.

Figure 5.9 – Schematic evolution of the scaled cumulant generating function $\lambda(k)$ when the drift velocity $\langle x \rangle$ changes sign, with the corresponding value of the coefficient of sedimentation α.

The coefficient α_{E} obtained from the classical Einstein relation reads, with the series expansion of $\langle x_1 \rangle$ and D_{x_1},

$$\begin{aligned} \alpha_{\mathrm{E}} &= \frac{2\varepsilon}{(2\varepsilon)^2} \frac{\langle x_1 \rangle}{D_{x_1}} \\ &= -\frac{1 - 2\varepsilon^2 + \frac{32}{3}\varepsilon^4 - \frac{776}{9}\varepsilon^6 + \mathcal{O}(\varepsilon^8)}{1 - 2\varepsilon^2 + \frac{32}{3}\varepsilon^4 - \frac{704}{9}\varepsilon^6 + \mathcal{O}(\varepsilon^8)} \\ &= -1 + 8\varepsilon^6 + \mathcal{O}(\varepsilon^8). \end{aligned} \tag{5.127}$$

As we can see, the deviation of the classical Einstein relation from the exact solution occurs at the order 6 in ε, meaning that the process $x_1(t)$ is weakly non-Gaussian.

One can derive a similar formula for the next order coefficient in the expansion of $\lambda(k)$. Explicitly, one obtains

$$\begin{aligned} c_3 &= \lim_{T\to\infty} \frac{1}{T} \int_0^T \mathrm{d}t_1 \int_0^T \mathrm{d}t_2 \int_0^T \mathrm{d}t_3 \, \kappa[x(t_1), x(t_2), x(t_3)] \\ &= 3! \left(\left\langle \phi_0 \middle| \hat{x}\hat{A}\hat{x}\hat{A} \middle| \Psi_0 \right\rangle - \langle x \rangle \left\langle \phi_0 \middle| \hat{x}\hat{A}\hat{A}\hat{x} \middle| \Psi_0 \right\rangle \right) \quad \text{with} \quad \hat{A} = (\hat{\mathcal{H}} + \hat{p})^{-1}(1 - \hat{p}). \end{aligned} \tag{5.128}$$

However, we have not managed yet to find similar expressions for the other coefficients c_n with $n \geq 4$.

5.5 Summary and conclusion

In this chapter, we studied the sedimentation process:

$$\dot{y} = x \tag{5.129}$$

where $x(t)$ is a fluctuating variable whose statistics do not depend on y, and this a non-zero mean $\langle x \rangle$. Under very general assumptions, the density of probability $P(y)$ is expected to follow an exponential distribution

$$P(y) \sim \exp(\alpha y). \tag{5.130}$$

We showed that the determination of the coefficient of sedimentation reduces to a problem of large deviation, and that α is linked to the root of the scaled cumulant generating function $\lambda(k)$ – namely, $\lambda(-\alpha) = 0$. The main result is that $\lambda(k)$ is a convex function and has a root in $k = 0$, with $\lambda'(0) = \langle x \rangle$ (see figure 5.9). It follows that there exists at most one non-zero value of α, and that in this case α and $\langle x \rangle$ have the same sign.

In the previous chapter we studied a one dimensional noisy dynamical system, which describes the transition from a regime where the instantaneous Lyapunov exponent is positive in average,

so that the trajectories fill the space, to a regime where the instantaneous Lyapunov exponent is negative in average, resulting in a clustering of trajectories. The transition between the two regimes is then described schematically in figure 5.9, where α, which can be identified with the correlation dimension, smoothly changes sign. Note that, as stated in chapter 4, the *fluctuations* of $x(t)$, here linked to the curvature of $\lambda(k)$, are primordial to obtain finite values of α.

We explicitly compute the expression of $\lambda(k)$ for a non-Gaussian and non-Markovian process: the telegraphic noise. For this particular process the classical Einstein relation, linking the coefficient α to the first two moments of the distribution, fails. We showed that such a relation is valid only for Gaussian processes, which corresponds to quadratic expressions of $\lambda(k)$ in k.

In the general case, however, the computation of the scaled cumulant generating function is a complicated task. In particular, one expects non-analytical behaviours of α, as it was the case for the model studied in chapter 4. Such behaviours cannot be observed with classical perturbation methods, and we are currently working on other approaches to compute $\lambda(k)$.

Chapter 6

Summary, conclusion and perspectives

6.1 Summary and reminder of the principal results

In this thesis, we studied two apparently different physical situations: first, the dynamics of tracers advected by turbulent flows, and in particular the case of three fluid particles in a two-dimensional flow (chapter 3); second, the motion of inertial particles in a one-dimensional turbulent flow (chapter 4). For both processes, we described *clustering processes* in the relevant phase space.

For advected triangles in isotropic and homogeneous turbulence, we considered an evolution dynamics which is independent of the scale of the triangle, so that the phase space is the shape space of the structure. This shape space is homeomorphic to a 2-sphere: the Kendall sphere [Ken77]. The action of like-scale eddies on the three-points structure results in the flattening of the triangle, which corresponds for the representative point to go towards the equator of the Kendall sphere, representing flat triangles.

Considering the case of inertial particles, we introduced a simple stochastic model for the one-dimensional motion of particles mostly subjected to the Stokes drag. A path coalescence transition is known to happen in the model [WM03]. Namely, two behaviours are possible: a regime where two close particles separate with probability one as time goes to infinity, in opposition with a regime where all trajectories eventually merge onto a single one.

The main contribution of this thesis is to show that, remarkably, the two phenomena discussed above are similarly described as simple dynamical systems presenting *fluctuating Lyapunov exponents*. Typically, the evolution dynamics for the departure from an attractor – the equator of the Kendall sphere for the advected triangles, and the master trajectory for the inertial particles –, say $\delta(t)$, reduces to a simple one-dimensional dynamical system:

$$\dot{\delta}(t) = \zeta(t)\delta(t) \tag{6.1}$$

where $\zeta(t)$ is the instantaneous Lyapunov exponent describing the dynamics near the attractor, a *fluctuating* quantity, which in the case of clustering processes is *negative* in average. As the statistics of $\zeta(t)$ do not depend on $\delta(t)$, we obtain generically stationary power-law distributions for the variable $\delta(t)$. The exponent of the power-law is linked to the correlation dimension of the attractor, so that in the case of clustering processes ($\langle\zeta\rangle < 0$), we extended this notion to negative cases, and showed how the determination of this exponent is linked to a quantity used in large deviation theory: the scaled cumulant generating function associated to the instantaneous Lyapunov exponent $\zeta(t)$. It is interesting to note that under this formalism the path coalescence transition appears to be actually smooth, as represented figure 5.9. In other words, the study of fluctuating Lyapunov exponents reduces to the analysis of sedimentations processes, for which the large deviation formalism provides a natural framework.

We also stressed out the importance of a re-injection mechanism to prevents the variable $\delta(t)$ to stay at 0 and to sustain fluctuations around the attractor. Such a mechanism is provided by similar terms in the equations of motion of the triangles and of the inertial particles, namely a homogeneous diffusion process in the physical space, which becomes prominent for two close trajectories in the phase space. Note that an explicit description of the sustaining term is not needed, as long as it allows positive fluctuations to occur. For the typical processes studied in chapter 5, we simply add a wall in the space of the variable $y = \ln \delta$.

To summarize, we recall the main results presented in this thesis:

- ▷ An effective description of the dynamics of flat triangles resulting from the action of a time-correlated strain matrix (section 3.4).
- ▷ A coherent extension of the notion of correlation dimension to negative values, when the corresponding Lyapunov exponent is negative in average but presents positive fluctuations (section 4.4.2).
- ▷ The general description of a sedimentation process, and the expression of the coefficient of sedimentation as (minus) the root of a convex function, the scaled cumulant generating function associated to the driving process (section 5.2.3).
- ▷ A perturbative expansion for the effective diffusion coefficient of a process driven by weakly non-linear Langevin equations (section 5.4.4).

6.2 Conclusion and perspectives

The careful reader may have noticed that, although this thesis presents the word “turbulent” in its title, we did not talk much about turbulent flows. In fact, we used very general feature of turbulent flows to obtain simple stochastic models in the form of noisy dynamical systems. Notably, few connections have been made with direct simulations of particles in turbulent flows or experimental results.

Triangle model

We showed in chapter 3 that introducing finite correlation times for the like-scale eddies acting on the triangle did not change the power-law distribution obtained for the variable z describing the shape of the triangle. Such an observation could be compared in the future with direct simulations or the analysis of the motion of actual tracers in turbulent flows.

Moreover, in the same chapter we sketched the beginning of a theory concerning the statistics of crossing of the Kendall sphere equator, which correspond the topological changes of the triangle. While we showed that time correlated eddies lead to normalisable statistics of crossing, we did not manage yet to propose a general description of the topological evolution of the triangle in terms of a braid group [TF06].

Note also that the model for an advected triangle is independent of the size of the triangle. However, during its temporal evolution the size of the initial structure typically grows, and the triangle encounter different eddies. The next step is then to consider size-dependant models, and to analysis the resulting dynamics.

Perturbative expansions and correlation dimension

In chapter 3 and 5 we presented perturbative methods to compute the mean drift velocity and the diffusion coefficient of a process generated by weakly non-linear Langevin equations, and tried to qualitatively determine whether a given non-linear system is likely to produce non-analytical behaviours in the expressions of this moments. Nevertheless, one still lacks a systematic criterion

for general non-linear systems. Moreover, if we observe non-analytical behaviours, we need to find a general theory to compute them reliably.

This statement, namely the possibility for the mean drift velocity and the diffusion coefficient to present non-analytical variations, is also true for the scaled cumulant generating function itself. While we managed to compute it exactly for a very particular process (see section 5.3), in the general case such a task in likely to be significantly more difficult, and we are currently working on this topic. We mainly studied what may be called strongly clustering processes, that is one-dimensional noisy dynamical systems with a negative mean Lyapunov exponent, but the description of the motion near the attractor as a sedimentation process is generic, so that the tools developed here, and in particular the use of the formalism of large deviation theory, can be applied to positive fluctuating Lyapunov exponents. Thus, a general approach of the scaled cumulant generating function, and in particular of its non-analytic aspects, may lead to a much deeper understanding of the evolution of the correlation dimension in a large class of dynamical systems.

Bibliography

[Abr98] Edward R Abraham. "The generation of plankton patchiness by turbulent stirring". In: *Nature* 391.6667 (1998), pp. 577–580.

[AV78] RA Antonia and CW Van Atta. "Structure functions of temperature fluctuations in turbulent shear flows". In: *Journal of Fluid Mechanics* 84.03 (1978), pp. 561–580.

[Bra+99] A Bracco et al. "Particle aggregation in a turbulent Keplerian flow". In: *Physics of Fluids (1994-present)* 11.8 (1999), pp. 2280–2287.

[CC88] Reiyu Chein and JN Chung. "Simulation of particle dispersion in a two-dimensional mixing layer". In: *AIChE Journal* 34.6 (1988), pp. 946–954.

[CGT85] CT Crowe, RA Gore, and TR Troutt. "Particle dispersion by coherent structures in free shear flows". In: *Particulate Science and Technology* 3.3-4 (1985), pp. 149–158.

[CK98] Shiyi Chen and Robert H Kraichnan. "Simulations of a randomly advected passive scalar field". In: *Physics of Fluids (1994)* 10.11 (1998).

[CP01] Patrizia Castiglione and Alain Pumir. "Evolution of triangles in a two-dimensional turbulent flow". In: *Physical Review E* 64.5 (2001), p. 056303.

[Cra38] Harald Cramér. "Sur un nouveau théoreme-limite de la théorie des probabilités". In: *Actualités scientifiques et industrielles* 736.5-23 (1938), p. 115.

[Csa73] GT Csanady. "Turbulent Diffusion in the Environment Reidel". In: *Dordrecht, Holland* (1973).

[DD73] Robert B Dingle and RB Dingle. *Asymptotic expansions: their derivation and interpretation*. Vol. 48. Academic Press London, 1973.

[Dri81] Wulf Driessler. "On the spectrum of the Rayleigh piston". In: *Journal of Statistical Physics* 24.4 (1981), pp. 595–606.

[DV75] Monroe D Donsker and SR Srinivasa Varadhan. "Asymptotic evaluation of certain Markov process expectations for large time, I". In: *Communications on Pure and Applied Mathematics* 28.1 (1975), pp. 1–47.

[Ein05] Albert Einstein. "Über die von der molekularkinetischen Theorie der Wärme geforderte Bewegung von in ruhenden Flüssigkeiten suspendierten Teilchen". In: *Annalen der physik* 322.8 (1905), pp. 549–560.

[Ell84] Richard S Ellis. "Large deviations for a general class of random vectors". In: *The Annals of Probability* (1984), pp. 1–12.

[ER85] J-P Eckmann and David Ruelle. "Ergodic theory of chaos and strange attractors". In: *Reviews of modern physics* 57.3 (1985), p. 617.

[Fal04] Kenneth Falconer. *Fractal geometry: mathematical foundations and applications*. John Wiley & Sons, 2004.

[Fen+98] DL Feng et al. "On-off intermittencies in gas discharge plasma". In: *Physical Review E* 58.3 (1998), p. 3678.

[FFS02] G Falkovich, A Fouxon, and MG Stepanov. "Acceleration of rain initiation by cloud turbulence". In: *Nature* 419.6903 (2002), pp. 151–154.

[Fia+12] Lionel Fiabane et al. "Clustering of finite-size particles in turbulence". In: *Physical Review E* 86.3 (2012), p. 035301.

[Fia+13] Lionel Fiabane et al. "Do finite-size neutrally buoyant particles cluster?" In: *Physica Scripta* 2013.T155 (2013), p. 014056.

[Fox78] Ronald Forrest Fox. "Gaussian stochastic processes in physics". In: *Physics Reports* 48.3 (1978), pp. 179–283.

[FP07] Gregory Falkovich and Alain Pumir. "Sling Effect in Collisions of Water Droplets in Turbulent Clouds". In: *Journal of Atmospheric Sciences* 64 (2007), p. 4497.

[Fuj+86] H. Fujisaka et al. "Intermittency Caused by Chaotic Modulation. II: –Lyapunov Exponent, Fractal Structure and Power Spectrum–". In: *Progress of Theoretical Physics* 76.6 (Dec. 1986), pp. 1198–1209. DOI: 10.1143/ptp.76.1198. URL: http://dx.doi.org/10.1143/PTP.76.1198.

[FY86] H. Fujisaka and T. Yamada. "Stability Theory of Synchronized Motion in Coupled-Oscillator Systems. IV: Instability of Synchronized Chaos and New Intermittency". In: *Progress of Theoretical Physics* 75.5 (May 1986), pp. 1087–1104. DOI: 10.1143/ptp.75.1087. URL: http://dx.doi.org/10.1143/PTP.75.1087.

[Gar+85] Crispin W Gardiner et al. *Handbook of stochastic methods*. Vol. 3. Springer Berlin, 1985.

[Gär77] Jürgen Gärtner. "On large deviations from the invariant measure". In: *Theory of Probability & Its Applications* 22.1 (1977), pp. 24–39.

[Gat83] Renée Gatignol. "The Faxén formulas for a rigid particle in an unsteady non-uniform Stokes-flow". In: *Journal de Mécanique théorique et appliquée* 2.2 (1983), pp. 143–160.

[GMW15] Kristian Gustavsson, Bernhard Mehlig, and Michael Wilkinson. "Analysis of the correlation dimension for inertial particles". In: *Physics of Fluids (1994-present)* 27.7 (2015), p. 073305.

[GP83] Peter Grassberger and Itamar Procaccia. "Measuring the strangeness of strange attractors". In: *Physica D: Nonlinear Phenomena* 9.1-2 (Oct. 1983), pp. 189–208. DOI: 10.1016/0167-2789(83)90298-1. URL: http://dx.doi.org/10.1016/0167-2789(83)90298-1.

[GP84] Peter Grassberger and Itamar Procaccia. "Dimensions and entropies of strange attractors from a fluctuating dynamics approach". In: *Physica D: Nonlinear Phenomena* 13.1 (1984), pp. 34–54.

[GPW16] Robin Guichardaz, Alain Pumir, and Michael Wilkinson. "Non-Thermal Einstein Relations". In: *arXiv preprint arXiv:1602.06059* (2016).

[GRH07] Melissa A Green, Clarence W Rowley, and George Haller. "Detection of Lagrangian coherent structures in three-dimensional turbulence". In: *Journal of Fluid Mechanics* 572.1 (2007), pp. 111–120.

[Ham+94] Philip W Hammer et al. "Experimental observation of on-off intermittency". In: *Physical review letters* 73.8 (1994), p. 1095.

[Hoa71] MR Hoare. "The linear gas". In: *Adv. Chem. Phys* 20 (1971), pp. 135–214.

[HPH94] JF Heagy, N Platt, and SM Hammel. "Characterization of on-off intermittency". In: *Physical Review E* 49.2 (1994), p. 1140.

[HS94] Mark Holzer and Eric D Siggia. "Turbulent mixing of a passive scalar". In: *Physics of Fluids (1994-present)* 6.5 (1994), pp. 1820–1837.

[JSB99] Thomas John, Ralf Stannarius, and Ulrich Behn. "On-off intermittency in stochastically driven electrohydrodynamic convection in nematics". In: *Physical review letters* 83.4 (1999), p. 749.

[Kam61] NG van Kampen. "A power series expansion of the master equation". In: *Canadian Journal of Physics* 39.4 (1961), pp. 551–567.

[Kár+00] György Károlyi et al. "Chaotic flow: the physics of species coexistence". In: *Proceedings of the National Academy of Sciences* 97.25 (2000), pp. 13661–13665.

[Ken+98] Wilfrid S Kendall et al. "A diffusion model for Bookstein triangle shape". In: *Advances in Applied Probability* 30.2 (1998), pp. 317–334.

[Ken77] David G Kendall. "The diffusion of shape". In: *Advances in applied probability* 9.3 (1977), pp. 428–430.

[Ken84] David G Kendall. "Shape manifolds, procrustean metrics, and complex projective spaces". In: *Bulletin of the London Mathematical Society* 16.2 (1984), pp. 81–121.

[Ken89] David G Kendall. "A survey of the statistical theory of shape". In: *Statistical Science* (1989), pp. 87–99.

[Kob+92] Hironobu Kobayashi et al. "Particle dispersion in a plane mixing layer with streamwise pressure gradient". In: *JSME international journal. Ser. 2, Fluids engineering, heat transfer, power, combustion, thermophysical properties* 35.1 (1992), pp. 29–37.

[Kub66] Rep Kubo. "The fluctuation-dissipation theorem". In: *Reports on progress in physics* 29.1 (1966), p. 255.

[KY79] JL Kaplan and JA Yorke. "Functional differential equations and approximation of fixed points". In: *Lecture notes in mathematics* 730 (1979), p. 228.

[Lan02] Serge Lang. "Algebra revised third edition". In: *Graduate Texts in Mathematics* 1.211 (2002), ALL–ALL.

[Lan08] Paul Langevin. "Sur la théorie du mouvement brownien". In: *CR Acad. Sci. Paris* 146.530-533 (1908), p. 530.

[Lan73] Oscar E Lanford. "Entropy and equilibrium states in classical statistical mechanics". In: *Statistical mechanics and mathematical problems*. Springer, 1973, pp. 1–113.

[LL65] Lev D Landau and EM Lifschitz. *Quantum mechanics. Nonrelativistic theory. 2-nd ed.* 1965.

[Lum92] JL Lumley. "Some comments on turbulence". In: *Physics of Fluids A: Fluid Dynamics (1989-1993)* 4.2 (1992), pp. 203–211.

[LZY03] Jing Z Liu, Lu D Zhang, and Guang H Yue. "Fractal dimension in human cerebellum measured by magnetic resonance imaging". In: *Biophysical Journal* 85.6 (2003), pp. 4041–4046.

[Man83] Benoit B Mandelbrot. *The fractal geometry of nature*. Vol. 173. Macmillan, 1983.

[Man90] Benoit B Mandelbrot. "Negative fractal dimensions and multifractals". In: *Physica A: Statistical Mechanics and its Applications* 163.1 (1990), pp. 306–315.

[Max87] MR Maxey. "The gravitational settling of aerosol particles in homogeneous turbulence and random flow fields". In: *Journal of Fluid Mechanics* 174 (1987), pp. 441–465.

[MBC10] Romain Monchaux, Mickaël Bourgoin, and Alain Cartellier. "Preferential concentration of heavy particles: a Voronoi analysis". In: *Physics of Fluids (1994-present)* 22.10 (2010), p. 103304.

[MBC12] Romain Monchaux, Mickael Bourgoin, and Alain Cartellier. "Analyzing preferential concentration and clustering of inertial particles in turbulence". In: *International Journal of Multiphase Flow* 40 (2012), pp. 1–18.

[MCB04] Nicolas Mordant, Alice M Crawford, and Eberhard Bodenschatz. "Experimental Lagrangian acceleration probability density function measurement". In: *Physica D: Nonlinear Phenomena* 193.1 (2004), pp. 245–251.

[Meh+05] Bernhard Mehlig et al. "Aggregation of inertial particles in random flows". In: *Physical Review E* 72.5 (2005), p. 051104.

[Mes82] Patrice Mestayer. "Local isotropy and anisotropy in a high-Reynolds-number turbulent boundary layer". In: *Journal of Fluid Mechanics* 125 (1982), pp. 475–503.

[Mor+01] Nicolas Mordant et al. "Measurement of Lagrangian velocity in fully developed turbulence". In: *Physical Review Letters* 87.21 (2001), p. 214501.

[Moy49] JE Moyal. "Stochastic processes and statistical physics". In: *Journal of the Royal Statistical Society. Series B (Methodological)* 11.2 (1949), pp. 150–210.

[MR83] Martin R Maxey and James J Riley. "Equation of motion for a small rigid sphere in a nonuniform flow". In: *Physics of Fluids (1958-1988)* 26.4 (1983), pp. 883–889.

[MW04] Bernhard Mehlig and Michael Wilkinson. "Coagulation by random velocity fields as a Kramers problem". In: *Physical review letters* 92.25 (2004), p. 250602.

[MY71] AS Monin and AM Yaglom. "Statistical fluid dynamics". In: *Vol. I and II MIT Press, Cambridge* (1971).

[Ose68] Valery Iustinovich Oseledec. "A multiplicative ergodic theorem. Lyapunov characteristic numbers for dynamical systems". In: *Trans. Moscow Math. Soc* 19.2 (1968), pp. 197–231.

[Ott02] Edward Ott. *Chaos in dynamical systems*. Cambridge university press, 2002.

[Oue12] Nicholas T Ouellette. "On the dynamical role of coherent structures in turbulence". In: *Comptes Rendus Physique* 13.9 (2012), pp. 866–877.

[Per13] Jean Perrin. *Les atomes*. Librairie Félix Alcan, 1913.

[PHH94] Nathan Platt, Stephen M Hammel, and James F Heagy. "Effects of additive noise on on-off intermittency". In: *Physical review letters* 72.22 (1994), p. 3498.

[PM80] Yves Pomeau and Paul Manneville. "Intermittent transition to turbulence in dissipative dynamical systems". In: *Communications in Mathematical Physics* 74.2 (1980), pp. 189–197.

[PPR09] Rahul Pandit, Prasad Perlekar, and Samriddhi Sankar Ray. "Statistical properties of turbulence: An overview". In: *Pramana* 73.1 (2009), pp. 157–191.

[PSC00] Alain Pumir, Boris I Shraiman, and Misha Chertkov. "Geometry of Lagrangian dispersion in turbulence". In: *Physical review letters* 85.25 (2000), p. 5324.

[PST93] NSEA Platt, EA Spiegel, and C Tresser. "On-off intermittency: A mechanism for bursting". In: *Physical Review Letters* 70.3 (1993), p. 279.

[PW13] Alain Pumir and Michael Wilkinson. "A model for the shapes of advected triangles". In: *Journal of Statistical Physics* 152.5 (2013), pp. 934–953.

[PW15] Alain Pumir and Michael Wilkinson. "Collisional Aggregation Due to Turbulence". In: *arXiv preprint arXiv:1508.01538* (2015).

[RČB95] F Rödelsperger, A Čenys, and H Benner. "On-off intermittency in spin-wave instabilities". In: *Physical review letters* 75.13 (1995), p. 2594.

[Ric26] Lewis F Richardson. "Atmospheric diffusion shown on a distance-neighbour graph". In: *Proceedings of the Royal Society of London. Series A, Containing Papers of a Mathematical and Physical Character* 110.756 (1926), pp. 709–737.

[Ris84] Hannes Risken. *Fokker-planck equation*. Springer, 1984.

[Roc70] R Tyrrell Rockafellar. *Convex Analysis, volume 28 of Princeton Mathematics Series*. 1970.

[Sre91] KR Sreenivasan. "On local isotropy of passive scalars in turbulent shear flows". In: *Proceedings of the Royal Society of London A: Mathematical, Physical and Engineering Sciences*. Vol. 434. 1890. The Royal Society. 1991, pp. 165–182.

[SS00] Boris I Shraiman and Eric D Siggia. "Scalar turbulence". In: *Nature* 405.6787 (2000), pp. 639–646.

[SS95] Boris I Shraiman and Eric D Siggia. "Anomalous scaling of a passive scalar in turbulent flow". In: *Comptes rendus de l'Académie des sciences. Série II, Mécanique, physique, chimie, astronomie* 321.7 (1995), pp. 279–284.

[SSS86] José M Sancho, F Sagues, and M San Miguel. "Mean first-passage time of continuous non-Markovian processes driven by colored noise". In: *Physical Review A* 33.5 (1986), p. 3399.

[Sut05] William Sutherland. "LXXV. A dynamical theory of diffusion for non-electrolytes and the molecular mass of albumin". In: *The London, Edinburgh, and Dublin Philosophical Magazine and Journal of Science* 9.54 (1905), pp. 781–785.

[Tan+09] Can Ozan Tan et al. "Fractal properties of human heart period variability: physiological and methodological implications". In: *The Journal of physiology* 587.15 (2009), pp. 3929–3941.

[Tan+92] L. Tang et al. "Self-organizing particle dispersion mechanism in a plane wake". In: *Physics of Fluids A: Fluid Dynamics* 4.10 (1992), p. 2244. DOI: 10.1063/1.858465. URL: http://dx.doi.org/10.1063/1.858465.

[Tay22] Geoffrey I Taylor. "Diffusion by continuous movements". In: *Proc. London Math. Soc* 20.1 (1922), pp. 196–212.

[TB09] Federico Toschi and Eberhard Bodenschatz. "Lagrangian properties of particles in turbulence". In: *Annual Review of Fluid Mechanics* 41 (2009), pp. 375–404.

[TF06] Jean-Luc Thiffeault and Matthew D Finn. "Topology, braids and mixing in fluids". In: *Philosophical Transactions of the Royal Society of London A: Mathematical, Physical and Engineering Sciences* 364.1849 (2006), pp. 3251–3266.

[TL72] Hendrik Tennekes and John Leask Lumley. *A first course in turbulence*. MIT press, 1972.

[Tou09] Hugo Touchette. "The large deviation approach to statistical mechanics". In: *Physics Reports* 478.1 (2009), pp. 1–69.

[Van74] NG Van Kampen. "A cumulant expansion for stochastic linear differential equations. II". In: *Physica* 74.2 (1974), pp. 239–247.

[Van76] Nicolaas G Van Kampen. "Stochastic differential equations". In: *Physics reports* 24.3 (1976), pp. 171–228.

[Van92] Nicolaas Godfried Van Kampen. *Stochastic processes in physics and chemistry*. Vol. 1. Elsevier, 1992.

[Wen+92] F Wen et al. "Particle dispersion by vortex structures in plane mixing layers". In: *Journal of fluids engineering* 114.4 (1992), pp. 657–666.

[WG14] Michael Wilkinson and John Grant. "Triangular constellations in fractal measures". In: *EPL (Europhysics Letters)* 107.5 (2014), p. 50006.

[Wil+12] Michael Wilkinson et al. "Clustering of exponentially separating trajectories". In: *The European Physical Journal B* 85.1 (2012), pp. 1–5.

[Wil+15] Michael Wilkinson et al. "Power-law distributions in noisy dynamical systems". In: *EPL (Europhysics Letters)* 111.5 (2015), p. 50005.

[Wio+89] Horacio S Wio et al. “Path-integral formulation for stochastic processes driven by colored noise”. In: *Physical Review A* 40.12 (1989), p. 7312.

[WM03] Michael Wilkinson and Bernhard Mehlig. “Path coalescence transition and its applications”. In: *Physical Review E* 68.4 (2003), p. 040101.

[WM05] M Wilkinson and Bernhard Mehlig. “Caustics in turbulent aerosols”. In: *EPL (Europhysics Letters)* 71.2 (2005), p. 186.

[WMB06] Michael Wilkinson, Bernhard Mehlig, and Vlad Bezuglyy. “Caustic activation of rain showers”. In: *Physical review letters* 97.4 (2006), p. 048501.

[WMG10] Michael Wilkinson, Bernhard Mehlig, and Kristian Gustavsson. “Correlation dimension of inertial particles in random flows”. In: *EPL (Europhysics Letters)* 89.5 (2010), p. 50002.

[WP11] Michael Wilkinson and Alain Pumir. “Spherical Ornstein-Uhlenbeck Processes”. In: *Journal of Statistical Physics* 145.1 (2011), pp. 113–142.

[WRR03] Michael E Wall, Andreas Rechtsteiner, and Luis M Rocha. “Singular value decomposition and principal component analysis”. In: *A practical approach to microarray data analysis*. Springer, 2003, pp. 91–109.

[XOB08] Haitao Xu, Nicholas T Ouellette, and Eberhard Bodenschatz. “Evolution of geometric structures in intense turbulence”. In: *New Journal of Physics* 10.1 (2008), p. 013012.

[YF86] T. Yamada and H. Fujisaka. “Intermittency Caused by Chaotic Modulation. I: –Analysis with a Multiplicative Noise Model–”. In: *Progress of Theoretical Physics* 76.3 (Sept. 1986), pp. 582–591. DOI: 10.1143/ptp.76.582. URL: http://dx.doi.org/10.1143/PTP.76.582.

[YG07] Hiroshi Yoshimoto and Susumu Goto. “Self-similar clustering of inertial particles in homogeneous turbulence”. In: *Journal of Fluid Mechanics* 577 (2007), p. 275.